DISSERTATION

DUAL FUEL ENGINE COMBUSTION AND EMISSIONS – AN EXPERIMENTAL

INVESTIGATION COUPLED WITH COMPUTER SIMULATION

Submitted by

Wan Nurdiyana Wan Mansor

Department of Mechanical Engineering

In partial fulfillment of the requirements

For the Degree of Doctor of Philosophy

Colorado State University

Fort Collins, Colorado

Fall 2014

Doctoral Committee:

    Advisor: Daniel B. Olsen

    Anthony J. Marchese
    Gao Xinfeng
    Sybil Sharvelle

ABSTRACT

DUAL FUEL ENGINE COMBUSTION AND EMISSIONS – AN EXPERIMENTAL

INVESTIGATION COUPLED WITH COMPUTER SIMULATION

Alternative fuels have been getting more attention as concerns escalate over exhaust pollutant emissions produced by internal combustion engines, higher fuel costs, and the depletion of crude oil. Various solutions have been proposed, including utilizing alternative fuels as a dedicated fuel in spark ignited engines, diesel pilot ignition engines, gas turbines, and dual fuel and bi-fuel engines. Among these applications, one of the most promising options is the diesel derivative dual fuel engine with natural gas as the supplement fuel.

This study aims to evaluate diesel and dual fuel combustion in a natural gas-diesel dual fuel engine. More dual fuel engines are being utilized due to stricter emission standards, increasing costs of diesel fuel and decreasing costs of natural gas. Originally sold as diesel engines, these units are converted to natural gas-diesel fuel engines using an aftermarket dual fuel kit. As natural gas is mixed with air intake, the amount of diesel used is reduced. The maximum natural gas substitution is limited by knock or emissions of carbon monoxide and total hydrocarbons.

In this research a John Deere 6068H diesel engine is converted to dual fuel operation. The engine is a Tier II, 6 cylinder, 6.8 liter, 4-stroke compression ignition engine with a compression ratio of 17:1 and a power rating of 168 kW at 2200 rpm. A natural gas fuel system is installed to deliver fuel upstream of the turbocharger compressor. The engine operates at 1800 rpm through five different load points in diesel and dual fuel operating modes. Crank angle resolved high speed combustion pressure data is obtained and analyzed. The natural gas

substitution values tested are representative of standard dual fuel tuning, with a maximum diesel displacement of 70%. Data for thermal efficiency, combustion stability, in-cylinder pressure and net heat release rate are also presented in this study. In addition, fuel consumption and pollutant emissions are measured. Elevated CO and HC emissions are observed at low loads for dual fuel operation. Overall, CO and unburned HC emissions increase for dual fuel operation. However, the average levels of PM and NOx substantially decreases. A series of natural gas and injection timing sweep are conducted to optimize the combustion and emission in dual fuel engine.

To understand the location of emissions inside the cylinder, a model study of a natural gas-diesel dual fuel combustion and emission is performed using the commercial CONVERGE CFD code. A reduced chemical kinetic mechanism with 86 species and 393 reactions for n-heptane, methane, ethane and propane is used. A preliminary hypothesis for these emissions is formulated based on the values of experiment equivalence ratio. Findings indicate that a large amount of CO and HC emissions in dual fuel engines are mainly located on the cylinder wall and nozzle area. High temperatures are not able to propagate through the lean mixture of natural gas and air in dual fuel engine hence high unburned fuel trapped at wall.

It is concluded that dual fuel engines are capable of reducing emissions and cost saving (through diesel displacement up to70%) in diesel fuel engines. CO and unburned HC can be reduced with the application of a dual fuel optimization map. Further investigation using oxidation catalyst is recommended in order to meet with emission regulations.

ACKNOWLDEGMENTS

TABLE OF CONTENTS

LIST OF TABLES

LIST OF FIGURES

LIST OF ACRONYMS

ICE	=	Internal Combustion Engine
CI	=	Compression-ignition
SI	=	Spark-ignition
Φ	=	equivalence ratio
NO_x	=	oxides of nitrogen
HC	=	Unburned Hydrocarbons
PM	=	Particulate Matters
CO	=	Carbon Monoxides
EPA	=	Environmental Protection Agency
DGE	=	Diesel Gallon Equivalent
LPG	=	Liquefied Petroleum Gas
CNG	=	Compressed Natural Gas
LNG	=	Liquefied Natural Gas
p-V	=	pressure-volume
°bTDC	=	Crank angle, measured in degrees before Top Dead Center.
°aTDC	=	Crank angle, measured in degrees after Top Dead Center
CR	=	Compression Ratio
η_t	=	Thermal efficiency
CFD	=	Computational Fluid Dynamics
SOI	=	the start of injection
AF	=	air fuel ratio
HRR	=	Heat Release Rate
Bsfc	=	brake specific fuel consumption

EGR   =   Exhaust Gas Recirculation

PLC   =   Programmable Logic Controller

OEM   =   Original Equipment Manufacturer

ECM   =   Engine Control Module

PWM   =   Pulse Width Modulation

VOCs   =   Volatile organic compounds

IR   =   Infra-Red Radiation

FID   =   Flame Ionization Detection

FTIR   =   Fourier Transform Infra-Red Spectrometer

HEPA   =   High Efficiency Particulate Air

IMEP   =   Indicated Mean Effective Pressure

COV   =   Coefficient of Variance

LHV   =   Lower Heating Value

NMHCs=   Non-Methane Hydrocarbons

IVC   =   intake valve closed

AMR   =   Adaptive Mesh Refinement

KH-RT=   Kelvin-Helmholtz Rayleigh-Taylor

KH-ACT=   Kelvin-Helmholtz-Aerodynamics Cavitation Turbulence

NTC   =   No Time Counter

RNG   =   Renormalization Group

RANS =   Reynolds Averaged Navier-Stokes model.

TKE   =   Turbulence Kinetic Energy

Eps   =   Turbulent Dissipation

NSC   =   Nagle and Strickland-Constable

1.0 INTRODUCTION

The internal combustion engine (ICE) is defined as a heat engine that converts chemical energy of fuel into thermal energy and later transforms this thermal energy into mechanical energy in a confined space called a combustion chamber. There are two types of ICEs, rotary and reciprocating engines, but the most commonly used are the reciprocating internal combustion engines. Reciprocating ICEs have pistons that move in a cylinder in a linear motion and transmit power through a connecting rod to a drive shaft. This reciprocating engine can have one or more cylinders and operates on either four-stroke, which has four piston movements over two resolutions for each cycle, or two-stroke cycle, which has two piston movements over one revolution for each cycle.

The ICE has undergone various improvements since it was demonstrated over a century ago. The focus had been on overcoming engine's shortcomings of low thermal efficiency and large engine sizes. In 1882, the German engineer Rudolf Diesel invented the compression-ignition (CI) engine by injecting a liquid fuel into air heated by compression. Since then, the diesel engine has become a favorable engine due to high fuel economy, reliability and power output.

1.1 Compression Ignition Engine Emissions

Emissions from a CI engine are a strong function of equivalence ratio (Φ) (1) (2). Common exhaust emissions from a CI engine are oxides of nitrogen (NO_x), carbon monoxides (CO), unburned hydrocarbons (HC) and particulate matters (PM). NO_x formation is dependent on the oxidation of atmospheric nitrogen and is strongly affected by the cylinder charge temperature. Total emission of NO_x in a CI engine is higher compared to lean burn spark-ignition (SI) engines because combustion takes place as a diffusion flame which occurs at Φ close to 1.0.

1

In this region, the stoichiometric air-fuel ratio reaches very high temperatures accounting for the high level of NO_x. CI engines that operate at a very lean mixture with excess air can help to control the NO_x. Combustion gases in lean mixture continue to mix with excess air resulting in lower temperatures that weakens the kinetics of NO_x formation. SI engines that operate close to stoichiometric produces higher NO_x levels than CI engines. Maximum flame temperature which occurs at stoichiometric air-fuel ratio leads to the dissociation of nitrogen (N) which then combines with oxygen to form NO_x. In lean mixture CI engines, because of the non-homogeneity of air-fuel mixture, some local spots in the cylinder will be too lean to burn, leading to misfire and poor combustion. Other spots may be too rich with not enough oxygen to react with all the carbons. Both conditions of lean and rich mixture produce high HC emission. For CO emission, it is formed when an engine runs rich, therefore its formation does not depend on the intake mixture condition. PM emission in CI engine is formed mostly in the fuel rich zone where Φ is higher than 1.0 within the cylinder during the combustion due to incomplete combustion of fuel hydrocarbons and some from lubricating oil (3).

1.2   The Effects of Exhaust Emission

Figure 1.1 represents a breakdown of country's percentage of global energy-related CO_2 emissions from fuel combustion in 2011. The USA contributes 17% of global CO_2 emissions while the rest of the world (29%), China (26%), European Union (11%), India (6%), Russian Federation (5%) and Japan (4%). The effects of greenhouse and other emissions are alarming. These emissions can result in unhealthy levels of air pollution, global climate change, acid rain and respiratory problems. In China, the ones most directly affected by its air pollution are the citizens. China's skies darken with pollution, forcing the citizens to take precautions when riding a bike or playing outside. Figure 1.2 shows a Chinese woman wearing a mask as she rides a bicycle though an area where the air is polluted by exhausts that are harmful to public health.

2
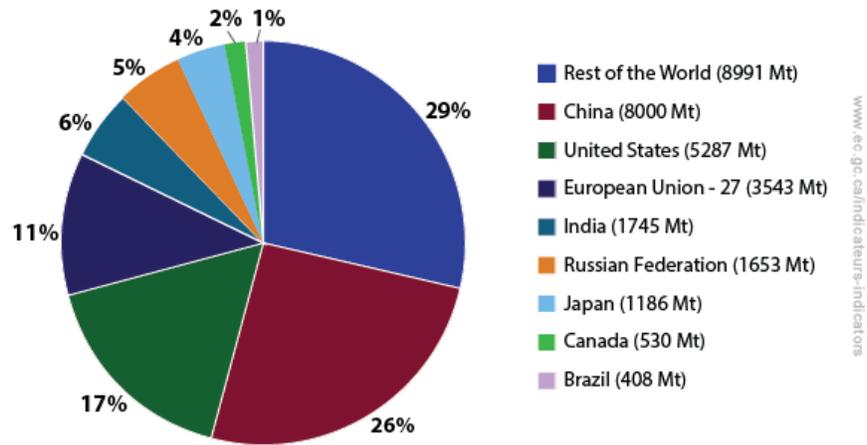
Figure 1.1: Global carbon dioxide emissions from fuel combustion (in megatons of

carbon dioxide equivalent) (4)

Figure 1.2: A woman protects herself from smog (4)

Figure 1.3 displays a clean air dome built by the International School of Beijing to enclose the playground and filter the air. Until the outside air is clean, students play and exercise in this costly dome every day. The health effects of these hazardous emissions are both acute

3

from short-term and chronic for long-term and repeated exposure. Therefore, it is crucial to control the production of air pollution. One way to reduce the emissions is by engine design and control of engine parameters but quite often, this will create other adverse effects. PM emission in the CI engine cannot be reduced to an acceptable level solely by engine design and control. It typically requires an after treatment system to reduce emission levels below regulator standards. Emission limits are implemented to regulate and control emissions from light-duty, heavy-duty and stationary engines.

Table 1.1 gives some of the emission standards for non-road and stationary CI engines that were established by Environmental Protection Agency (EPA). Tier 4 requires more than 90% reduction in NO_x emission. Tier 4 also requires substantial reduction in HC emission as well as PM emission. In natural gas engine, non-methane hydrocarbon (NMHC) is considered as HC emission. CO emission limits are unchanged since Tier 2 and 3. Looking at the data below, the standards are significantly tightened over time. Therefore, it is crucial for the engine manufacturers to continuously improve the engine efficiency and technology in order to meet the regulations.

Another concern for manufactures and operators of CI engines is the fuel cost. Diesel fuel cost is generally high and increases when the high worldwide demand for diesel fuel and other distillate oil is increased, especially in Europe, China and the USA (5). In the USA, on-highway diesel fuel prices have been continuously higher than gasoline since September 2004 (6). Since alternative fuel such as natural gas is considerably lower, utilizing natural gas in diesel operations may promote fuel cost savings.

Figure 1.3: Kids play under the dome for air filtering in Beijing (7)

Table 1.1: Emission standard for non-road and stationary CI engines with power more than 900 kW

	Tier 1	Tier 2	Tier 3	Tier 4
Year released	2004	2006	2011	2015
NO_x Limit (g/kWh)	9.2	Sum 6.4	0.67	0.67
HC (NMHC) Limit (g/kWh)	1.3		0.4	0.19
CO Limit (g/kWh)	11.4	3.5	3.5	3.5
PM Limit (g/kWh)	0.54	0.2	0.1	0.03

Figure 1.4 shows price comparisons between on-highway diesel fuel and city gate natural gas fuel in dollars per diesel equivalent between year 2000 and 2013. In 2008, city gate natural gas prices reached the highest at $1.5 per diesel gallon equivalent (DGE). The same trend is observed in on-highway diesel fuel cost at more than $4.5 per DGE. In recent years, city gate natural gas prices are more stable at less than $1.0 per DGE, while on-highway diesel fuel price remains higher at $4.0 per DGE. The cost saving in city gate natural gas is approximately 80% lower than on-highway diesel fuel with diesel to natural gas ratio as more than 6.

In the effort to reduce undesirable emissions and expensive diesel fuel cost, many have proposed alternative ways to combine cleaner and lower cost gaseous fuel with diesel fuel as a diesel fuel supplement. Gaseous fuels are considered to be good alternative fuels for passenger cars, truck transportation and stationary engines that can provide both reduced pollutant emissions and energy security (8). Most combustion devices are easily adaptable to the use of gaseous fuels for power production. Gaseous fuels with high octane numbers such as natural gas and biogas have a knock resistance which makes them suitable for engines with relatively high compression ratios. Gaseous fuels produce less pollutant exhaust emissions if appropriate conditions are satisfied for its mixing and combustion (9).
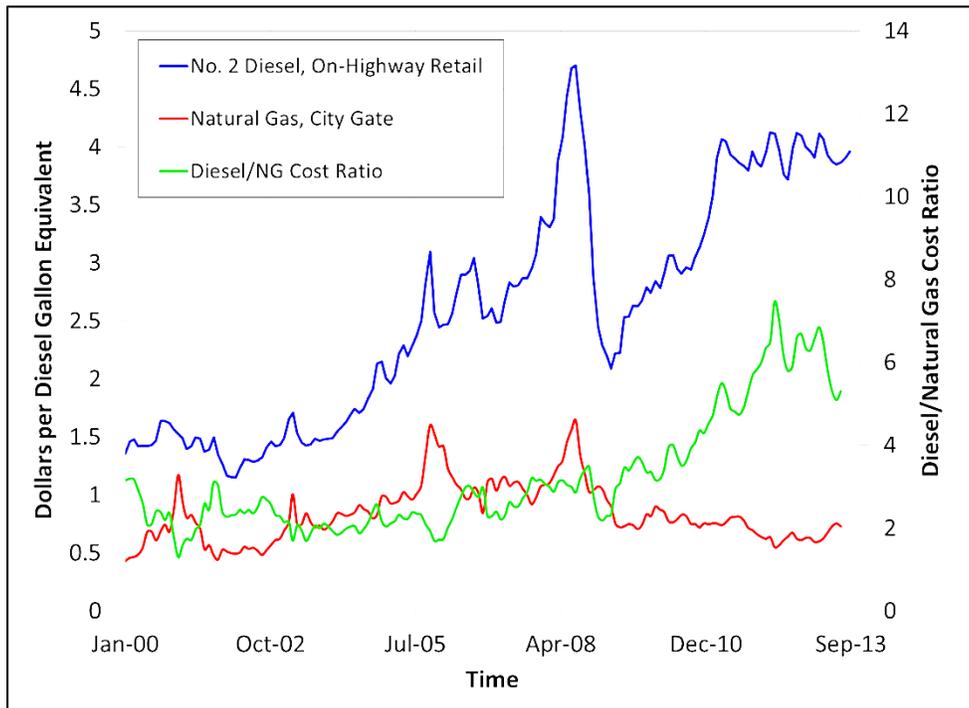
Figure 1.4: Diesel fuel and natural gas price comparisons (6)

1.3   Gaseous Fuels in CI Engines

There have been many published studies on the use of gaseous fuels in CI engines such as biogas, producer gas, natural gas and liquefied petroleum gas (LPG). These fuels vary in chemical composition, which has a significant impact on engine emissions and performance. Therefore, the choice of fuel is important.

Biogas is also known as swamp gas, sewer gas, fuel gas, marsh gas and wet gas. It is produced by fermenting organic material in absence of air with the help of bacteria to break the materials to intermediates such as alcohols and fatty acids and finally to methane, carbon dioxide and water. The process is called anaerobic fermentation (10). The main components of biogas are methane and carbon dioxide (CO_2) (11). Biogas has a high octane number and auto ignition temperature which makes it suitable for CI engines. When it is used in diesel engines as a primary fuel, it reduces NO_x and PM emission level and increases premixed combustion. However, it has negative effects on engine performance and HC and CO emissions due to longer ignition delay and poor flame propagation of the gaseous fuel-air mixture, especially at part load (12). The presence of CO_2 in biogas reduces the burning velocity and peak pressure inside the cylinder, which leads to a decrease in maximum power (13). And since biogas composition varies depending on the origin of the anaerobic fermentation process (14), varying heating values of biogas could be problematic in this engine where a larger amount of biogas is required to displace diesel fuel.

Producer gas, also known as syngas, in dual fuel applications is reported to lead to power loss due to lower heating value of the combustible mixture (15). In one case the power de-rating of engine was between 20-30% (16) attributing to the fact that the producer gas is a low energy density fuel when compared to natural gas. This fuel also has negative impacts on engine

efficiency and CO emissions with longer ignition delay (17). The fuel is not readily available; a gasifier where solid material is turned into producer gas is needed to continuously supply the fuel to the engine.

LPG is known as auto gas and is composed of a mixture of propane and butane. When LPG used in diesel engines, it produces substantially less CO and NO_x emission as well as a smaller percentage of CO_2 (18). LPG is described as a high octane number and a low cetane number fuel. This characteristic makes it suitable to be used in SI engines but difficult to self-ignite in conventional compression ignition engine. If LPG is to be used as alternative fuel to diesel fuel, the addition of cetane enhancer can improve the auto ignition characteristic and achieve stable engine operation (19) (20). LPG as a secondary fuel in diesel engines use a fumigation approach where the LPG fuel is inducted to the intake air stream using a low pressure injector (21). Using this approach along with diesel as a pilot fuel produced a low power output and lower thermal efficiency than pure methane and natural gas due to its tendency to self-ignite earlier. The combustion noise in the cylinder is reported the highest among those fuels (8). With LPG fumigated into compression ignition engines, nitric oxide (NO) and PM decrease, but significant increases in CO and HC emissions occur (22). One way to improve the performance of this fuel is to mix LPG with hydrogen   in a ratio of 70:30 (23) (24). When this mixture is used as a secondary fuel in diesel engines it increases the brake thermal efficiency and reduces HC emission. It also increases the maximum pressure rise rate, heat release rate, and peak cylinder pressure as well as reduces the combustion duration.

Interest in natural gas replacement of diesel fuel in compression ignition engines have substantially increased in recent years. Natural gas in dual fuel engines produce high output torque and a better thermal efficiency compared to LPG due to a larger heating value (8). It also

helps to reduce the NO_x emissions by lowering the charge temperature, which reduces the NO_x formation (25) (26). Methane is the main component in natural gas and has a high octane number, greater than 120, which makes it knock resistant and suitable for high compression ratio engines. Natural gas is favorable because it contains minimal impurities such as sulfur and when used with diesel as a dual fuel engine, tends to reduce PM compared to conventional diesel engines (27) (28).

The natural gas composition varies based on geographic location and the processing of the gas as shown in Table 1.2. Typically natural gas contains methane, ranging between 85-95%, and a small percentage of ethane and propane.

The natural gas that is stored at high pressure is called compressed natural gas (CNG) and as a sub-cooled liquid is call liquefied natural gas (LNG). If CNG or LNG is to be used in fumigated diesel engines, a pressure regulator is required to bring down the pressure to a more sufficient level.

Among these alternative fuels, natural gas is considered very promising as a primary fuel in dual-fuel mode (29). It is abundant, low cost and reduces emissions of both NO_x and PM. In this research, natural gas is provided by the city supply network and the composition varies slightly at each point (30).

Table 1.2: Variations of pipeline quality natural gas compositions from around the world (31)

Origin	Methane %	Ethane %	Propane %	Butane %	Nitrogen %
Malaysia	89.8	5.2	3.3	1.4	0.3
Qatar	89.9	6.0	2.2	1.5	0.4
Australia	89.3	7.1	2.5	1.0	0.1
USA	94.0	3.14	0.45	0.11	1.0

1.4   Natural Gas

The natural gas contains a mixture of methane, ethane, propane, butanes, pentanes and other hydrocarbons. It is formed from decayed animals and plants million years ago, built up in thick layers and trapped beneath the surface of the earth. Over time, intense heat and pressure changed these fossils into black oils, coals and natural gases. Natural gas is extracted from the underground formation through a well with other liquid hydrocarbons and non-hydrocarbons, which later are filtered from these components and sent through pipelines for distribution.

Technology advances have enabled the domestic energy production to rapidly grow in Canada, China, Netherlands, Poland, Germany and the USA (32). The developments of horizontal drilling and hydraulic fracturing technologies have improved the exploration of natural gas from shale reservoirs. Shale gas, which is a natural gas that is trapped within the shale formations, has become the fastest growing source of natural gas in the USA. In the USA, at least 2 million wells of oil and shale gas have been hydraulically fractured since 1860. Today 95% of new wells are hydraulically fractured which accounts for more than 43% of total U.S. oil production and 67% of natural gas production (33).

Even though natural gas fumigated CI engines can reduce the NO_x and PM emissions, it is also observed that CO and HC emissions were higher especially at part load compared to conventional diesel engine (34) (26). The combustion in natural gas fumigated diesel engines is slower at part load but improved at higher load. This way of reducing pollution from diesel exhaust emissions is becoming more common. A diesel engine fumigated with natural gas is called a diesel derivative dual fuel engine.

1.5   Engine Cycles

The dual fuel system is a retrofit to the CI engine. The dual fuel engine works using a CI engine but operates on a combustion process with characteristics from both SI and CI engines. To illustrate the process of the SI and CI engine operating cycle, a pressure-volume (p-V) diagram associated with an ideal air-standard cycle is considered. A heat addition term is used to replace the combustion process since air alone cannot combust. The Otto cycle is the ideal air cycle for the SI engine which is differs from the actual cycle. The cycle is divided into intake, compression, combustion, expansion and exhaust processes. Figure 1.5 shows the pressure-volume diagram for the Otto cycle. This cycle consists of an isentropic compression process 1-2, which compresses the mixture of air and gas and brings the piston to top dead center (TDC), a constant volume heat addition process 2-3 which raises the temperature of the mixture at constant volume to point 3, an isentropic expansion process 3-4 to the bottom dead center (BDC), and constant volume heat rejection 4-1.
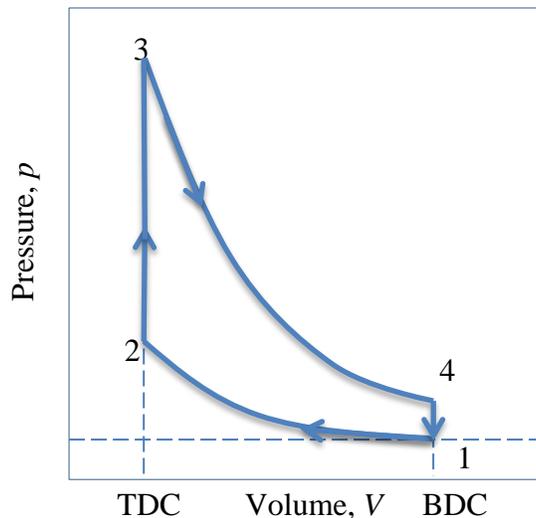
Figure 1.5: Otto Cycle p-V diagram (3)

The working processes for Diesel cycle is presented in Figure 1.6. The processes for this cycle are isentropic compression 1-2, constant pressure heat addition 2-3, isentropic expansion 3-4, and constant volume heat rejection 4-1. All processes are the same as the Otto cycle except the heat addition process 2-3.

The dual cycle contains features of both Otto and Diesel cycles. This can be considered a model for dual fuel combustion since it contains features of the ideal cycle for the SI engine (Otto cycle) and the ideal cycle for the CI engine (Diesel cycle). The process of Dual cycle is illustrated in Figure 1.7. The isentropic compression process 1-2, the isentropic expansion process 4-5, and the constant volume heat rejection process 5-1 are the same as in the Otto and Diesel cycles with different numbering of states. The heat addition process is different for the dual cycle. The heat addition process is composed of a dual mechanism, which is where the dual cycle name comes from. Heat addition consists of constant volume heat addition 2-3 followed by constant pressure heat addition 3-4.

Comparing the Otto, Diesel and Dual cycles at the same inlet conditions and compression ratio (CR) shows that Otto has the highest work output and thermal efficiency (η_t), while Diesel has the lowest.

$$(\eta_t)_{OTTO} > (\eta_t)_{DUAL} > (\eta_t)_{DIESEL}$$

However, since CI engines have much higher CR values than SI engines, CI engines typically have higher efficiencies than SI engines.

$$(\eta_t)_{DIESEL} > (\eta_t)_{DUAL} > (\eta_t)_{OTTO}$$

From these concepts, it is suggested that the most efficient engine would have combustion close to constant volume as in the Otto cycle but operates at high compression ratios as with the Diesel cycle (1).
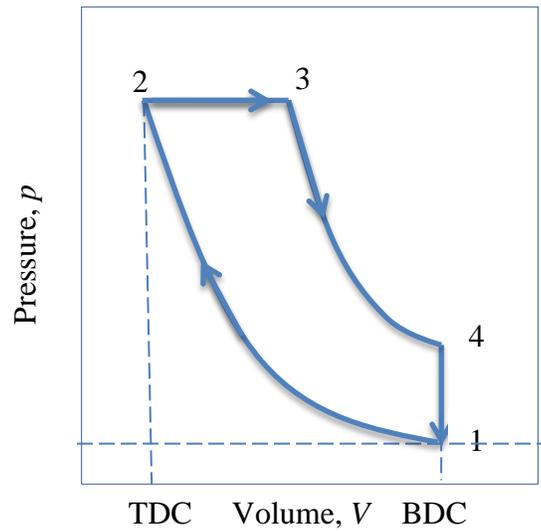
Figure 1.6: Diesel cycle *p-V* diagram (3)
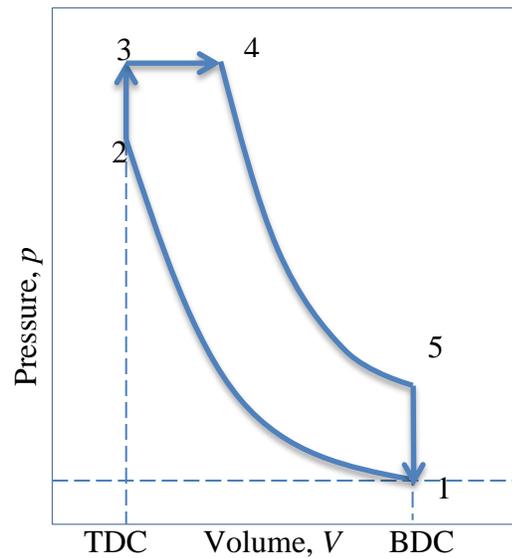
Figure 1.7: Dual cycle *p-V* diagram (3)

1.6   Dual Fuel Operation

The basic operation of dual fuel engines is shown in Figure 1.8. In the dual fuel engine, natural gas is fumigated with air in the intake stream by a venturi installed before the turbocharger. Natural gas flow is controlled by a throttle. The amount of natural gas admitted into the intake air stream is dependent on the engine load and speed. The mixture is compressed and a small amount of diesel fuel is injected near the end of compression stroke to initiate combustion. No modifications are made to the internal workings of the engine or the diesel injection system. The natural gas will displace some of the diesel required to run the engine, decreasing diesel fuel consumption for the same power output (30).
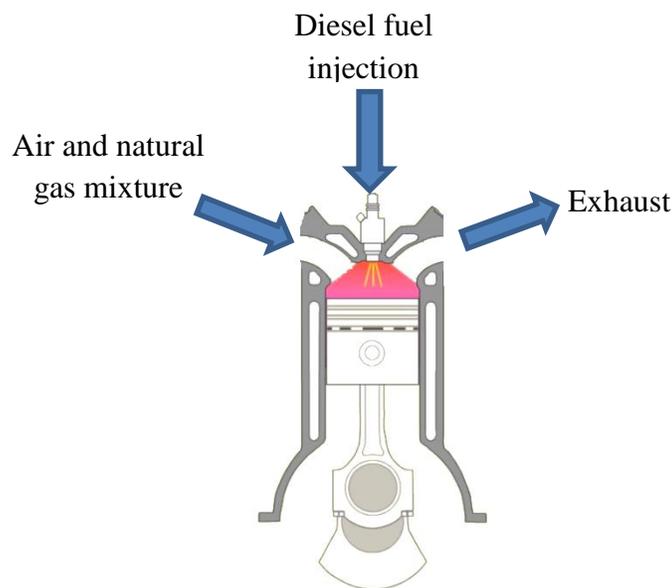
Figure 1.8: Basic dual fuel operation

1.7   Dual Fuel Advantages and Applications

The major advantages of the dual fuel natural gas-diesel engine are reduced NO_x and PM emissions as well as reduced fuel cost due to substantially lower cost of natural gas compared to

diesel. Other potential advantages are increased thermal efficiency, which is load dependent, and reduced fuel transport impacts if natural gas is available locally. The maintenance cost after the conversion will not increase as the majority of the engine parts remain unchanged. Since a significant amount of diesel is displaced by natural gas, up to 70%, carbonization is reduced in the dual fuel engine. Therefore, the number of times the engine needs to be de-carbonized and overhauled is reduced (35). In the dual fuel natural gas-diesel engine, the transitions between diesel and dual fuel modes can be achieved while the engine is running without any interruption to the required engine load. If natural gas is not available, the control valve will be shut off and the engine continues on diesel fuel as a conventional diesel engine.

The dual fuel system is offered by several manufacturers such as Solaris, Green Fuel Pro, Altronic, Hythane and Landi Renzo USA. The cost for a complete dual fuel system by Green Fuel Pro ranges from $30,000 to $35,000 for heavy duty engine. Lower natural gas fuel costs (about half of diesel cost) help pay for a conversion.

The application of diesel engines employing natural gas ranges from on-site power production to transportation vehicles. Various cities in the USA have been implementing the dual fuel engine in trucks and heavy duty tractors as shown in Figure 1.9. Dual fuel technology has also been used in land-based oil, well-drilling and fracking applications itself. Dual fuel is implemented on the engines that drive the hydraulic fracturing pumps, normally run on 100% diesel. This reduces the truck traffic by requiring that less diesel be trucked in to run the hydraulic fracturing trucks. By applying dual fuel engines in tanker trucks and using natural gas near the well site, truck traffic and fuel cost can be saved tremendously.

In addition, the natural gas from the formation is also useful to power the high pressure pump and diesel engine in the fracturing trunks. Figure 1.10 shows a hydraulic fracturing truck

15

and Figure 1.11 shows a well pad site with fracturing pumps that can be implemented with dual fuel engine.

Figure 1.9: A diesel truck running on CNG and diesel. Conversion kit by Landi Renzo USA
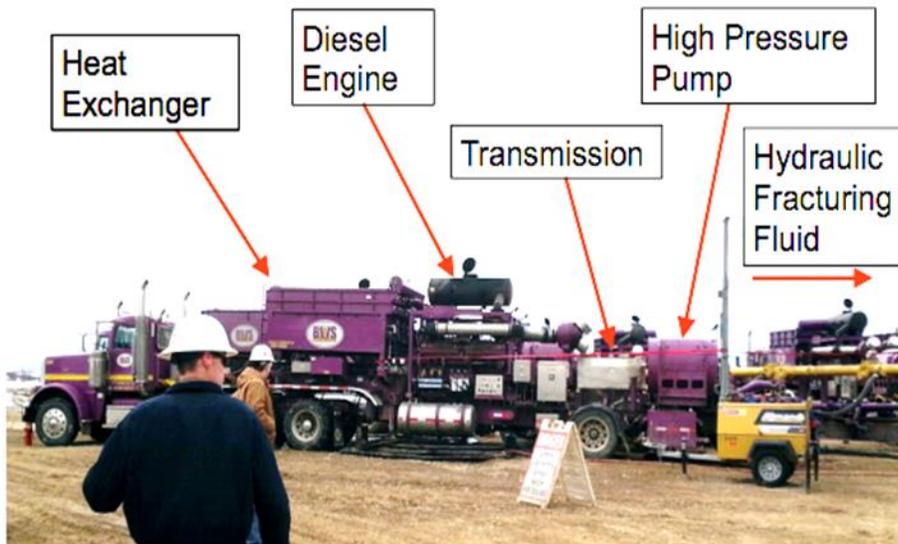
Figure 1.10: Potential fuel cost saving in equipment of a fracking truck
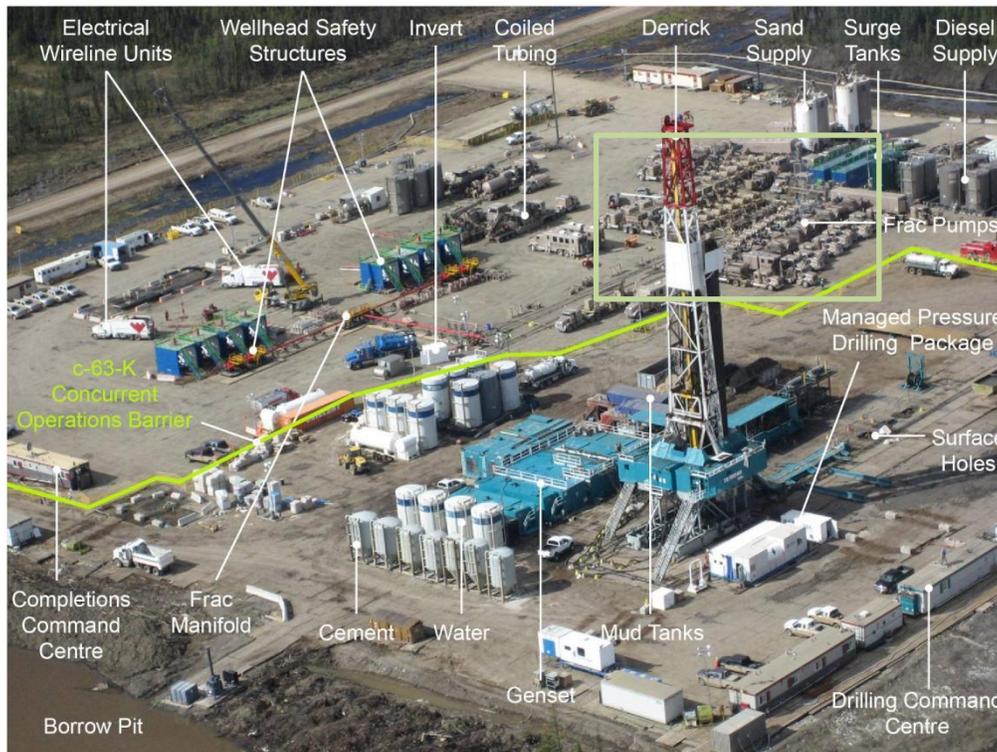
Figure 1.11: An example of a well pad site with fracturing pumps, another dual fuel application

1.8   Problem Statement and Research Objectives

Higher fuel costs and increasingly stringent emission regulations are concerns for manufacturers and operators of compression ignition engines. By converting the CI unit to dual fuel operation and utilizing lower cost natural gas, both lower fuel costs and lower emissions can be achieved. However, the cost savings through diesel displacement and emission reductions need to be quantified.   Thus, the main purpose of this research is to address the challenges associated with dual fuel engines in order to improve efficiency and to obtain better control of the exhaust emissions. Since dual fuel engines produce higher HC and CO emissions than regulations allow, concepts should be developed to advantageously control combustion and emissions. In addition, in-cylinder combustion is very complex. While experimental data are able

to approximate in-cylinder combustion, parameters such as temperature field, air fuel ratio distributions and emission locations are not understood completely using experimental data. Therefore, the detail analysis of combustion is one of the most important key factors to determine engine's efficiency. Consequently, a computational fluid dynamics (CFD) is proven to be an efficient tool to predict combustion events and emission formation inside the cylinder. Therefore, the primary challenges of this research and hypotheses to the questions are as follows:

1) Does dual fuel operation save cost compared to diesel operation?

Hypothesis: Over the past five years, natural gas fuel prices have remained well below that of diesel fuel and have been more consistent compared to diesel fuel. When natural gas is introduced in diesel engine, it should displace some of the diesel fuel in CI engine, therefore reduce the fuel cost in dual fuel engine.

2) Do dual fuel engines reduce NO_x and PM emission compared to diesel engines?

Hypothesis: Being a lowest member in paraffin family, the diesel combustion with natural gas in dual fuel engine is expected to produce less PM. In addition, since the premixed combustion happens, the opportunity for locally rich mixtures to form is reduced. Therefore, with lean conditions, the flame temperature should be lower, thus reducing the NO_x formation in a dual fuel engine.

3) Do dual fuel engines emit excessive HC and CO?

Hypothesis: The ratio for the natural gas and air entering the cylinder is not controlled. It is speculated that at these load conditions, the natural gas air mixture is below the flammability limit in the cylinder and the penetration of the diesel fuel jet does not extend across the cylinder. Consequently, regions near the edge of the combustion chamber with natural gas

and air mixtures below the flammability limit are either unburned (HC emission) or partially

burned (CO emission).

Given the problem statement above, the research objectives are as follows:

1) To evaluate the emissions and performance of a dual fuel engine and compare the results with the diesel equivalent.

2) To develop an emissions control methodology in order to maintain applicable regulatory standards on emissions levels.

3) To investigate in-cylinder combustion by implementing the CFD simulation using CONVERGE code with a reduced chemical-kinetic mechanism for time saving. The location where the emission is formed will be investigated as well.

1.9   Thesis Outline

An overview of previous research is presented in chapter two. Chapter two begins with a dual fuel combustion description followed by emissions trends. Comparison with conventional diesel engine is carried out where applicable. Chapter three describes the experimental procedure and data analysis method used in this research. Chapter four discusses the results of the experimental and modeling study. A detailed discussion is presented at five loads comparing diesel and dual fuel engines in the experimental section and the development of the flow, heat transfer and combustion phenomena in the modeling section. Chapter five discusses a CFD technique for internal combustion engine simulations and describes the state of the art sub-models used in this research. Chapter six discusses the CFD results on combustion and emission location in dual fuel engine. Conclusions of this research and future perspectives are presented in Chapter seven.

2.0   LITERATURE REVIEW

2.1   Natural Gas

Natural gas has been known for many centuries. It was first found by the people of Mount Parnassus in ancient Greece (36). Around 500 B.C., it is known that the Chinese started using natural gas that seeped to the surface to boil sea water for drinking water. The first usage of commercial natural gas was in Britain in the 1780s, where gas derived from coal or coal gas was used for powering houses and streets. In the USA, Natural gas was discovered in the 1620s when natives were sighted by French explorers igniting gases that seeped into and around Lake Erie. Centuries later in 1821, the first well was dug by William Hart in Fredonia, New York; Fredonia Gas Light later became the first American Natural gas distribution company in the USA.

During most of the 19th century, Natural gas was used almost exclusively as a source of light, but the invention of the Bunsen burner by Robert Bunsen in 1885 opened new opportunities to use Natural gas. Since then, Natural gas applications have expanded to home appliances such as stoves, clothes dryers, and furnaces and industrial applications such as engines for electrical power generation, pumping, and compression and boilers for process heating.

2.2   Dual Fuel Background

The discovery of the dual fuel engine is credited to Cave in 1929 and Helmore et al. in 1930 when hydrogen fuel was introduced as a supplementary fuel in diesel engines (37). However, at that time, dual fuel had limitations which made it less popular for commercialization. The challenges included mechanical complexity, expensive components, large inefficiencies, and significant knocking. Serious attention to dual fuel began during the

Second World War when petroleum supplies were lacking, leading to new technology exploration including the dual fuel engine. In their early days, many dual fuel engines, especially heavy-duty engines, ran on waste gas from the oil industry or sewage gas from sewage treatment plants (38).

After the war, the market returned to fuel oil because of environmental concerns associated with coal and the large supply of very inexpensive oil from Saud Arabia. This enabled the petroleum gas industry to expand and many gas transport companies started to increase production and expand pipeline systems during this time.

In recent engines, the development of dual fuel technology is motivated by emissions regulations which require specific limits be met for pollutants released into the atmosphere. Development is also motivated by the potential savings on operations costs for dual fuel engines compared to diesel engines. For these reasons, many diesel engines are converted to run with gaseous fuels such as natural gas and retain positive features of diesel operation. Natural gas is preferred because it is cheap and widely available. It is also shown to reduce emission problems in diesel engines.

2.3   Diesel Engine

The combustion process of a diesel engine starts when fuel is injected into the cylinder at the end of compression stroke. During the compression stroke, pure air is compressed with a high compression ratio, heating the gas above the diesel self-ignition temperature. A small amount of diesel fuel is injected and ignited in the high temperature air. Just after the ignition and before the combustion occurs, a short ignition delay exists followed by a sudden and rapid rise in cylinder pressure known as the premixed combustion phase. (Heywood, 1988) Heywood summarized four stages of the CI diesel combustion on the typical heat-release diagram in Figure

2.1 and the in-cylinder pressure diagram, p-θ in Figure 2.2. The AB phase is the ignition delay period. This ignition delay is determined from the change in slope on the p-θ diagram. This data is from a pump-line-injector mechanical system, as opposed to a high pressure common rail system. The BC phase is described as a premixed or rapid combustion phase. In this phase, the heat release rate has a high peak because the burning mixture is premixed. The burning mixture is composed of the injected fuel at the start of injection (SOI), which has mixed with surrounding air to within the flammability limits during period AB. The premixed portion of the charge undergoes rapid combustion. This phase is often referred to as chemically controlled combustion.

Period CD is the combustion phase where the heat release rate is controlled by the rate of mixing, termed mixing controlled combustion. At the end of combustion phase DE, during the expansion stroke, the heat release rate becomes slower. This happens as the temperature of the cylinder gases drop during this part of the stroke.
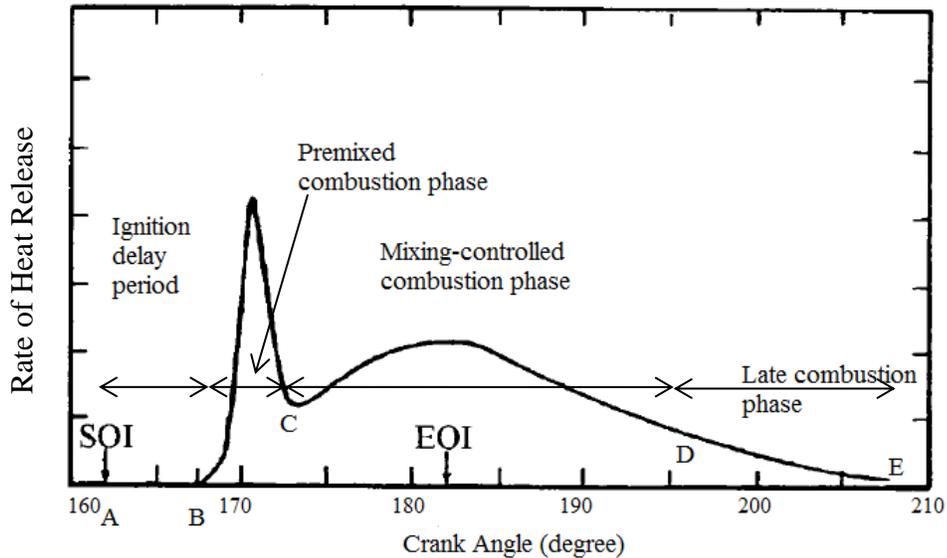
Figure 2.1: Diesel combustion stages by Heywood (3)
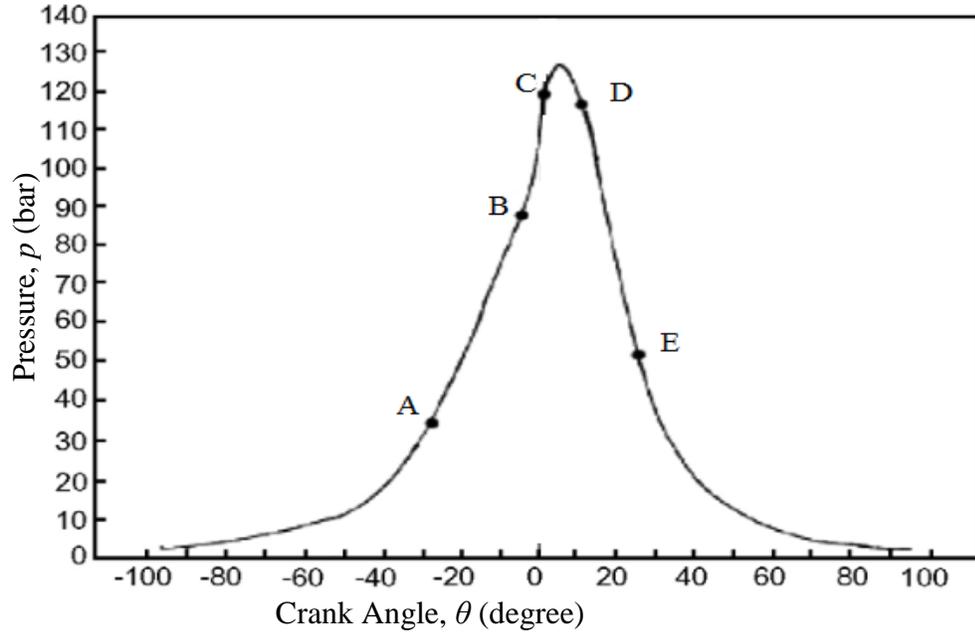
Figure 2.2: Cylinder pressure, p of a conventional diesel engine (3)

There are several forms of diesel emissions that are created during the combustion process, primarily PM, NO_x, CO, and HC. The PM is generated in fuel-rich zones where there is insufficient oxygen to oxidize all carbon to CO_2.

$$C(s) \quad + \quad O_2 \quad \rightarrow \quad CO_2$$
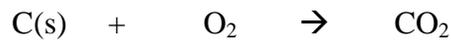
Equation 2.1

In diesel engines, 90% of carbon particles that are originally generated early in the combustion process are consumed later in the end of the combustion and power stroke (1).

Exhaust gases of diesel engines also contain NO_x emissions, primarily NO, with lower levels of NO_2 and other nitrogen-oxygen combinations. NO_x emissions do not form until the cylinder charge temperature reaches about 2800°F (1540 °C) as shown in Figure 2.3. For premixed SI engines, HC emissions have a direct relation with Φ as shown in Figure 2.4 (for

23

premixed SI engines). HC emissions are significant at richer conditions when there is not enough

oxygen to react with the excess fuel, resulting in a high concentration of HC emissions in the

exhaust products. HC emissions are also significant at low load when the mixture is too lean to

burn and the flame is quenched, leaving some fuel particles unreacted.
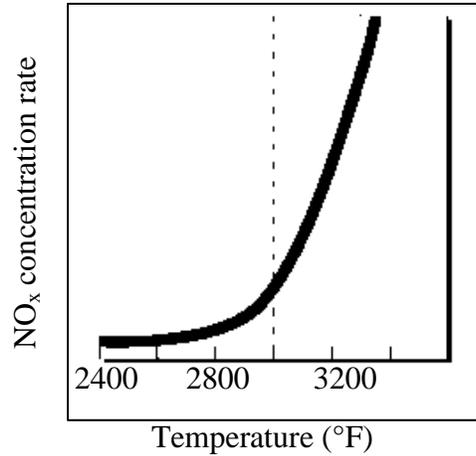
Figure 2.3: The formation of NO_x as a function of temperature (39)
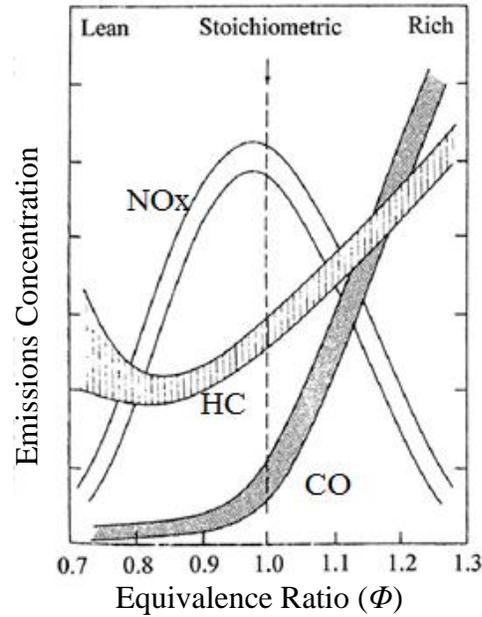
Figure 2.4: NO_x, CO and HC missions as a function of equivalence ratio (1)

2.4   Dual Fuel Operation

In dual fuel operation, combustion ideally consists of a diesel fuel flame progressing through a lean premixed air and gaseous fuel mixture which is locally homogenous. The premixed air and gaseous fuel burn in the presence of the diesel flame and a premixed flame is initiated by the diesel flame and propagates through the remaining air and gaseous fuel mixture. During the compression stroke, the premixed mixture's temperature and pressure is greatly increased, forming the pre-ignition reaction environment. During this phase, partial oxidation products can form at the end of compression to induce diesel fuel ignition and combustion. The spread of the diesel flame front is greatly influenced by turbulence, swirl, and squish within the cylinder.

(Nwafor, 2001) The combustion process of a dual fuel engine is described by Nwafor with five stages. The data is taken on a single cylinder pre-chamber diesel engine with a pump-line-injector mechanical diesel injection system. The combustion phases of a dual fuel engine are illustrated with a cylinder pressure trace in Figure 2.5. After diesel fuel is injected at point A, a longer ignition delay period AB is observed in dual fuel combustion than in conventional diesel engines due to the reduction in oxygen concentration resulting from the introduction of natural gas to the intake charge. The premixed combustion phase BC in dual fuel is slower compared to conventional diesel premixed combustion. This is because the dual fuel engine is injecting a smaller amount of liquid fuel, therefore a smaller amount of burning mixture is added to the fuel. Period CD shows a decrease in pressure until it rises at period DE. Period CD is described as the primary fuel (premixed air and natural gas fuel) delay period. The DE phase is the actual combustion of the natural gas fuel starting with the flame propagation initiated by the spontaneous liquid fuel ignition. Nwafor described the period EF as a diffusion combustion

stage starting at the end of gaseous fuel combustion. It is unclear why this phase of combustion is characterized as diffusion combustion. It may be more appropriate to characterize it as the late combustion phase.
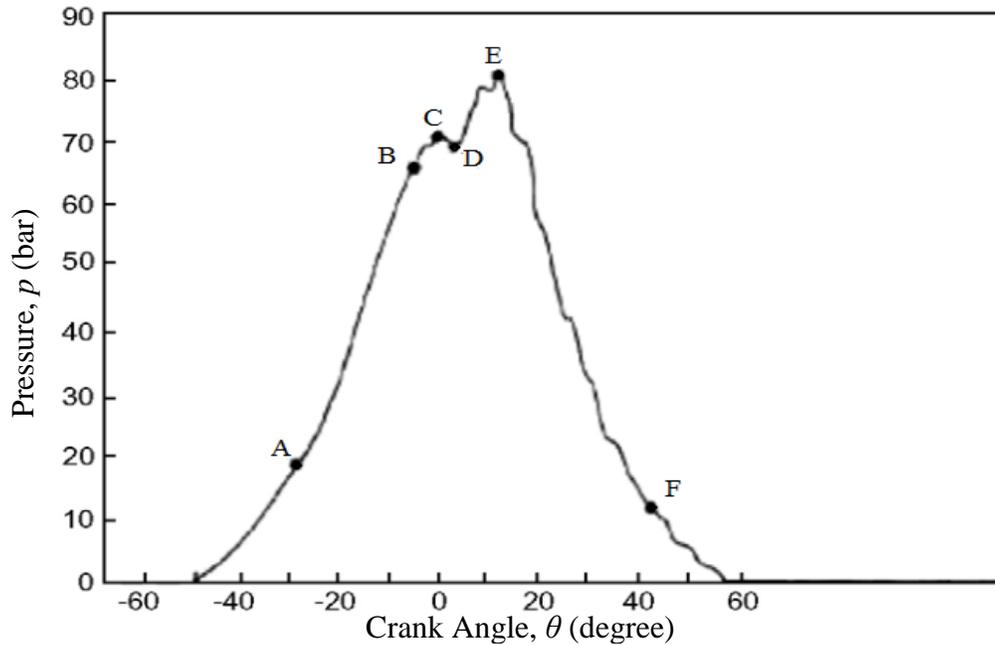
Figure 2.5: Combustion process of a dual fuel engine

(Rajput, 2005) In diesel engines, higher peak cylinder pressures are observed compared to dual fuel engines. This is due to the CR being not knock-limited ratio in CI dual fuel engine, while the CR value of SI and dual fuel engines are knock limited. The conventional diesel engine uses a heterogeneous mixture, where the cylinder charge is pure air. The mixture undergoes a non-premixed, or diffusion flame, combustion process except when rapid premixed combustion occurs (period BC in Figure 2.1 and Figure 2.2). In the diesel engine, the ignition starts at several points in the chamber where a local stoichiometric air/fuel ratio (AF) is formed, regardless of the overall AF in the cylinder. On the other hand, in the dual fuel engine the primary fuel

combustion is homogeneous (premixed). The cylinder charge is a mixture of air and natural gas and ignited by the injection of diesel fuel. It is characterized as non-premixed combustion of diesel fuel, followed by premixed combustion of the natural gas. The premixed combustion is very sensitive to AF; therefore, in lean combustion as observed in dual fuel engines the in-cylinder pressure has a lower peak value.

Since the dual fuel operates at lean mixtures, the flame temperature is lowered, therefore reducing the formation of NO_x. Other factors that affect the formation of NO_x in dual fuel engines are the quantity of gaseous fuel and Φ of the air-fuel mixture (1). The effect of Φ on emissions is shown in Figure 2.4. This figure is specific to SI engines but the general trends are similar for CI and dual fuel engines. This figure shows that maximum NO_x is formed at slightly lean conditions, around $\Phi = 0.95$. As the mixture goes leaner, increasing excess air concentration reduces the gas temperature. At low temperature, atmospheric nitrogen is a stable diatomic molecule (N_2) and less oxides of nitrogen are produced. In contrast, at high temperatures some of N_2 breaks down to reactive monotonic nitrogen radicals (3). At high temperatures with excess oxygen available oxygen can combine with the nitrogen to form nitric oxide:

$$O \quad + \quad N_2 \quad \rightarrow \quad NO \quad + \quad N$$

$$N \quad + \quad O_2 \quad \rightarrow \quad NO \quad + \quad O$$
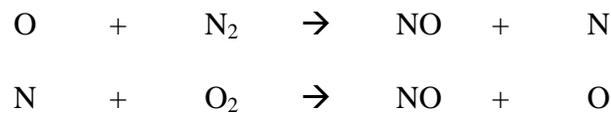
Oxygen radicals (O) are produced from the dissociation of oxygen molecules (O_2) or from a collision between the H radical and O_2. These oxygen radicals combine with N_2 to start the simple chain shown, called the Zeldovich mechanism. Nitric oxide can further oxidize to form NO_2. In order to minimize NO_x formation in ICEs, reducing flame temperature is crucial, which slows the reaction rates in the Zeldovich mechanism.

There are substantial numbers of studies investigating emissions from dual fuel engines. (Uma et al., 2004) Uma and associates published a paper on their study on a turbo-charged CI engine with producer gas. They mentioned that the presence of gaseous fuels in dual fuel operation reduces the amount of diffusion combustion and replaces it with lean premixed combustion, which affects the rate of NO_x formation. This statement is supported by Lounici et al. in their study using single cylinder, naturally aspirated Lister Petter-TS1 diesel engine (Lounici et al., 2014). However, the NO_x formation at high load is lower for the diesel engine as shown in Figure 2.6. The author of this study attributes this to the combustion of liquid fuel near TDC creating a high charge temperature which remains at a high temperature longer in gas-diesel dual fuel engine than in the diesel case.

Figure 2.7 compares CO and HC emissions for diesel and dual fuel by Lounici et al. at 2000 rpm. The data shows extremely lower CO emissions for the dual fuel case at high load, while HC emissions are significantly higher in the dual fuel case.
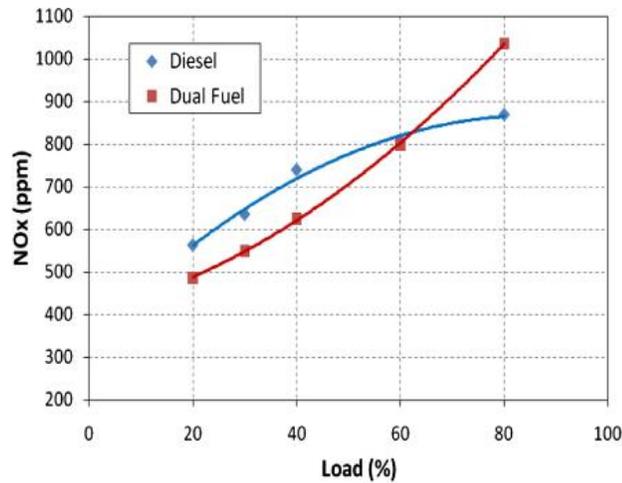
Figure 2.6: Variations of NO_x as a function of load (40)
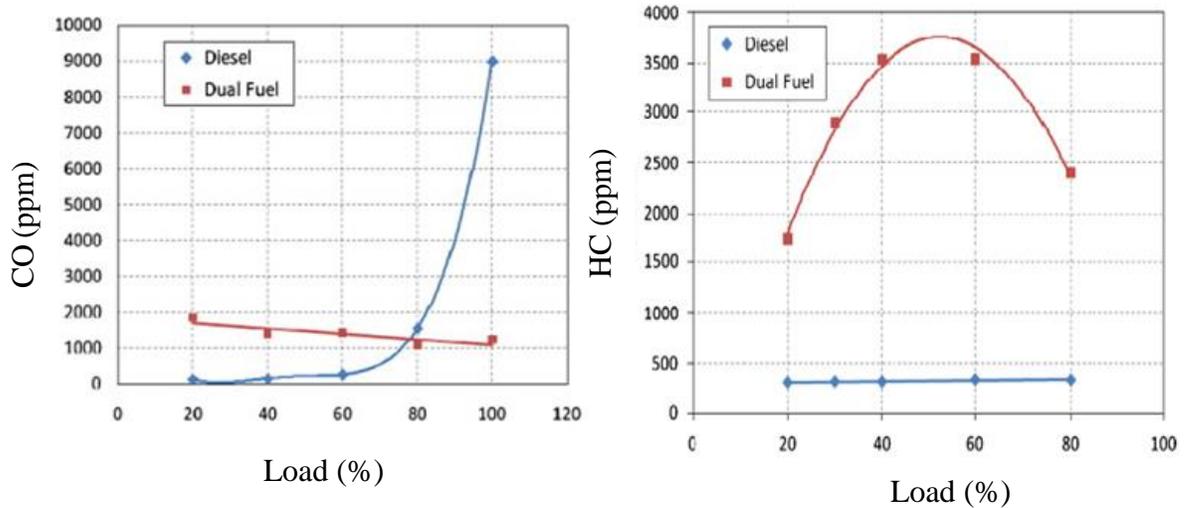
Figure 2.7: HC and CO emissions as a function of load and type of fuel (40)

(Namasivayam et al., 2009) HC emissions trend higher at all conditions in the dual fuel natural gas-diesel engine. This is consistent with the data in Figure 2.7. It is theorized that HC emissions are substantially higher because natural gas survives through the combustion process and ends up in the exhaust gas stream. Flame quenching at the wall and very lean mixtures also result in high levels of HC emissions.

(Bueno et al., 2012) Another important parameter in determining an engine's performance is the heat release rate (HRR) calculation. The net HRR is calculated by computing the amount of energy release from the fuel to obtain the experimentally observed pressure, while the combustion reaction extent is evaluated through the released fraction of the total fuel chemical energy. (Abdelaal et al., 2012) Abdelaal et al. in their study using naturally aspirated diesel engine, describe that longer ignition delays in the dual fuel engine have a negative impact on the HRR. Generally, the diesel engine exhibits better HRR trends than the dual fuel engine. In the diesel engine, a large amount of diesel is utilized especially at high load resulting in high in-

29

cylinder temperatures. The reduced HRR in dual fuel operation is mainly due to the very lean mixture of air and gaseous fuels. This affects the combustion in dual fuel; a portion of natural gas usually escapes the combustion process resulting in low combustion efficiency and high HC emissions.

Some experimental studies show similar trends in thermal efficiency between dual fuel and diesel operation and some observed lower efficiencies in dual fuel than diesel engines (41) (42). This suggests that the thermal efficiency comparison is dependent on engine design and operating conditions. (Papagiannakis et al., 2003) The authors identify that dual fuel experiences lower thermal efficiencies because of the reduced combustion duration, which also reduces cylinder charge temperature. This is exacerbated by very lean mixtures of air and gaseous fuels at low load. (Abdelaal et al., 2012) As previously mentioned, in their work using a naturally aspirated diesel engine, at part load some of the air and gaseous fuel mixture is burned but some escape from the combustion process due to valve overlap. Increased valve overlap at part load causes the intake charge to flow directly into the exhaust leading to poor combustion especially during idling. The authors also define better fuel utilization in dual fuel engine at high loads. This is due to larger amount of natural gas introduced leading to better combustion and higher brake thermal efficiency at high loads. In contrast, at high loads diesel engine combustion sees increment in heat loss to the cylinder wall, therefore negatively impacting the thermal efficiency. As a consequence, more power may be produced in dual fuel combustion.

Brake specific fuel consumption (bsfc) depends on CR and Φ (1). As mentioned earlier, Lounici and associates used a naturally aspirated diesel engine to investigate dual fuel engine performance at several engine speeds. Figure 2.8 compares dual fuel and diesel totsl bsfc at 2000

rpm. The authors conclude an improvement in total bsfc in conventional diesel engine at low load, but lower at high loads.
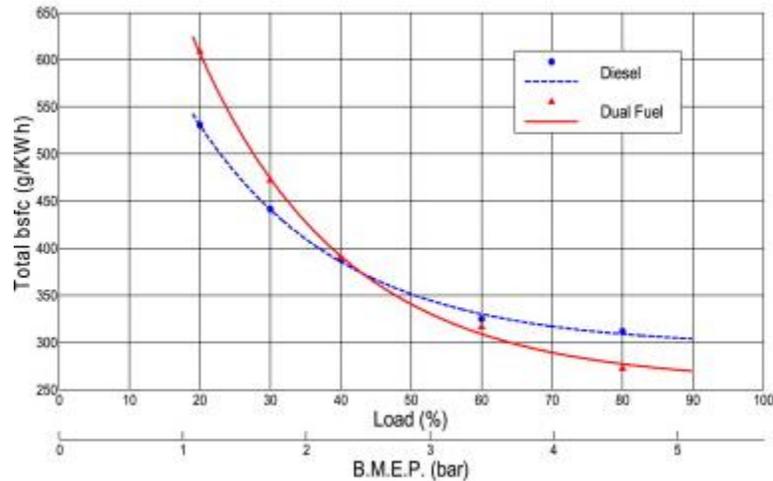
Figure 2.8: Brake specific fuel consumption variations (40)

2.5 Improving Performance and Emissions

Performance and emissions in dual fuel can be reduced by engine design and controlling operating parameters. The following parameters were studied by previous researchers in order to improve engine performance and efficiency, along with the reduction of HC, CO, and NO_x emissions at high load.

2.5.1 Fuel Injection Timing

(Sayin et al., 2009) Sayin et al. studied the effect of injection timing on dual fuel engine's performace and emission. The injection timing has a significant effect on the engine performance and emissions of CI engines. When injection timing is advanced, a large portion of fuel is burned during the latter part of the compression stroke. Consequently, more combustion occurs earlier which increases cylinder temperature and results in higher peak in-cylinder

31

pressure, occurring near TDC, as shown in Figure 2.9. Since advancing the injection timing results in high cylinder charge temperature, the formation of NO_x is also higher. If injection starts later, or is retarded, the peak pressure and cylinder temperature occur after TDC where the cylinder volume is larger. Retarding injection timing also continues to decrease ignition delays. Further retarding the injection timing past TDC leads to low in-cylinder temperature and energy losses resulting in low thermal efficiency and high bsfc.
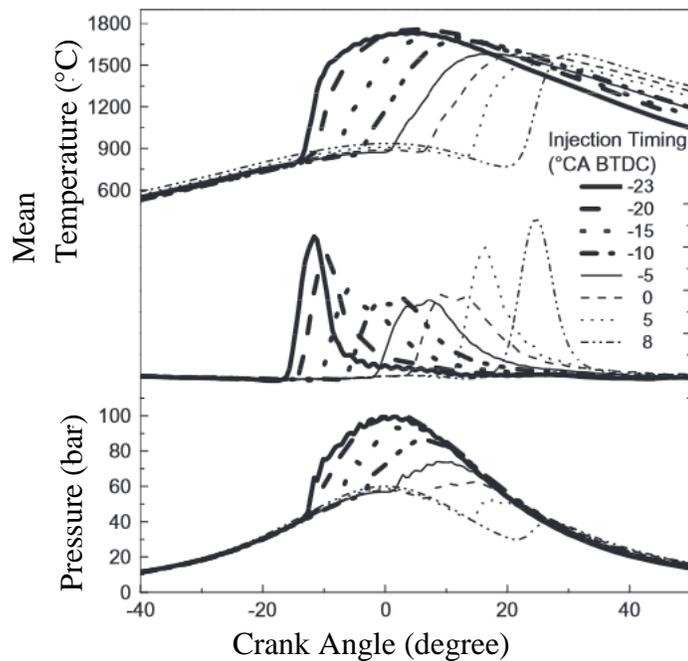
Figure 2.9: Effect of injection timing to in-cylinder pressure and mean temperature (43)

2.5.2   Pilot Fuel Quantity

(Sombatwong et al., 2013) Sombatwong et al. in their investigation using a naturally aspirated diesel engine describe quantity of pilot fuel as an important parameter for controlling the combustion process and emissions in a dual fuel engine. In this study using methane and diesel, the authors experimented on producer gas as primary fuel over diesel fuel. It is shown that

by increasing the amount of pilot fuel, in this case the diesel fuel, resulted in high in-cylinder temperatures due to the large energy release from diesel fuel. Larger amounts of diesel fuel also create a larger reaction zone with more ignition centers. Thus, the flame consumes the gaseous air fuel mixture in a shorter time. Figure 2.10 shows the impact of pilot fuel quantity on HC emissions. Improved combustion efficiency also decreases the CO emissions since the fuel is more completely burned. This is again due to a larger pilot fuel envelope being created thus increasing the burned fraction of the gaseous fuel and, subsequently, decreasing the products of partial combustion emitted in the exhaust. However, while CO and HCs are reduced, NO_x is more likely to increase).
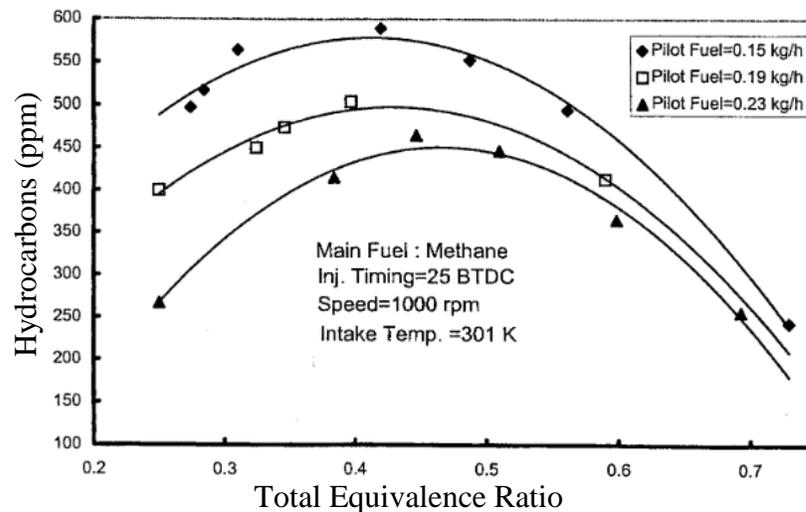
Figure 2.10: Unburned HC as a function of pilot fuel quantity and equivalence ratio (44)

2.5.3 Intake Manifold Temperature

(Krishnan et al., 2004) It is described that intake manifold temperature affects the performance and emissions of an engine. When the manifold temperature is increased to over 100°C, the mass burning rate during the flame propagation (period DE in Figure 2.5) is also

increased leading to more complete combustion at higher temperature. Improvements in bsfc are observed and HC and CO emissions are reduced; however, this comes with a moderate increase in NO_x emission.

2.5.4   Exhaust Gas Recirculation

(Selim, 2003) Low load conditions in dual fuel engines suffer low efficiency and higher emissions. By applying exhaust gas recirculation (EGR), the combustion improves and the efficiency increases. By re-circulating exhaust gas into the combustion chamber, active radicals in the exhaust gas enhance the pre-flame activities and the exhaust gases are re-burnt. (Hussain et al., 2012) NO_x emission is reduced substantially due to reduced oxygen concentration (some oxygen is displaced by EGR) and decreased flame temperature in the chamber. However, increasing the rate of EGR too high can deteriorate engine performance and result in increases in HC and CO emissions, even though doing so can further reduce NO_x formation. (Poonia et al., 1999) The addition of EGR along with increasing intake manifold temperature and pilot fuel quantity can improve brake thermal efficiency considerably, but these measures also increase ignition delay. At high load, no significant improvements on thermal efficiency or ignition delay are observed at any EGR ratio.

2.6   Dual Fuel Technology

An engine where diesel displacement occurs by introducing natural gas as a concurrently combusted fuel source is called a dual fuel engine. In a dual fuel engine with a conventional injection system, up to 86% substitution rate by energy is reported by Mbawara (45). The maximum diesel fuel displacement is limited by engine stability and knocking. Maximum diesel displacement varies according to the engine parameter, but usually takes place when the dual fuel engine runs at intermediate and high loads. In general, current displacement of diesel in dual

fuel engines with conventional diesel fuel injectors is 70% by energy at high load. Current manufacturers of OEM dual fuel engines for stationary applications are Cummins, Wärtsilä, Caterpillar,Waukesha, and Dresser-Rand Guascor.

Cummins Inc. produced Cummins Dual Fuel™ engines for land-based oil and gas drilling applications. Figure 2.11 shows their QSK50 dual fuel engine for well servicing. QSK50 engine power rating is up to 1864 kW (2500 hp). The QSK50 engine offers 30% reduction in NO_x and 65% reduction in PM to meet Tier 2 emission standard. The engine provides up to 70% substitution rates and is able to run solely on diesel fuel. Total fuel savings vary depending on the natural gas type used (CNG, LPG or field gas). Annual cost saving using CNG for a 2500hp pressure pumping engine is almost 20%.

Other than Cummins Inc., Dresser-Rand Group Inc. is among the largest supplier of oil and gas equipment. Guascor dual fuel engines by Dresser-Rand run on diesel and natural gas (Figure 2.12). The engine operation is based on diesel engine with maximum natural gas substitution rate of 85%. Engine maximum power rating is up to 768 kW (1029 hp). The diesel fuel is used to initiate combustion inside the cylinder.

Another technology in dual fuel engines is a micro-pilot injection system, where very little diesel fuel is injected to ignite the air-gas mixture. Micro-pilot technology is currently being developed by Clean Air Power under the project name MicroPilot™. It also has been developed by Colorado State University as a retrofit diesel pilot ignition system (46) (47). In a micro-pilot injection engine, only 1-2% of total fuel is diesel fuel injected to ignite a premixed mixture of air and natural gas. The 1-2% pilot fuel can provide ignition power more than 5000 times than a conventional SI system. The micro-pilot injector has a very small nozzle opening diameter to

accommodate the small percentage of diesel fuel injection. The micro-pilot injection engine is a natural gas SI engine with a small injection of diesel fuel acting as the spark plug.
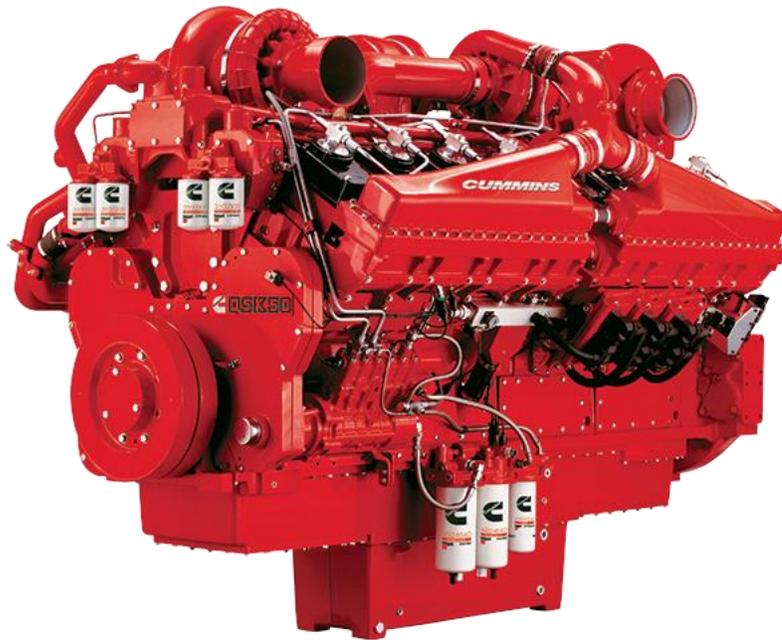
Figure 2.11: Cummins QSK50 Tier 2 well servicing applications (48)

Figure 2.12: Dresser-Rand Guascor dual fuel engine

3.0   EXPERIMENTAL SETUP AND TEST PLAN

The purpose of testing is to investigate performance and emission characteristics of the engine when it runs on a diesel and a dual fuel natural gas-diesel system. The first goal of this study is to examine the performance and emissions at different loads for both diesel and dual fuel operations. Then, the effect of diesel injection timing and diesel fuel displacement on dual fuel performance and emissions will be characterized. The gaseous fuel used in this experiment is natural gas supplied by the Fort Collins, CO city distribution system. Experimental results will serve as validation data for combustion modeling.

3.1   Experimental Apparatus

The engine used in this research is a John Deere diesel engine retrofitted with a dual fuel system. A photograph of the engine test setup is illustrated in Figure 3.1and the schematic of the system is shown in Figure 3.2. From the natural gas supply, the incoming gas first encounters two pressure regulators. The first regulator regulates the pressure to 5 psi and the second regulator reduces the pressure to approximately 2 psi. A gas filter is located in the gas train to remove any particulates from the gas stream, thus protecting the control valves and engine componentry. A gas shut-off solenoid valve is also included and is controlled by the programmable logic controller (PLC). It must be energized for the gas control valve to open. A zero-pressure regulator is located at the end of the gas train upstream of the control valve and mixer. This regulator maintains a small vacuum to draw gas into the mixer and to ensure proper air-fuel ratio is achieved, determined by the gas control valve position. This control valve is a Woodward L-Series Air/Fuel Ratio Control which provides precise air-fuel ratio control for engines. It is a microprocessor-based actuator with built-in speed control and internal fault detection. The valve is directly mounted to the mixer, which is located between the clean air

intake and turbocharger. The air-gas mixture is then fed to the turbocharger, which facilitates complete mixing of the natural gas with air before it is fumigated into the intake stream.

Figure 3.1: Engine test setup
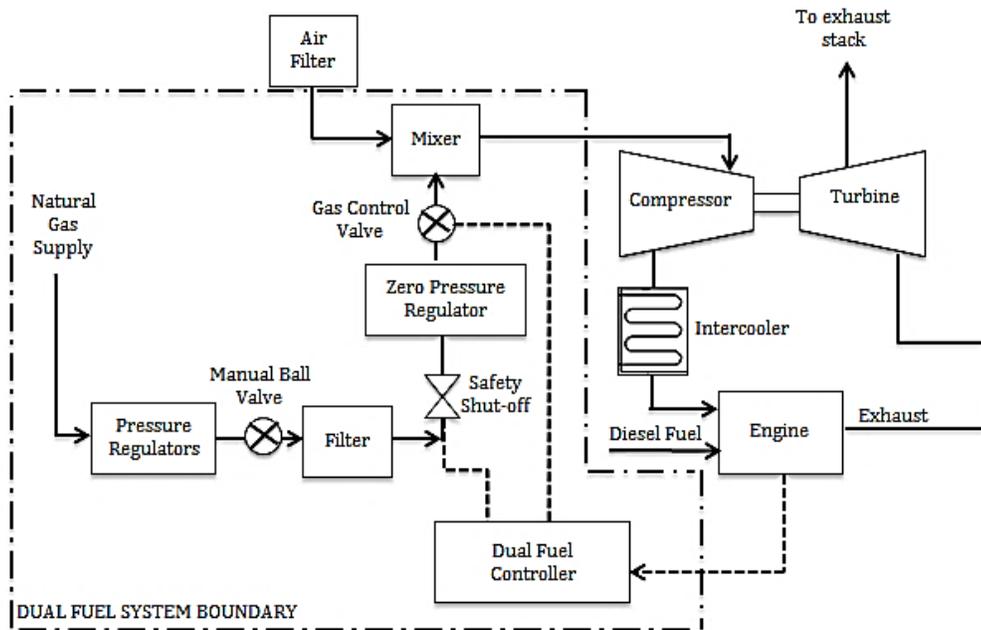
Figure 3.2: The schematic diagram of John Deere diesel engine with a dual fuel kit

The engine used is a 6-cylinder Tier II, 6.8 liter John Deere 6068H diesel engine with bowl-shaped pistons/combustion chambers. The basic specifications of the engine are presented in Table 3.1. It is equipped with a fixed geometry turbocharging system and a high-pressure common rail diesel fuel injection system. High diesel injection pressures at all engine speeds are supplied by using a high pressure pump and a pressure accumulator which provides high pressure fuel to the common rail. The engine is loaded with an AC motoring dynamometer with a maximum power of 300hp at maximum speed of 2800rpm. The dynamometer is manufactured by Marathon Electric, model number JVN. It is controlled by a variable frequency drive by Eaton Corporation that has a rating of 350hp at 480 VAC. A LabView Virtual Instrument VI is programmed to remotely control the system.

Table 3.1: John Deere diesel engine specification

Engine Model	6068HF475
Number of Cylinders	6
Bore and Stroke	106 x 127 mm
Connecting Rod	203 mm
Compression Ratio	17:1
Engine Type	In-line, 4-cycle
Aspiration	Turbocharged and Aftercooled
Displacement	6.8 liters
Rated Power	205 kW (275 hp)
Rated Speed	2400 rpm
Normal operation speed	1800 rpm
Inlet Valve Opening (measured)	-156.75 °
Number of Injector Nozzle Holes	6
Injector Nozzle Hole Diameter	1.75E-04 cm
Nominal Start of Injection Timing	6.5 bTDC

The dual fuel system is a retrofit to the diesel engine. No modifications are made to the internal workings of the engine or the diesel injection system. The natural gas will displace some of the diesel required to run the engine, decreasing diesel fuel consumption for the same power output. The original equipment manufacturer (OEM) engine control module (ECM) will detect this discrepancy in power production and automatically reduce diesel quantity injected when natural gas is present. Incoming natural gas composition to the laboratory varies and was slightly different at each point. The typical composition is shown in Table 3.2. Some of the sensors used in this experiment are as follows:

1) The Omega gas flow meter measures natural gas fuel flow in mass basis.

2) K-type thermocouples sense temperature of the intake, exhaust, and gas supply.

3) Kistler PiezoStar Type 6056A in-cylinder pressure sensors. The sensors measure combustion pressure. These sensors rely on a piezoelectric crystal to detect changes in pressure at measurement speeds below the natural frequency of 160 kHz (measurement frequency further limited by data acquisition system used) (49). Nominal operation lies between $0 - 250$ bar up to 350 °C.

4) Motor, torque and engine speed sensors.

Table 3.2: Typical natural gas composition seen during testing. Percentages by volume

Methane	94%
Nitrogen	1%
Carbon dioxide	1.3%
Ethane	3.14%
Propane	0.45%
Butane	0.11%

3.2   Flow Meters

3.2.1   AVL Fuel Balance and DevX Measurement

Diesel fuel mass flow is measured using an AVL flow meter. It is also calculated using DevX software provided by John Deere. AVL fuel balance works on a direct gravimetric measurement technique with an accuracy of 0.12%. The amount of fuel consumption is determined directly by measuring the time related weight decrease of the measuring vessel by means of a capacitive sensor (50). Data from DevX based on the engine control system is also available. DevX measures diesel fuel flow from a standard diesel fuel density, knowledge of injector design, and duty cycle of pulse width modulation (PWM) cycle feeding the injectors.

3.2.2   Natural Gas Flow Measurement

The natural gas throttling valve position was recorded for all dual fuel engine test data. Upstream natural gas pressure was held constant throughout testing. An Omega FMA-1700 series thermal mass flow meter was installed for a calibration engine test. The dual fuel system was operated through the full range of natural gas flow while recording natural gas flow rate, natural gas supply temperature, and throttle valve position. A flow fit was created from the thermal mass flow meter data to correlate throttle valve position to natural gas flow rate. From this fit, natural gas flow rate was computed from the gas throttle valve position and temperatures of the gas supply. The equation used is:

$$\frac{dm}{dt} = K \times C_v \times \sqrt{SG}$$

Equation 3.1

where *dm/dt* is the natural gas mass flow rate, *K* is the constant as a function of load, C_v is the coefficient as a function of plate angle and *SG* is the specific gravity of gas.

3.3   Emission Concentration Measurement

The exhaust emissions captured in this test include CO, total HC (THC), NO_x, CO_2, O_2, PM, volatile organic compounds (VOCs), methane, and ethane. The following devices are used to measure their respective emissions.

3.3.1   5-Gas Analyzer

The 5-gas analyzer measures CO, CO_2, O_2, NO_x, and THC concentrations. Originally the entire panel comprised of Rosemount instruments; however, the CO, CO_2 and NO_x measuring devices have since been replaced with Siemens instruments. The techniques used in this measurement are presented in Table 3.3. Shown in Figure 3.3 is the 5-gas analyzer rack with Siemens instruments in the Rosemount panel. Before the exhaust gas enters the analyzer, a Peltier-type condenser is used to remove water from the exhaust sample. To measure CO and CO_2 concentrations, infra-red radiation (IR) adsorption technology is used. A flame ionization detection (FID) method is used to measure the THC concentration in the exhaust.

In the FID method, the sample gas flows through a hydrogen gas (H_2) flame inside the instrument and any hydrocarbons in the sample are burnt. The combustion of organic compounds produces ions which are collected by a negatively charged electrode called the collector plate. The current induced across this collector plate is proportional to the rate of ionization which in turn depends upon the concentration of THC in the sample gas. A chemiluminescence technique is used to detect NO_x formation. The chemiluminescence method for gas analysis of NO_x relies on the measurement of light produced by the gas-phase reaction of NO and ozone (O_3) (51). NO is a relatively unstable molecule which will readily oxidize to NO_2 especially in the presence of O_3. This reaction produces a quantity of light for each NO molecule which is reacted and measured by a photodiode. The concentration of NO_x is directly proportional to the intensity of

the chemiluminescence. The O_2 concentration is measured using a paramagnetic technique. This approach utilizes the strong paramagnetic property of O_2 compared to other gases.

Table 3.3: Specifications and measurement technology of the 5-gas emissions bench

	Device	Measurement Technology	Minimum Concentration Range	Maximum Concentration Range	Linearity
CO	Ultramat 6	IR	0 – 10.0 ppm	0 – 10000 ppm	< 0.5% of full-scale value
CO_2	Ultramat 6	IR	0 – 5.0 ppm	0 – 30 %	< 0.5% of full-scale value
THC	NGA 2000, FID	FID	0 – 1.0 ppm	0 – 10000 ppm	< +/- 1% of full scale
NO_x	NO_x MAT 600	Chemiluminescence	0 – 1.0 ppm	0 – 3000 ppm	< 0.5% of full-scale value
O_2	NGA 2000, PMD	Paramagnetic	0 – 1.0 ppm	0 – 100 %	+/- 1% of full scale

Figure 3.3: Rosemount 5-Gas analyzer rack with Siemens analyzers

3.3.2 Fourier Transform Infra-Red Spectrometer

The Fourier Transform Infra-Red Spectrometer (FTIR) is used to measure the concentration of hazardous air pollutants (HAPs). The primary HAPs of interest are formaldehyde, acrolein, and acetaldehyde. Ammonia and hydrogen cyanide can also be measured. The FTIR spectrometer used at the EECL is a Nicolet Magna 560 FTIR shown in Figure 3.4. FTIR spectroscopy is used to measure species concentrations by analyzing the infra-red absorption spectra of the exhaust gas.

Figure 3.4: Nicolet Magna 560 FTIR spectrometer used in the research

3.3.3 PM Concentration Measurement

For PM measurement in the exhaust, a dilution tunnel is used (52). The main purpose of the dilution tunnel is to simulate the mixing of engine exhaust with ambient air by diluting the exhaust gas sample. A schematic diagram in Figure 3.5 demonstrates the application of a dilution tunnel. The dilution tunnel collects particulates suspended in the exhaust and mixes them with clean laboratory air. Laboratory air is inducted by a pump and drawn through a High Efficiency

Particulate Air (HEPA) filter. A secondary activated charcoal filter further purifies the incoming

air. The exhaust sample flow is measured using a venturi/differential pressure measurement and

the dilution air flow is measured with a turbine meter. The purified air and exhaust sample flow

are mixed in the dilution tunnel, then cooled down and equilibrated in a large residence chamber.

The mixture is pulled from the base of residence chamber by a pump and passed through the

filter assembly. Teflon or quartz filters designed to collect particulate matter are held by filter

cassettes. The particulate sample is collected onto a pre-weighed Teflon or quartz filter which is

then weighed again to give the mass of sample collected. Ball valves located upstream and

downstream of the filter holder are used to stop the flow when a data point is not being taken and

to isolate the filter housing when filters are being changed. Figure 3.6 shows the dilution tunnel

used for PM measurement at the laboratory.
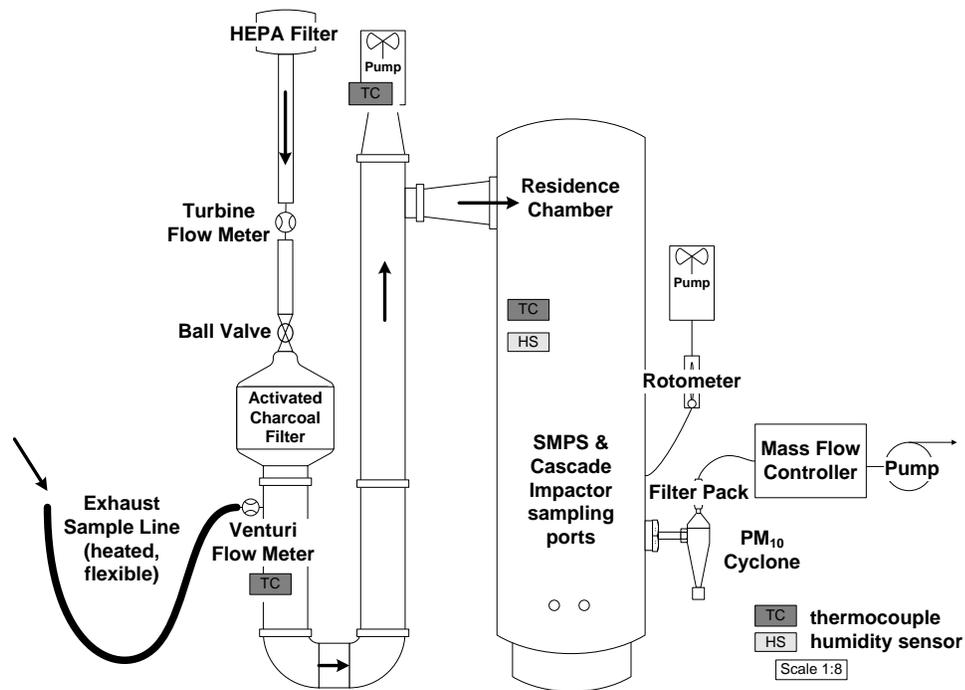
Figure 3.5: Dilution tunnel schematic diagram

Figure 3.6: Particulate matters dilution tunnel

The ISO Standard 8178:4 Cycle D2 procedure for exhaust emission measurement for non-road engine applications is used. The engine operating modes and weighing factors for cycle D2 is listed in Table 3.4.

Table 3.4: Weighting factors of ISO 8178 type D2 test cycles

Load	12%	25%	50%	75%	100%
Weighing factor	0.1	0.3	0.3	0.25	0.05

3.4   Test Plan

Tests were conducted for the diesel engine with dual fuel system turned off (diesel baseline) and for normal dual fuel operations. Baseline dual fuel operation corresponds to the nominal natural gas substitution map recommended by the manufacturer. Table 3.5 shows the

tests performed and the analyzers used on each test. Points at five engine loads were taken corresponding to 12%, 25%, 50%, 75% and 100% of the 165kW maximum load attainable from the test setup at altitude. The engine speed was maintained at 1800 rpm for all cases. These testing parameters were determined after consulting ISO Standard 8178:4 Cycle D2. Experiments were carried out at steady state with intake manifold temperature of 43°C and block coolant temperature reaching 88°C.

Table 3.5: Testing plan and analyzers used in each test

Test No.	Test Description	5-gas	Combustion	FTIR	Fuel GC	Dilution Tunnel / PM
1	Baseline diesel, ISO 8178 Cycle D2 5-mode	✓	✓	✓	•	✓
2	Baseline dual fuel, standard tuning, ISO 8178 D2 5-mode	✓	✓	✓	✓	✓
3	Final configuration, ISO 8178 D2	✓	✓	✓	✓	✓
4	Diesel displacement sweep, ISO 8178 Cycle D2 5-mode	✓	✓	•	•	•
5	Injection timing sweep, ISO 8178 Cycle D2 5-mode	✓	✓	✓	✓	•

During dual fuel operation, the power output of the engine is controlled by varying the amount of natural gas inducted into the system. This is achieved by adjusting the gas control valve. The injection timing was left at stock configuration and is varied by the ECM according to the amount of diesel fuel injected. At high loads for the diesel case, the engine automatically

retards the timing to be nearer to top dead center. However, in dual fuel operation, the engine automatically advances the timing as shown in Figure 3.7. During dual fuel operation, the timing does not retard until the full load point. This is because the ECM calculates engine load from diesel fuel consumption and sets the timing as if the engine were at a lower load, consistent with the reduced diesel consumption in dual fuel operation. During dual fuel operation, significantly less diesel is injected, resulting in a low operating load calculated by the ECM.

The air flow rate inducted to the system is not throttled. Because of this, the air and natural gas mixture becomes leaner as the load is reduced. At lower loads it is expected that combustion will degrade as the mixture becomes leaner, leaving large amounts of partial reaction products in the exhaust (70).
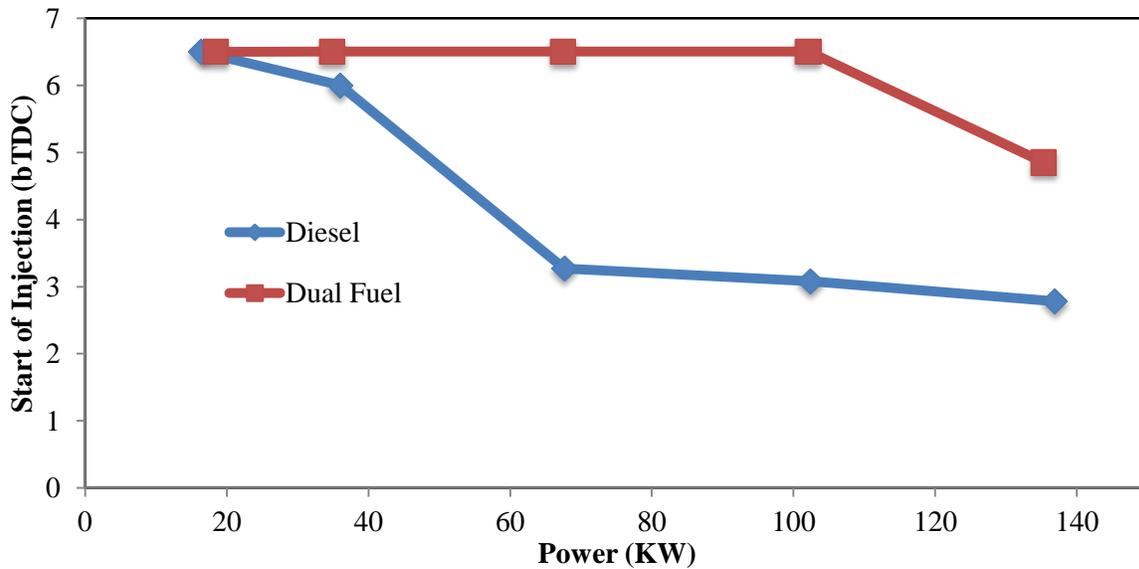
Figure 3.7: Diesel fuel injection timing at various loads

Therefore, it is important to evaluate the Φ of the air and natural gas mixture. This mixture Φ at each load entering the cylinder during the intake stroke is shown in Table 3.6. It is calculated using Equation 3.2:

$$\Phi = \frac{A/F_{Stoichiometric}}{A/F_{Actual}}$$

<div align="right">Equation 3.2</div>

where $A/F_{Stoichiometric}$ is the AF at stoichiometric conditions and A/F_{Actual} is the actual AF. The actual natural gas AF was evaluated in several steps. The actual AFs were calculated for diesel baseline using exhaust gas analysis. Using measured fuel consumption and the AF, the air flow through the engine was computed. The volumetric efficiency was determined from the air flow and intake air properties. The volumetric efficiency values for diesel operation at each load were utilized to compute intake flow for dual fuel operation. Finally, the intake flow and measured natural gas flow rates were used to calculate natural gas Φ for dual fuel operation.

Diesel displacement is calculated using Equation 3.3 and is shown in Table 3.6. The diesel displacement represents the percentage of natural gas substitution in the diesel engine.

$$\text{Diesel Displacement (\%)} = 100 \times \frac{\dot{m}_{Baseline\ Diesel} - \dot{m}_{Diesel\ in\ Dual\ Fuel\ Mode}}{\dot{m}_{Baseline\ Diesel}}$$

<div align="right">Equation 3.3</div>

It is computed by measuring the diesel fuel mass flow rate for diesel baseline, $\dot{m}_{Baseline\ Diesel}$, and the diesel fuel mass flow rate in the dual fuel engine, $\dot{m}_{Diesel\ in\ Dual\ Fuel\ Mode}$. The difference of these mass flow rates represents how much natural gas is substituted in the dual fuel engine. It

is shown in Table 3.6 that the maximum displacement in the dual fuel engine is 70%, which is limited by engine stability and knocking. Further increasing the natural gas flow in the system caused engine instability, observed as significant vibrations in the test cell. In-cylinder pressures also dropped significantly. Considering these issues, maximum diesel displacement for this setup is 70%.

Table 3.6: The diesel displacement of natural gas by mass and Φ of air and natural gas

Load	12%	25%	50%	75%	100%
Diesel displacement (%)	35.0	59.6	70.0	69.4	58.7
Equivalence ratio	0.15	0.23	0.22	0.27	0.24

3.5 Combustion Analysis

In-cylinder data such as pressure and HRR provide important insights about combustion behavior in the cylinder. This data can be used to obtain information about the combustion process such as the HRR and burn durations. The method of analysis is adapted from Gatowski et al., 1984 (53). In a diesel engine, the combustion chamber is treated as closed system where only flow of fuel is considered and the crevice flow is neglected. The overall heat release using the energy balance equation is derived as:

$$\frac{dQ}{d\theta} = \left(\frac{C_P P}{R}\right)\frac{dV}{d\theta} + \left(\frac{C_V V}{R}\right)\frac{dP}{d\theta} - \frac{dQ_w}{d\theta}$$

Equation 3.4

where $\frac{dQ}{d\theta}$ is the heat transfer rate across the system with respect to crank angle degree, C_p and C_v are the gas specific heats at constant pressure and volume, R is the specific ideal gas

constant, $dV/d\theta$ is the displaced volume across the system and $dP/d\theta$ is the differential pressure as piston travels.

The indicated mean effective pressure (IMEP) is used to quantify indicated work per piston displacement (work density), while the combustion stability is determined by the coefficient of variance (COV). The COV represents the standard deviation of the data as a percentage of its mean value. The COV of IMEP is used to indicate the cyclic variability in indicated work per cycle. Crank angle locations of peak pressure and 10, 50, and 90% mass fraction burned are analyzed to indicate combustion speed. Other parameters involved are thermal efficiency (η_t) and bsfc which represent the engine's performance.

3.6   Effects of Diesel Displacement and Injection Timing

Effects of pilot fuel quantity and injection timing will be considered in order to improve performance and to reduce the emissions. A diesel displacement sweep is conducted at each of the five loads to find limits of operation and formulate an optimized substitution scheme that will maximize diesel displacement. A sweep of injection timing is also conducted to note the effects of combustion phasing on combustion and emissions. In this particular testing, the timing is both advanced and retarded around the SOI until engine instability or extremely high emissions levels were observed.

3.7   Optimization Testing

The data in Section 3.6 is used as indicators for two major factors influencing the decision of the optimized testing parameters. The testing is carried out to investigate the optimized load map for minimizing THC and CO emissions while maintaining loading capabilities over the full range of operating conditions.

4.0   RESULTS AND DISCUSSION

Measurements were taken under two different operational modes, baseline diesel and dual fuel operation as described in the Experimental Setup section. To examine the phenomena inside the combustion chamber, the combustion stability, cylinder pressure, net heat release rate, and mass fraction burned data are presented. The raw net heat release data in section 4.3 is smoothed a running average of ten data points. Emissions were collected according to the appropriate ASTM, EPA, and ISO standards and analyzed using the equipment described previously. For the baseline conditions, the primary parameters presented here are cost analysis, bsfc, efficiency, NO_x, PM, CO and THC. An analysis is also presented showing the dual fuel performance in terms of ISO weighted average emissions based on the appropriate ISO test cycle. Additionally, emissions and engine performance data are presented for the diesel displacement and injection timing sweeps.

Table 4.1 shows overall cost saving associated with dual fuel engine. It shows that dual fuel engine provides maximum cost saving at 50% load with 61% fuel cost reduction and 60% fuel cost reduction at 75% load.

Table 4.1: Cost analysis comparing diesel and dual engine in $/kWh at various loads

Load	12%	25%	50%	75%	100%
Diesel engine ($/kWh)	0.38	0.27	0.25	0.23	0.23
Dual fuel engine ($/kWh)	0.25	0.15	0.10	0.09	0.12

4.1   Combustion Stability

4.1.1   Coefficient of Variance

The stability of engine combustion is determined by the coefficient of variance (COV) computed from combustion pressure data. The COV represents the standard deviation of the data as a percentage of its mean value, shown in Equation 4.1 and 4.2.

$$COV_{Peak} = 100 \; \frac{\sigma_{Peak}}{\overline{Peak\ Pressure}}$$

Equation 4.1

$$COV_{IMEP} = 100 \; \frac{\sigma_{IMEP}}{\overline{IMEP}}$$

Equation 4.2

where σ is the standard deviation, $\overline{Peak\ Pressure}$ is the mean of peak pressure and $\overline{IMEP}$ is the mean of indicated mean effective pressure (IMEP). The COV of peak pressure and IMEP in cylinder for load variation are presented in Figure 4.1and Figure 4.2.
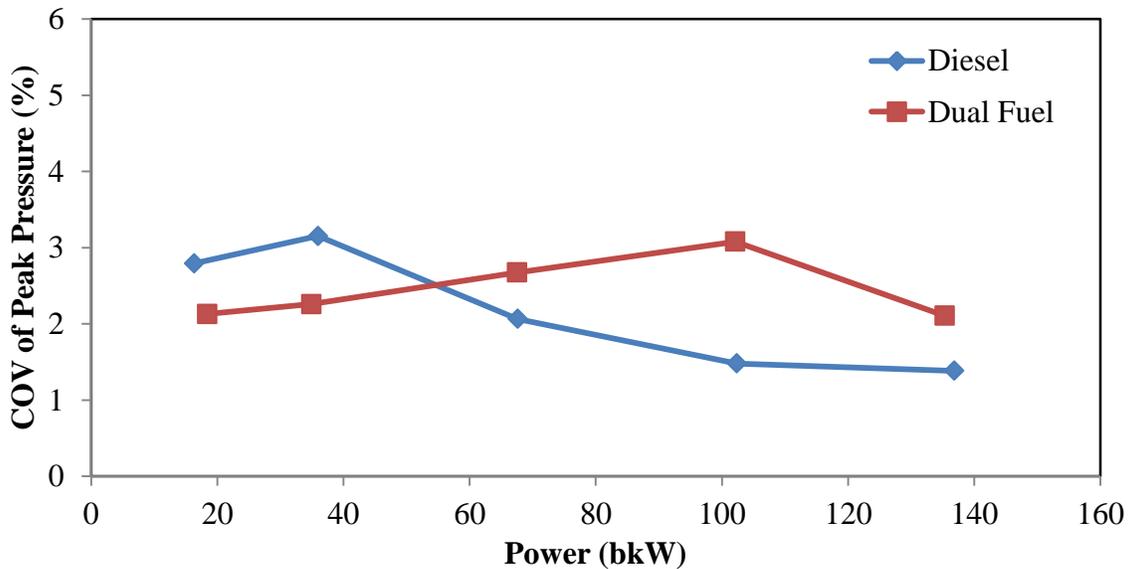
Figure 4.1: COV of peak pressure diesel and dual fuel engines at various loads

53
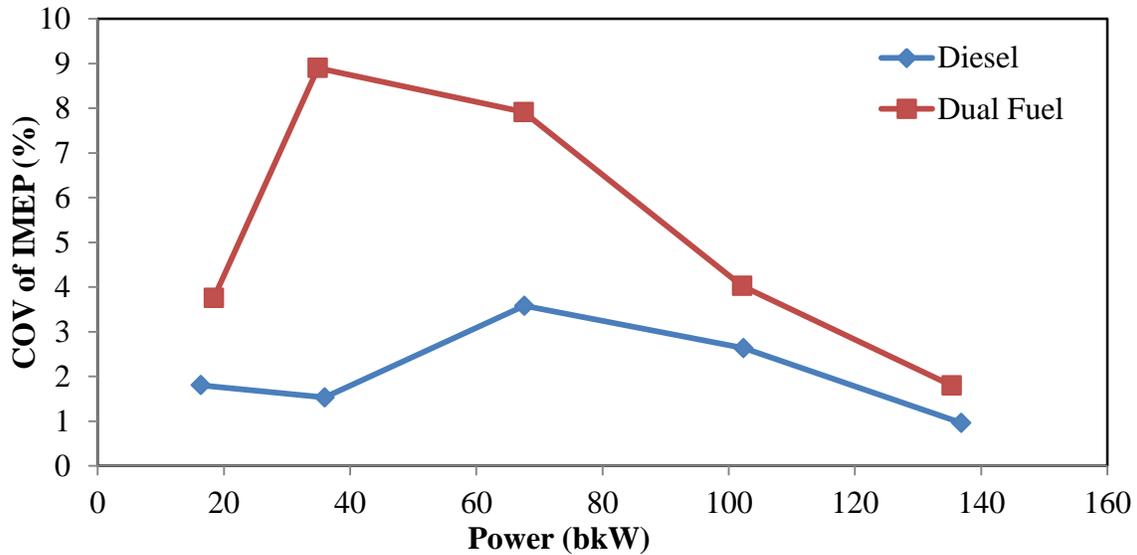
Figure 4.2: COV of IMEP of diesel and dual fuel engines as a function of brake power

Considering the COV for all five load cases, Figure 4.1 and Figure 4.2 show generally lower COVs during diesel operation except at low loads for peak pressure COV, implying that the combustion process is more repeatable for diesel operation. The peak pressure COV in diesel operation is lower than observed values during dual fuel operation. This is expected since diesel combustion is highly stable and this represents the stock, as-engineered operation for this engine. Two exceptions are the two lower loads COV of peak pressure data points, where diesel is higher than dual fuel.

In general for diesel the combustion process occurs at stoichiometric conditions as a diffusion flame, which results in low COVs. For dual fuel operation, a significant fraction of the heat released occurs as lean premixed combustion. The premixed air and fuel (natural gas) in the combustion chamber just before diesel injection are characterized by lean Φs below the flammability limit of laminar premixed methane flames (0.46). Consequently, oxidation of natural gas and air likely occurs as distributed reactions rather than a self-propagating flame. As

54

diesel is injected, the temperature in the cylinder increases which accelerates oxidation of the natural gas. The combustion stability and the extension of reaction of natural gas are dependent on the penetration of the diesel burning jets and subsequent mixing of hot combustion gases with the lean premixed air and natural gas. At low loads high CO and HC emissions are observed. This is probably due to poor diesel jet penetration at low loads since the diesel fuel mass injected per cycle is significantly lower.

4.1.2 Combustion Duration

The speed of the initial phase of combustion is represented by the 0-10% burn duration, often referred to as the ignition delay period. The 0-10% burn duration is calculated using Equation 4.3:

$$0\text{-}10\% \text{ Burn Duration=SOI (°bTDC)} + \text{mass fraction burned at 10\% (°aTDC)}$$

Equation 4.3

The primary phase of combustion is represented by the 10-90% burn durations. The 10-90% burn duration is calculated using Equation 4.4. The 0-10% burn duration and 10-90% burn duration are shown in Figure 4.3.

$$10\text{-}90\% = 90\% \text{ mass fraction burned location (°aTDC)} - 10\% \text{ mass fraction burned location (°aTDC)}$$

Equation 4.4

The general trend is for the 10-90% burn duration to go up as load increases because the required mass of fuel burned increases. However, the trend levels as load increases, indicating faster combustion rate at higher loads. For diesel this comes about since the fuel injection system is optimized for 100% load and combustion temperature increases with load, which also applies to

dual fuel. The data show that at all loads dual fuel experiences shorter 10-90% burn duration compared to diesel. The premixed natural gas equivalence ratio shown earlier in Table 3.6 is leaner at low loads and results in a slower combustion rate, which is supported by a larger difference between dual fuel and diesel 10-90% burn duration at low load. Additionally, the dual fuel injection timing is retarded at intermediate and high loads, which can slow combustion during the latter stages of combustion due to volume expansion cooling. The 0-10% burn duration data show a larger ignition delay for dual fuel at all loads except the highest load, where dual fuel and diesel are about the same. Two possible reasons for the dual fuel 0-10% burn values being larger than diesel, 1) the mole percentage of air in the cylinder is smaller for dual fuel because some of the air is displaced by natural gas (the decreased availability of oxygen most likely slows ignition reactions), 2) the ratio of specific heats of natural gas is substantially lower than air, decreasing the mixture average ratio of specific heats. A lower ratio of specific heats reduces the compression temperature, which will reduce ignition reaction rates.
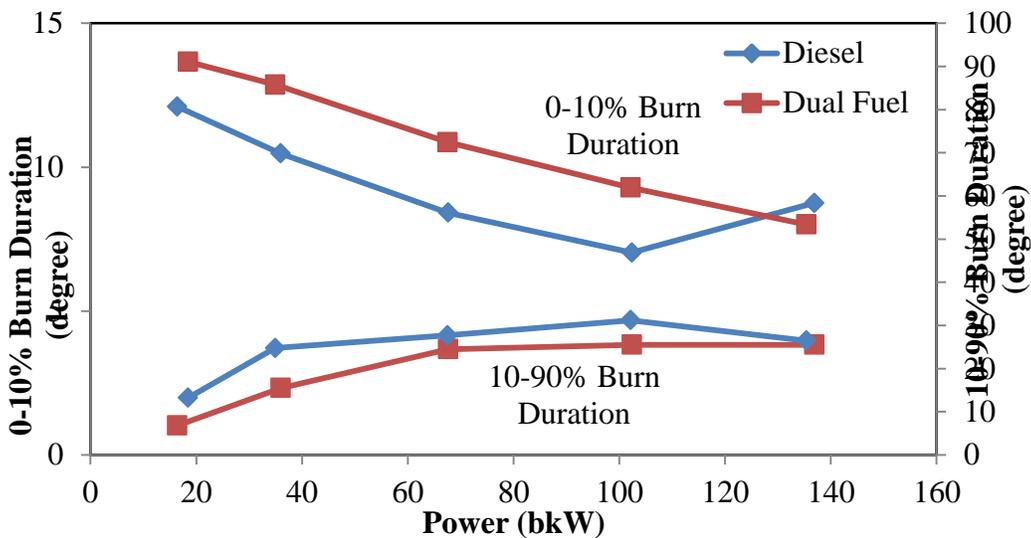
Figure 4.3: 0-10% burn duration and 10-90% burn duration comparisons

4.2   Engine Performance

4.2.1 Thermal efficiency and bsfc

The bsfc is calculated by dividing the total fuel mass flow rate (diesel and natural gas) by engine shaft power as shown in Equation 4.5. The brake thermal efficiency is calculated by using inverse proportion of bsfc and the weighted average lower heating value (LHV) as shown in Equation 4.6.

$$bsfc \;=\; \frac{\dot{m}_f}{\dot{W}_b}$$

Equation 4.5

$$efficiency \;=\; \frac{1}{bsfc \times LHV}$$

Equation 4.6

Comparisons of efficiency and bsfc of diesel and dual fuel engine are shown in Figure 4.4 and Figure 4.5. At low loads, the efficiency is lower for the dual fuel operation compared to normal diesel operation while the bsfc is higher for dual fuel operation. This may be due to slower combustion rate and poor utilization of the gaseous fuel in the combustion chamber. Additionally, on a mass basis the specific heat of natural gas is higher than pure air and higher than diesel vapor. This may also play a role by reducing combustion temperature and consequently slowing the combustion process. The trends are improved at intermediate and high loads. It is observed that ignition delay (Figure 4.3) is decreased at high loads in dual fuel operation, which promotes faster combustion. Additionally, the diesel injection timing is advanced for dual fuel compared with diesel at the upper three loads by 2 to 3.5 degrees (see Figure 3.7). Timing is advanced and has a significant impact on engine efficiency.

57
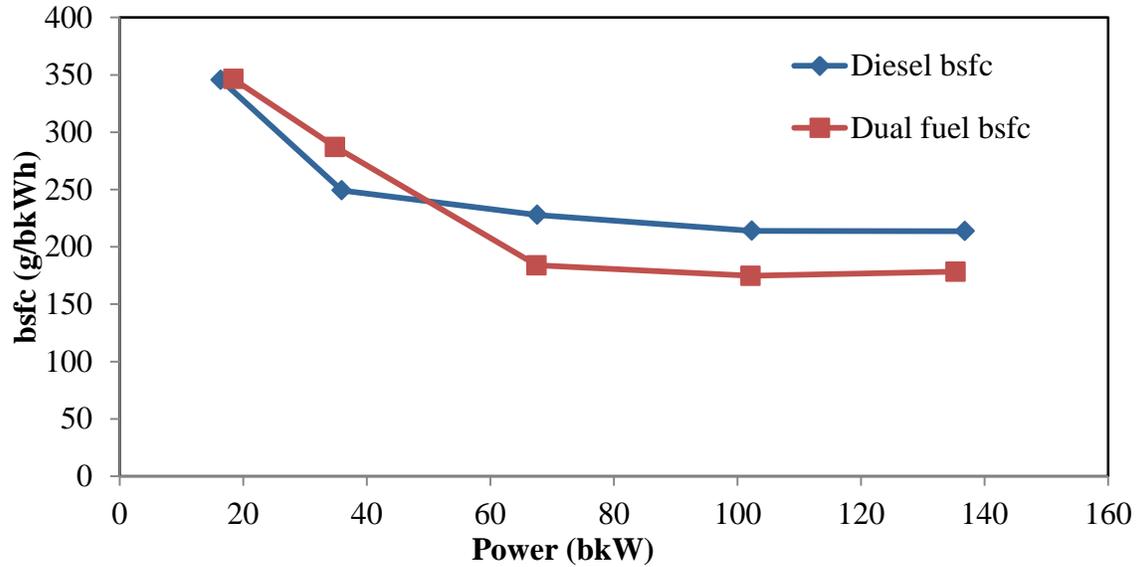
Figure 4.4: Engine's bsfc for diesel and dual fuel operation as a function of brake power
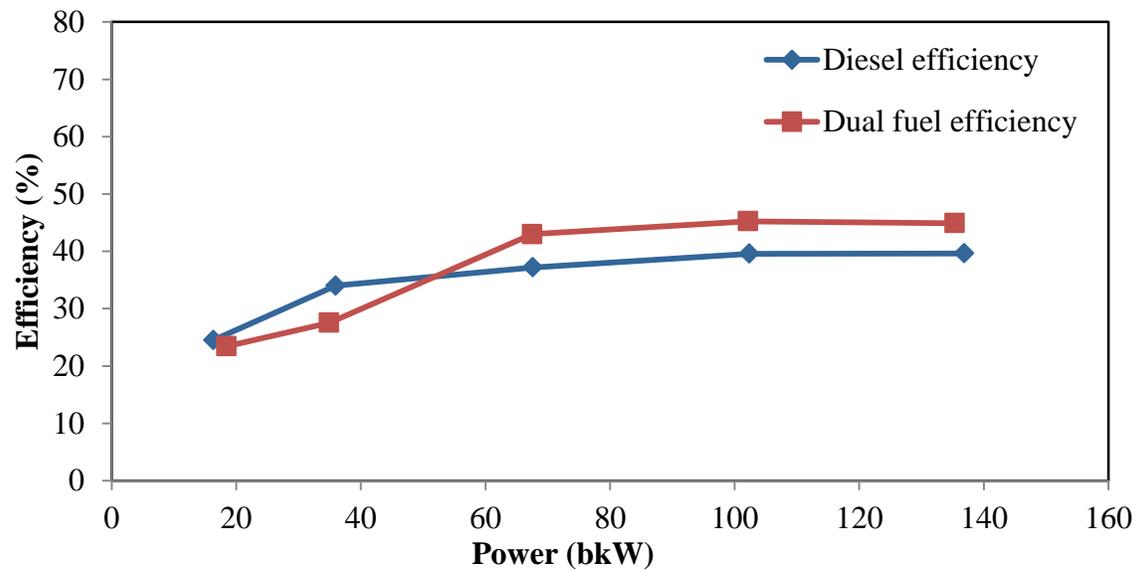
Figure 4.5: Engine's efficiency for diesel and dual fuel operation as a function of brake power

4.2.2 *Combustion Pressure and Heat Release Profile*

Figure 4.6 and Figure 4.7 show combustion pressures and net heat release rates vs. crank angle at low loads. At low loads, the cylinder pressure is lower in dual fuel operation due primarily to later heat release. While the motoring pressure peaks of both traces are nearly identical, the dual fuel case fails to reach similar peak pressures as the diesel case due to a late

58

pressure peak. Also at both loads, the diesel case reaches complete combustion more quickly. Complete combustion is shown as a mass burn fraction value of one. In both low load cases, the mass burn fraction rises much faster for diesel than dual fuel.

Figure 4.8 shows pressure and heat release rate trend at 50% load. Dual fuel motoring and peak combustion pressures are slightly lower than the diesel condition. The heat release rate is also lower in dual fuel engine. The diesel case shows two heat release peaks, the first premixed combustion and the second mixing controlled combustion. For dual fuel only one heat release peak is observed.

The pressure and heat release rate profile at higher loads are presented in Figure 4.9 and Figure 4.10. The motoring pressures for dual fuel are lower at 75 and 100% loads. Peak combustion pressures double over the selected testing range. Although the compression ratio is fixed, the intake air pressure is much higher at 100% load compared to 12% load. Two heat release peaks are present for diesel and dual fuel at the higher loads. At high loads, dual fuel and diesel combustion appears similar, with dual fuel mass burn fraction rising slightly faster. Both regimes have completed combustion by approximately 45° aTDC.
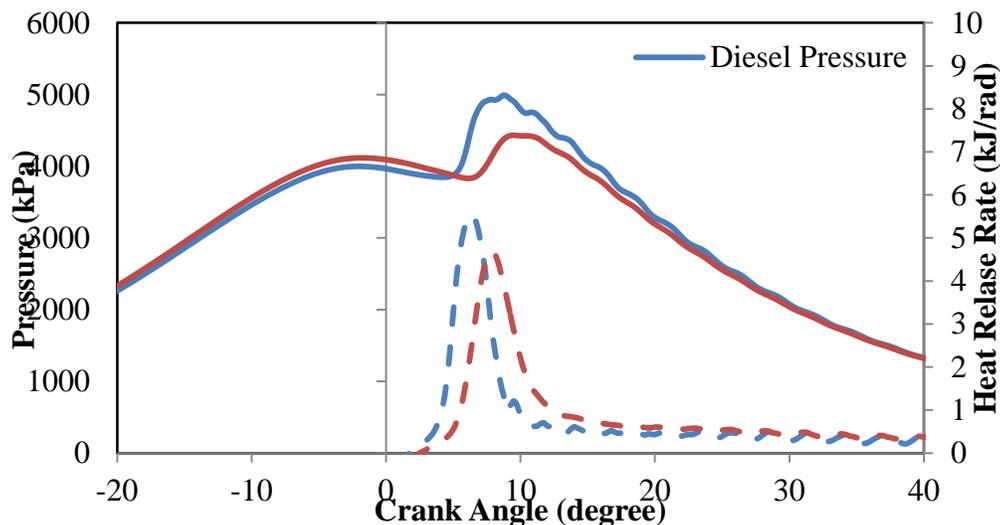
Figure 4.6: Pressure trace and heat release rate profile at 12% load
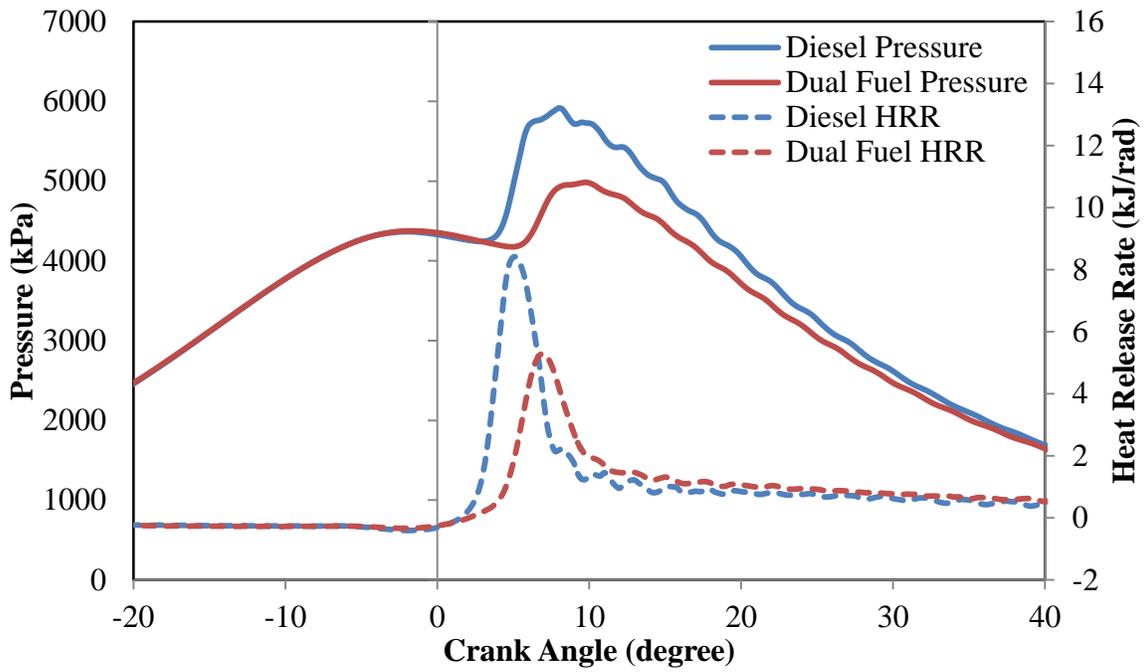
Figure 4.7: Pressure trace and heat release rate profile at 25% load
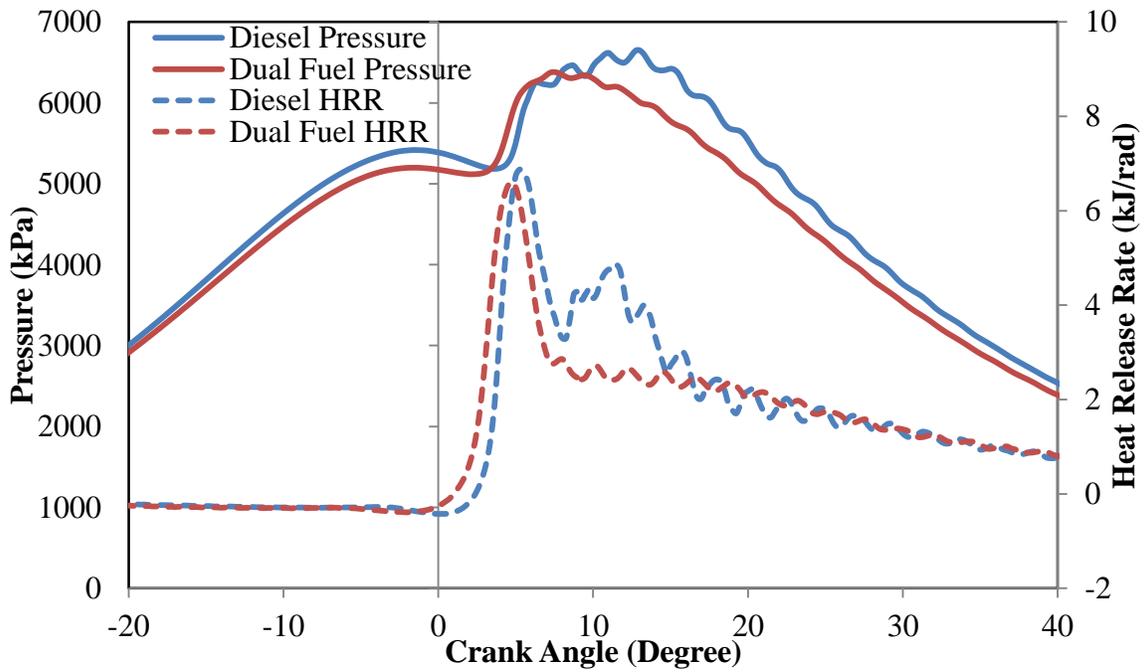
Figure 4.8: Pressure trace and heat release rate profile at 50% load

60
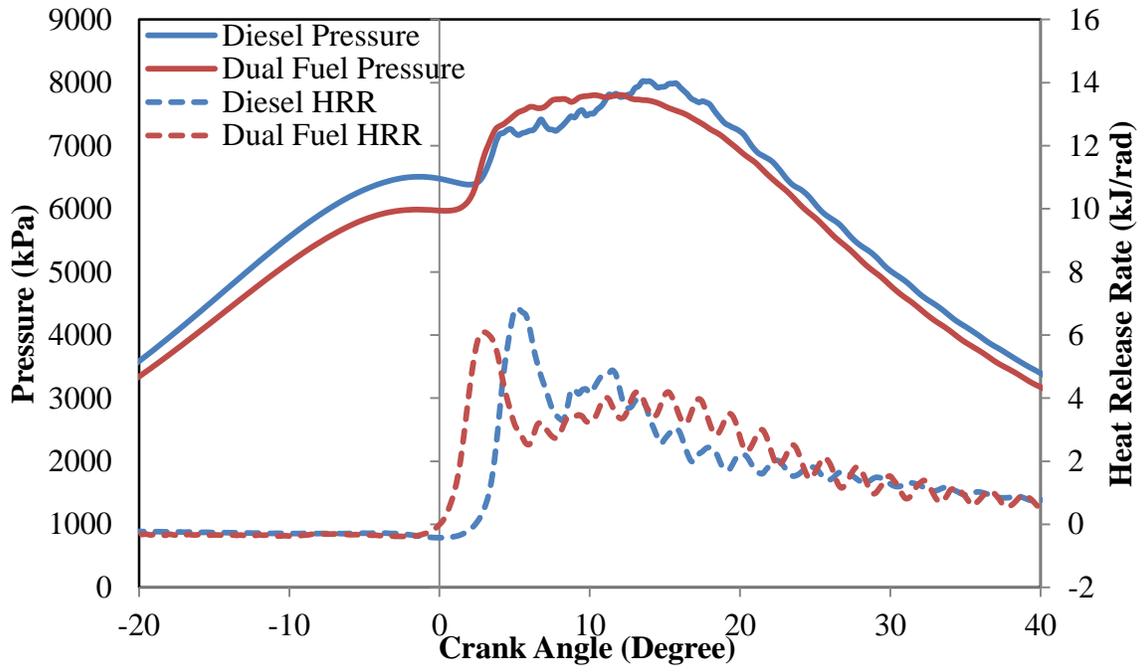
Figure 4.9: Pressure trace and heat release rate profile at 75% load
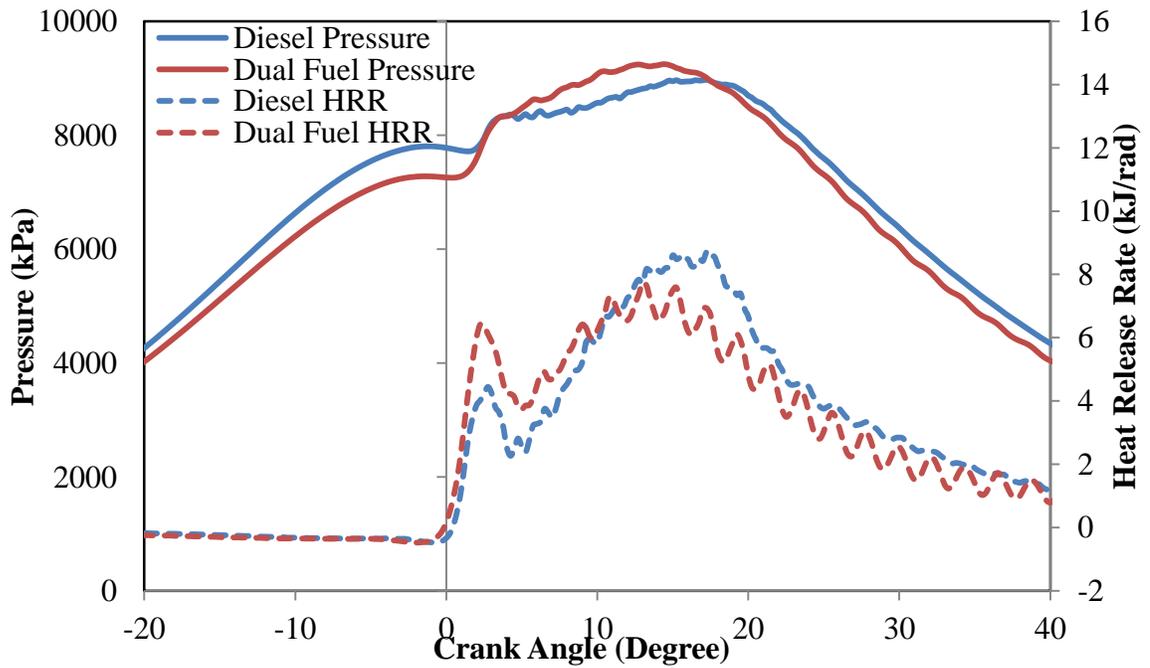
Figure 4.10: Pressure trace and heat release rate profile at 100% load

4.3   Emission Analysis

4.3.1   NOx Emissions

NO_x is the sum of NO and NO_2. There are other oxides of nitrogen sometimes included, but they are insignificant in diesel and natural gas engines. Figure 4.11 shows measured NO_x emissions at five loads for the two operating modes. The figure indicates that dual fuel operation emits less NO_x throughout the load map. NO_x formation is dependent on the oxidation of atmospheric nitrogen. The most significant component, NO is described by the extended Zeldovich mechanism, which is strongly affected by cylinder charge temperature. In dual fuel operation, part of the combustion process occurs in the lean, premixed regime. For normal diesel operation, most of the fuel is burned as a diffusion flame near stoichiometric equivalence ratio. Stoichiometric combustion produces higher NO_x due to higher combustion temperatures. Both operating modes display minimum NO_x production at about 75 kW and follow similar trends. Thus, it appears that the same combustion and engine operating phenomena are affecting both operating modes. At low loads the 0-10% burn duration is higher and 10-90% burn duration is lower (Figure 4.3) for both operating modes. Consequently, the premixed diesel combustion phase is more predominant, which produces more NO_x. This is more pronounced for diesel mode. At high loads the overall AF ratio decreases (Φ increases) due to turbocharger limitations. For example, in the dual fuel case the overall Φ, considering both fuels, is 0.55 at 68 kW and 0.71 at 135 kW. This effect impacts both operating modes by increasing average combustion temperatures at high loads, tending to increase NO_x.
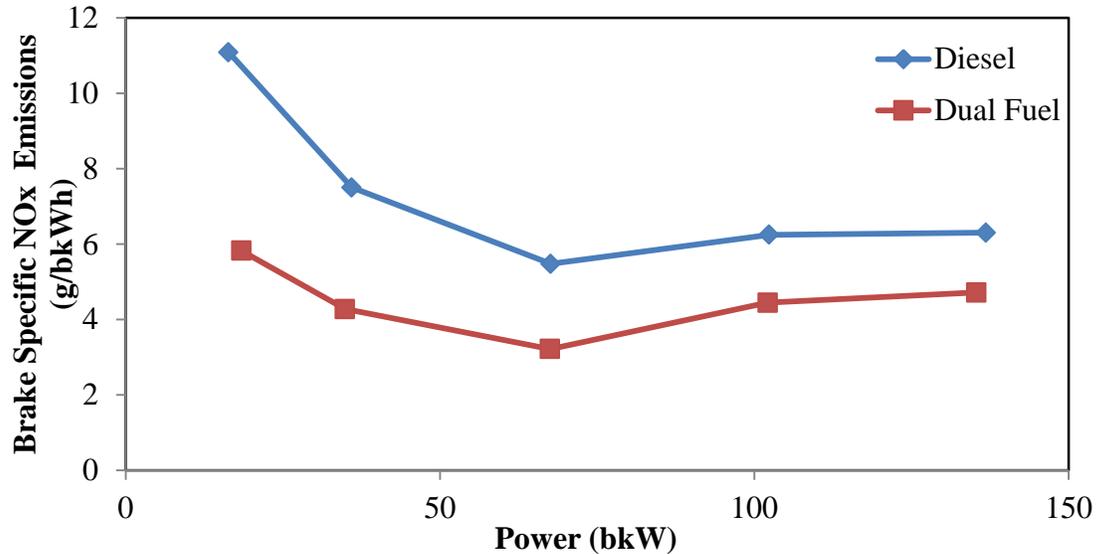
Figure 4.11 : NO$_x$ formation comparison for diesel and dual fuel operation

4.3.2   PM Emissions

Figure 4.12 shows the variation of PM with load. Under dual fuel operation, PM emissions are lower for every load except high load, which exhibits 60% higher PM than normal diesel operation. In normal diesel operation, the PM emissions show a decreasing trend with increasing load. The general PM reduction in dual fuel operation is expected. Natural gas contains primarily methane, the simplest hydrocarbon, which tends to produce lower PM emission. PM formation is dependent on the fuel composition. The carbon content of diesel is higher than natural gas and tends to produce more PM. PM formation is also dependent on the combustion regime. CI diesel engines are characterized by mixing controlled combustion. In dual fuel operation, the fraction of premixed natural gas combustion increases while the fraction of mixing controlled diesel combustion decreases. Generally this tends to reduces PM emissions. The high load data was unexpected, and the explanation is unclear. The high load data points were subsequently repeated on a different test days, confirming the result.

63
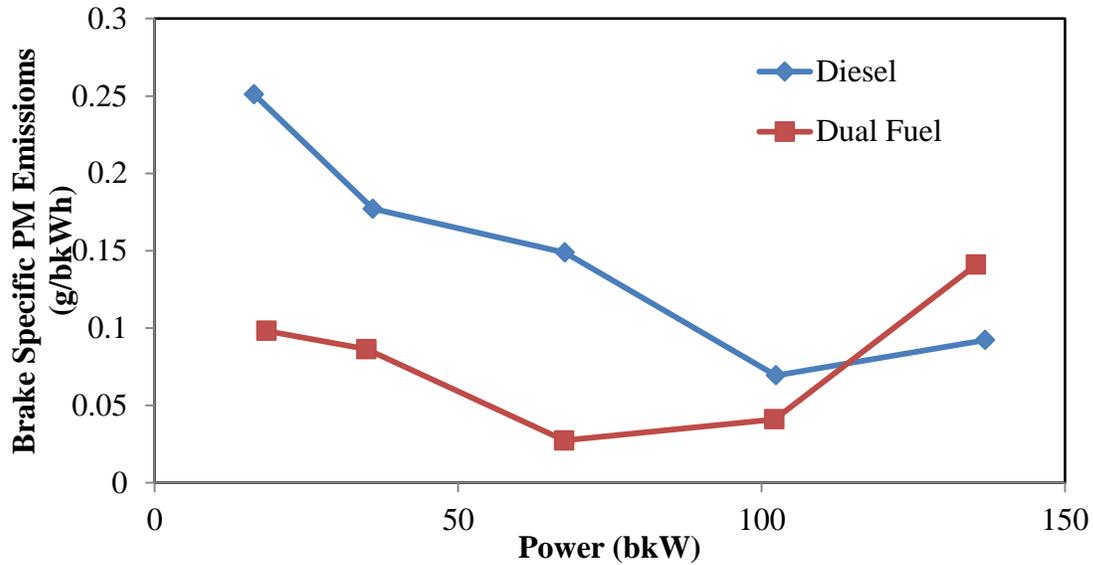
Figure 4.12: PM emissions comparison for diesel and dual fuel operation

4.3.3   CO Emissions

The relationship between CO emissions and load is shown in Figure 4.13 for both operating modes. Emission of CO is indicative of incomplete combustion. CO emissions are dependent on equivalence ratio, partially burned gaseous fuel, and cylinder charge temperature. According to the figure, it is revealed that dual fuel operation suffers from high CO emissions, particularly at low loads. Diesel operations, on the other hand, produce low CO emissions. At low loads, duel fuel combustion is characterized by slower combustion rates (Figure 4.6 and Figure 4.7) compared to diesel, which results in lower cylinder charge temperature and poor quality combustion. At intermediate loads, dual fuel combustion is improved with lower CO emissions compared to low loads. This declining trend continues at high loads. However, even with this reduction, CO emissions are still higher than normal diesel operation. The extent of diesel jet penetration is another factor that likely influences incomplete combustion and CO emissions at low loads. At low loads, the mass of diesel fuel injected is much smaller (about 70%

reduction) than high load for dual fuel operation. When less mass is injected the diesel jet penetration is not as great and less likely to extend throughout the combustion chamber. This reduces the probability of complete combustion of the entire air and natural gas mixture.
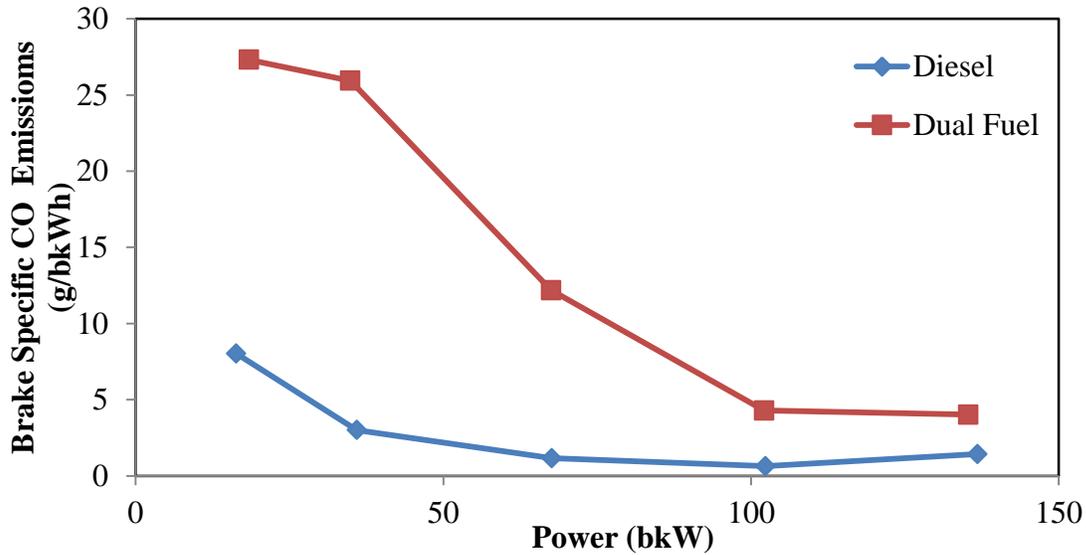
Figure 4.13: CO emissions comparison for diesel and dual fuel operation

4.3.4   THC Emissions

Figure 4.14 shows THC levels in the exhaust for dual fuel and diesel operating modes across the load map. THC emissions for both cases decrease with increasing load and are minimum at 100% load. THC emissions are controlled by the quality of the combustions process inside the cylinder. The trend in THC emissions is similar for dual fuel and diesel, but dual fuel THC emissions are nearly 100X that of diesel THC emissions. An explanation can be made similar to that made for CO emissions. The air and natural gas is very lean, especially at low loads. Referring to Table 3.6, the natural gas Φ varies from 0.15 to 0.27. At Φ s this low, flame

propagation is slow or non-existent. The extent of penetration of the burning diesel jet may play a critical role in oxidizing the lean natural gas/air mixture. At low loads the natural gas Φ and diesel jet penetrations are the lowest, likely contributing to high THC emissions at low load. The high THC emissions for dual fuel are therefore a product of incomplete combustion, primarily, of the lean air and natural gas mixture.
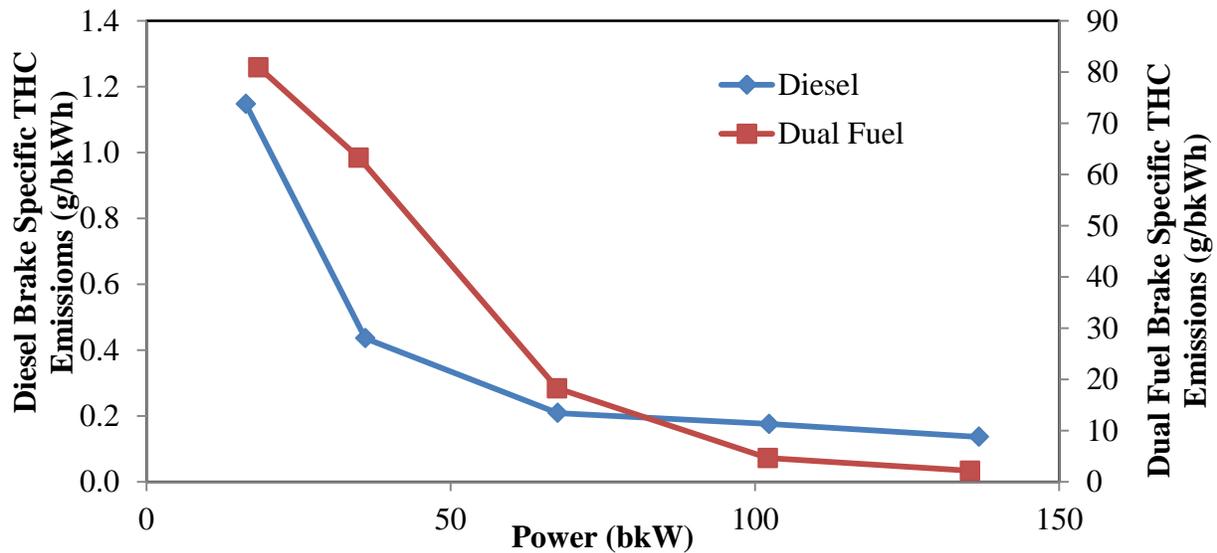
Figure 4.14: THC emissions comparison for diesel and dual fuel engine

4.3.5 Regulated Emissions

Figure 4.15 shows ISO 8178 weighted emissions for diesel and dual fuel operation. The John Deere Tier II 6068H compression ignition engine is required to meet the US EPA limits at sea level conditions. These limits are indicated in the figure. NO_x is combined with NMHCs. The NMHC emissions are evaluated by subtracting methane measured with the FTIR from HC. In normal diesel mode the engine meets the Tier II limits with the exception of NO_x + NMHC,

which is slightly above the limit. The test was carried out at an altitude of 5000 feet. The turbocharger system does not provide as much boost at high altitude, which decreases the air fuel ratio and increases NO_x. This is most likely why NO_x + NMHC is slightly above the limit. In dual fuel mode NO_x + NMHC and CO limits are significantly exceeded. PM emissions are reduced further below the Tier II limit. The limit for NO_x + NMHC is exceeded because, although NO_x is reduced, the increase in NMHC emissions is much larger.
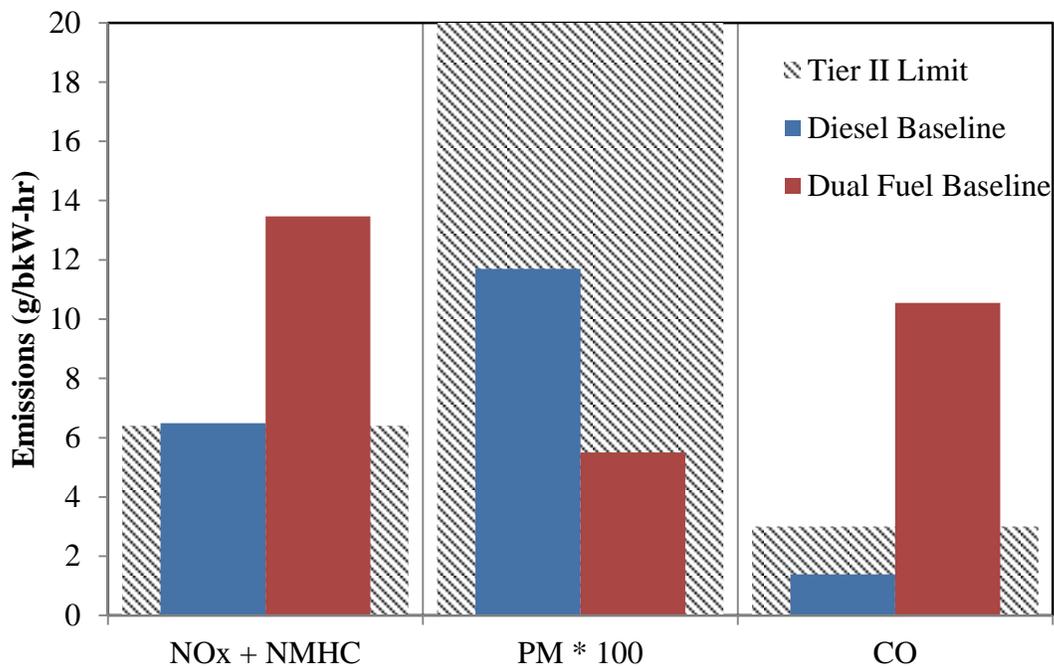
Figure 4.15: ISO 8178 weighted emissions compared to EPA Tier II limits

4.4   The Effects of Diesel Displacement

Low and intermediate loads in dual fuel operation suffer from high CO and incredibly high THC emission levels. In order to optimize diesel displacement over the load map, a natural gas substitution sweep was conducted at each load in order to find the limits of operation and

formulate an optimized substitution scheme that would maximize diesel displacement while reducing emissions. Figure 4.16 and Figure 4.17 shows brake specific variations at low loads. These figures show that THC and CO emissions increase with increasing diesel displacement at low loads. NO_x displays a slight decreasing trend with increasing diesel displacement. At 25% load the THC emissions are reduced for the first diesel displacement point (~17.5%), but then increases for further increases in diesel displacement. At 50% load each emission species displays a different trend.

Figure 4.18 shows the brake specific emissions trend with diesel displacement. THC emissions start below 1 g/bkW-hr at 0% diesel displacement and increases to about 25 g/bkW-hr at maximum diesel displacement. CO emissions gradually increase as diesel displacement increases, peaking near 60% diesel displacement, then significantly decrease as diesel displacement increases further. NO_x emissions display a gradual decreasing trend as diesel displacement increases. As diesel displacement increases from 0% to maximum diesel displacement NO_x emission are approximately cut in half.

Figure 4.19 shows the emissions trend when the amount of diesel replaced with natural gas is varied at 75% load. NO_x emissions gradually decrease as diesel is replaced with natural gas until about 40% replacement, at which point NO_x increases. In an opposite fashion, emissions of CO significantly increase with increasing diesel replacement up to about 40%, where the trend reverses. Natural gas Φ is shown earlier in Table 3.6. The equivalence ratio steadily increases as diesel replacement is increased. At an equivalence ratio between 0.16 and 0.21 the CO and NO_x trends are reversed. THC emissions increase with increasing diesel replacement throughout the entire sweep. As the mass of diesel injected decreases, it is likely that more regions in the

cylinder are not ignited by the diesel jets. At high diesel replacement values above 60%, the CO
trend reverses again and CO increases.
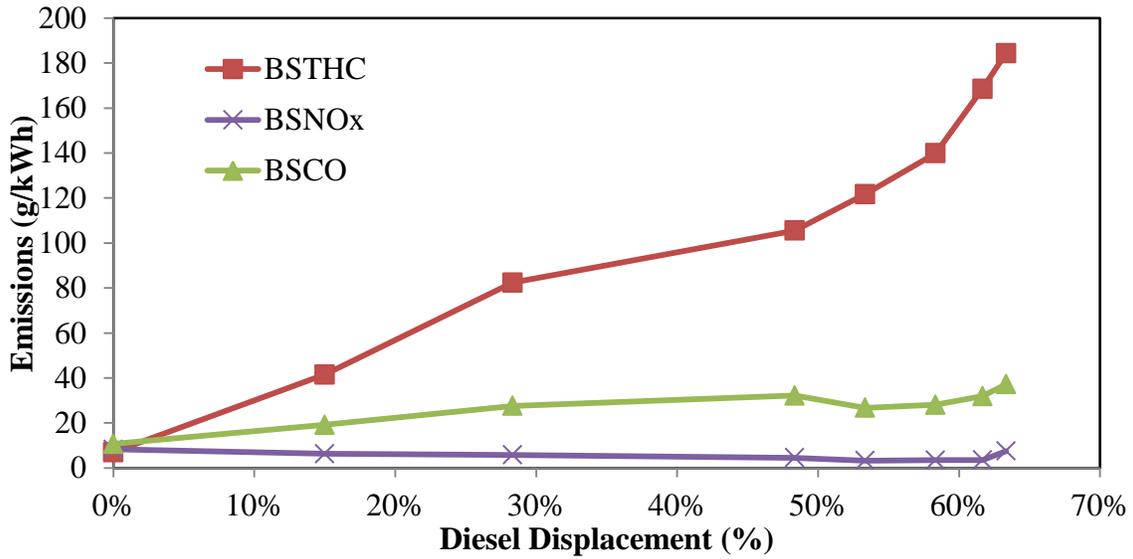
Figure 4.16: Emissions as a function of diesel displacement at 12% load
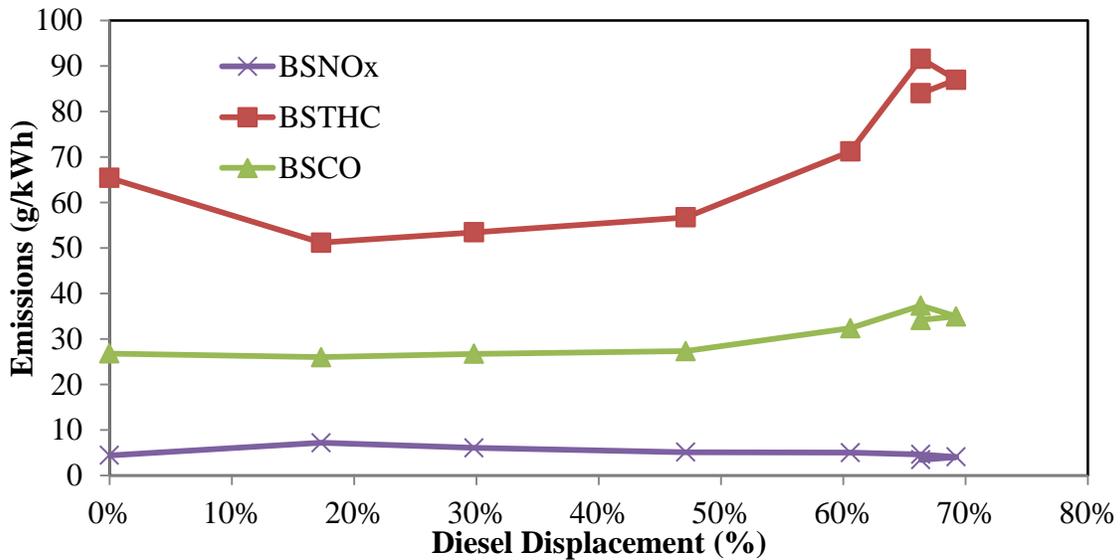
Figure 4.17: Emissions as a function of diesel displacement at 25% load
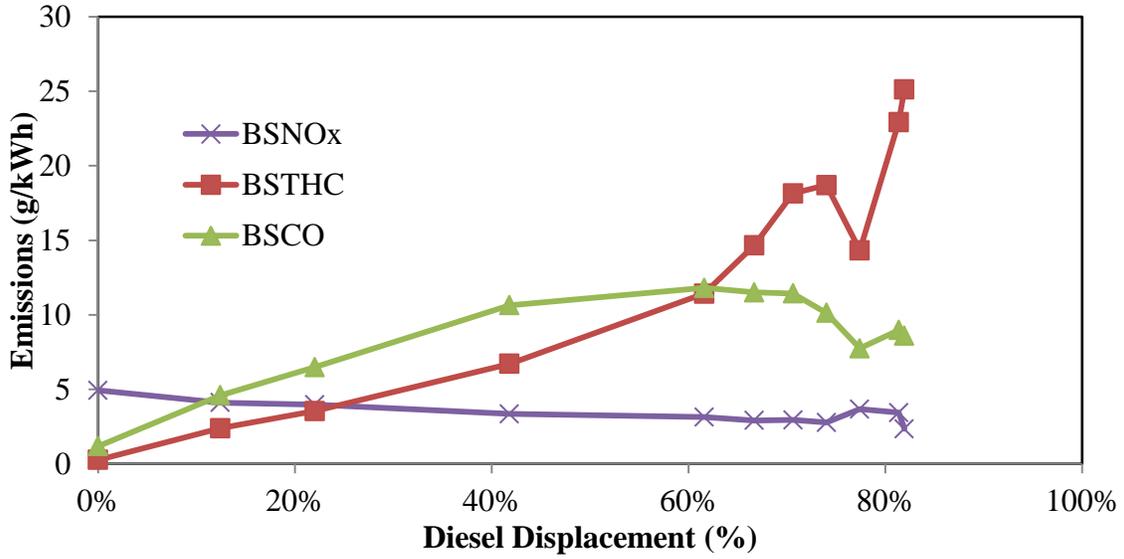
Figure 4.18: Emissions as a function of diesel displacement at 50% load
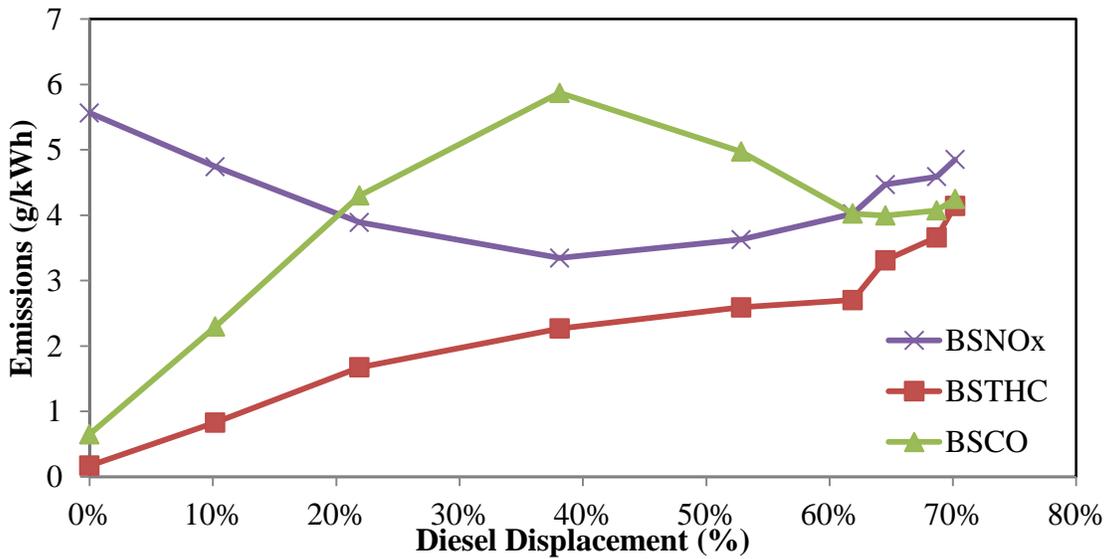
Figure 4.19: Various emissions as a function of diesel displacement at 75% load

Similar trends are noted for the 100% load point, shown in Figure 4. 20. However, there appears to be an outlier at 22% diesel displacement. Extremely high THC emissions are noted at

this point. It is unclear why there would be such a large increase at this condition. However, a corresponding increase in CO indicates that the increase may be a real effect since CO and THC often trend in the same direction. NO_x emissions gradually decrease with increasing diesel displacement, reaching a minimum at 40% diesel displacement, followed by a significant increase in NO_x continuing to the maximum diesel displacement.
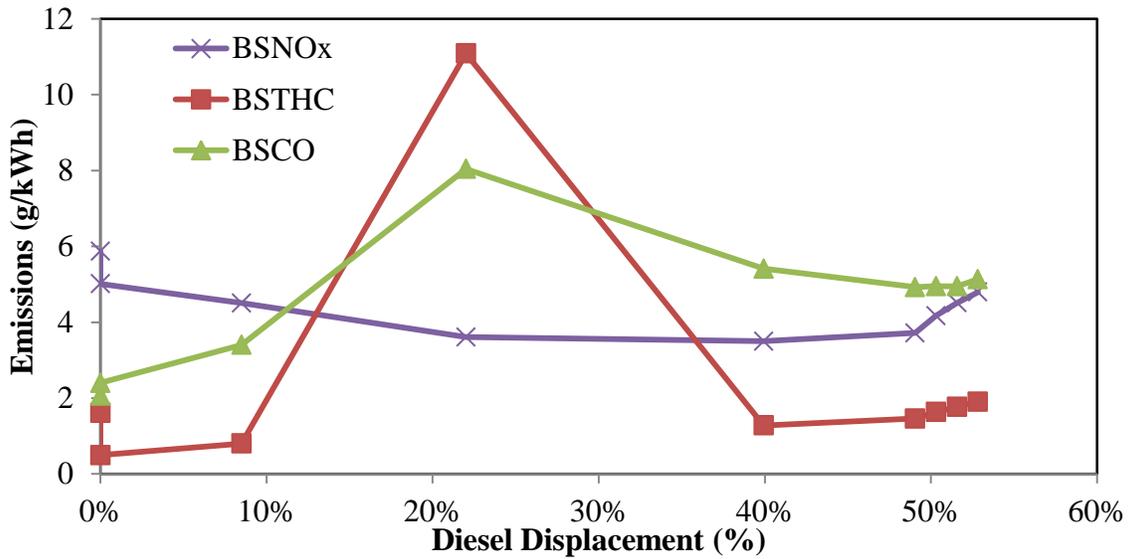
Figure 4. 20: Emissions trend as diesel displacement is varied at 100% load

4.5   The Effects of Diesel Injection Timing

A sweep of injection timing was also conducted at each load to note the effects on combustion and emissions. At each load, timing was both advanced and retarded around the stock SOI until engine instability (demonstrated by COV values greater than 8) or extremely high emissions levels were noted.

Figure 4.21 presents emission variations as injection timing is varied at 12% load. This shows all emissions trend upward with advancing timing until 14° bTDC. At more advanced

timings, emissions slightly decrease. It should be noted that at 12% load, it was occasionally difficult to maintain the target engine load of ~15 kW, and even a 5 kW deviation from the target represents a 30% change in load. This uncertainty is a potential factor in the variation of the brake-specific emissions at these loads. It shows that THC and NO_x emissions trend oppositely – with advances in timing, HC emissions decrease and NO_x increase. CO emissions are relatively independent of injection timing. As injection is advanced, more time as allotted for the production of NOx and peak pressure occurs earlier, producing higher peak pressure and temperature. THC decreases as due to higher combustion temperature and more time for combustion to occur before expansion.

Figure 4.22 illustrates emission variations as a function of injection timing at 25% load. At intermediate load, Figure 4.23 shows that THC and CO trend similarly, while NO_x trends in the opposite direction. Figure 4.24 and Figure 4.25 show brake specific emission variations when injection timing is varied at 75% and 100%, respectively. These show the same trending pattern as intermediate load, but at high loads all three emissions are on the same order of magnitude. CO emissions overtake THC emissions at high loads, whereas previously THC emissions were larger in magnitude. For all loads, it was observed that the ideal trade-off between minimizing both THC and NO_x emissions occurred at or very near the stock SOI. For this reason, stock timing was not changed during optimized testing.
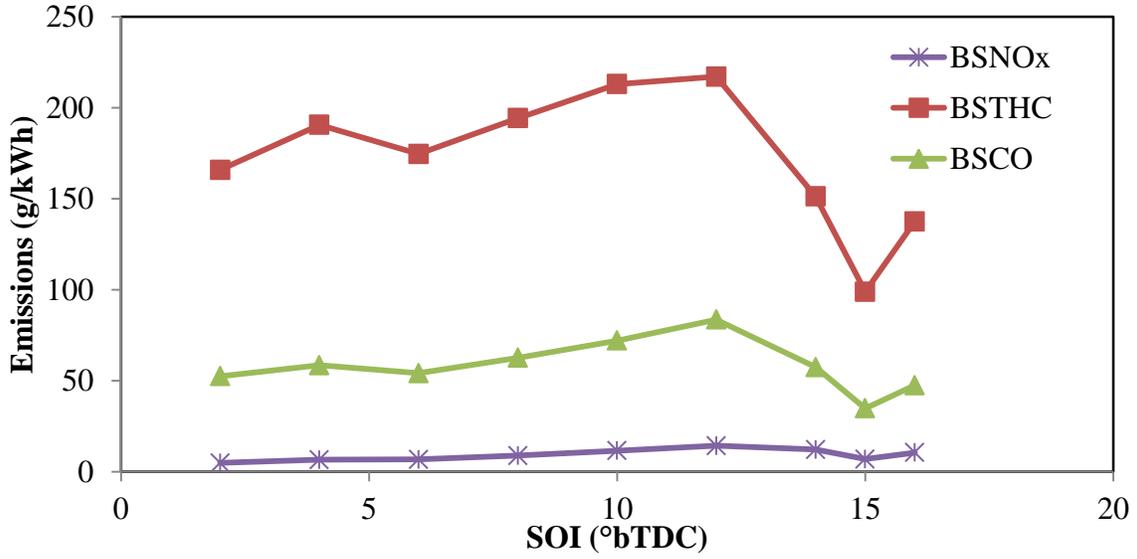
Figure 4.21: Emissions as a function of injection timing, 12% load.
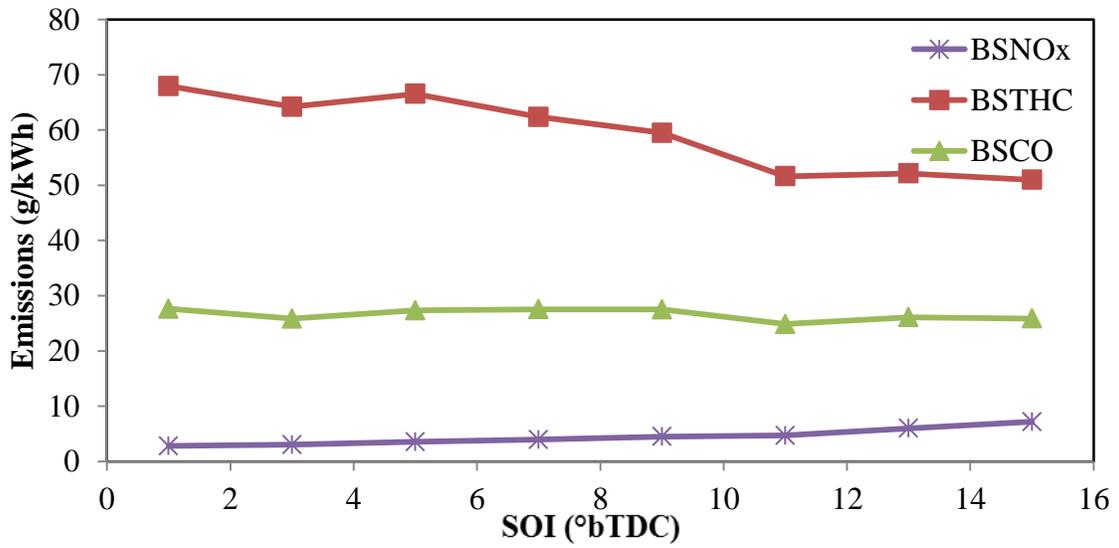
Figure 4.22: Emissions as a function of injection timing, 25% load.
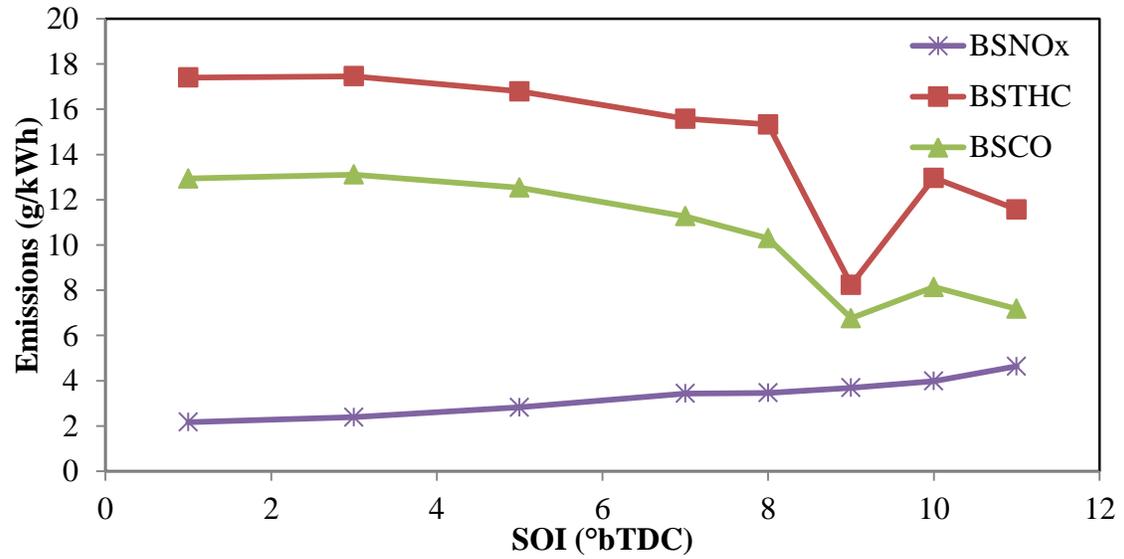
Figure 4.23: Emissions as a function of injection timing, 50% load
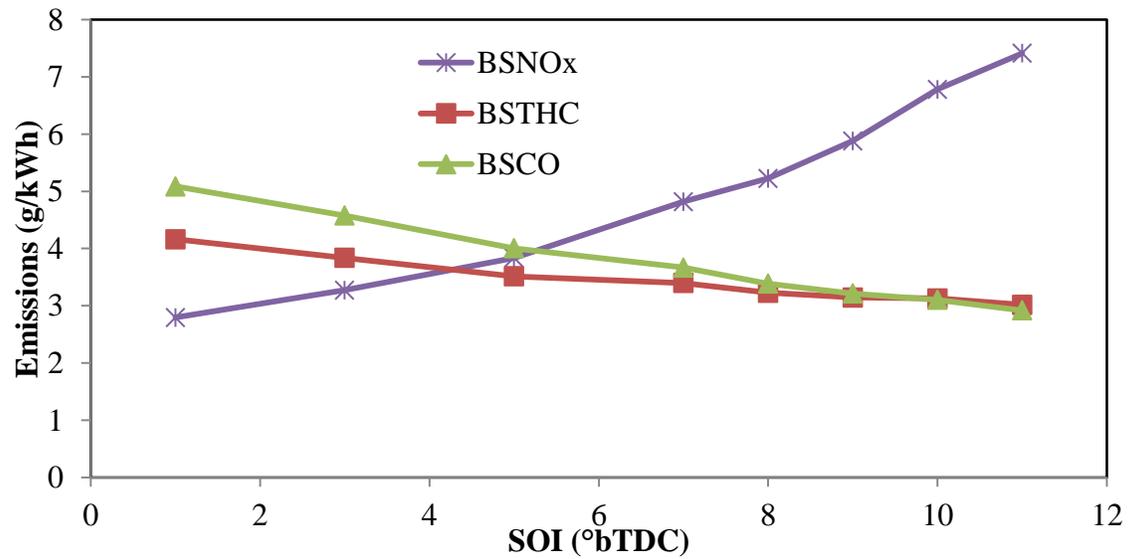
Figure 4.24: Emissions as a function of injection timing, 75% load
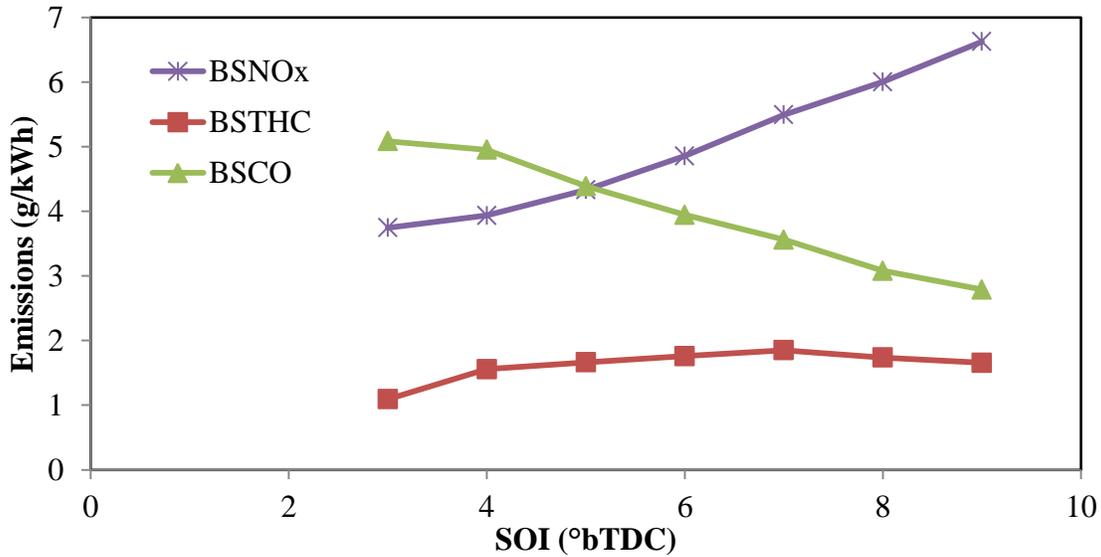
Figure 4.25: Emissions as a function of injection timing, 100% load

4.6   Optimization Testing

The two sweeps performed indicated two major factors influencing the decision of the "optimized" testing parameters:

1) At low loads, the dual fuel system provides more gas than can be utilized, resulting in very high THC and CO emissions.

2) Stock injection timing already represents a good compromise between THC and NO_x emissions, which trend in opposite directions. Moving the injection timing setpoint to improve one of these emissions would other emissions increasing.

Taking these factors into account, it was decided that the following load map as shown in Table 4.2 would represent an optimized profile. Because of the high THC and CO emissions at low loads, it was decided that dual fuel would be turned off until intermediate loads were reached. Subsequent target diesel displacements were determined by selecting the highest diesel displacement observed during the natural gas substitution sweeps which maintained engine

75

stability. Figure 4.26 shows emissions levels in diesel and dual fuel baseline, optimized dual fuel, and Tier II limit. Although emissions with optimized substitution map are still higher than limits, it shows an improvement when compared with dual fuel baseline emission.

Table 4.2: Dual fuel baseline and optimized loading map

Load	Baseline Dual Fuel Diesel Displacement	Target Diesel Displacement
12%	35%	0%
25%	60%	0%
50%	70%	76%
75%	70%	66%
100%	59%	52%
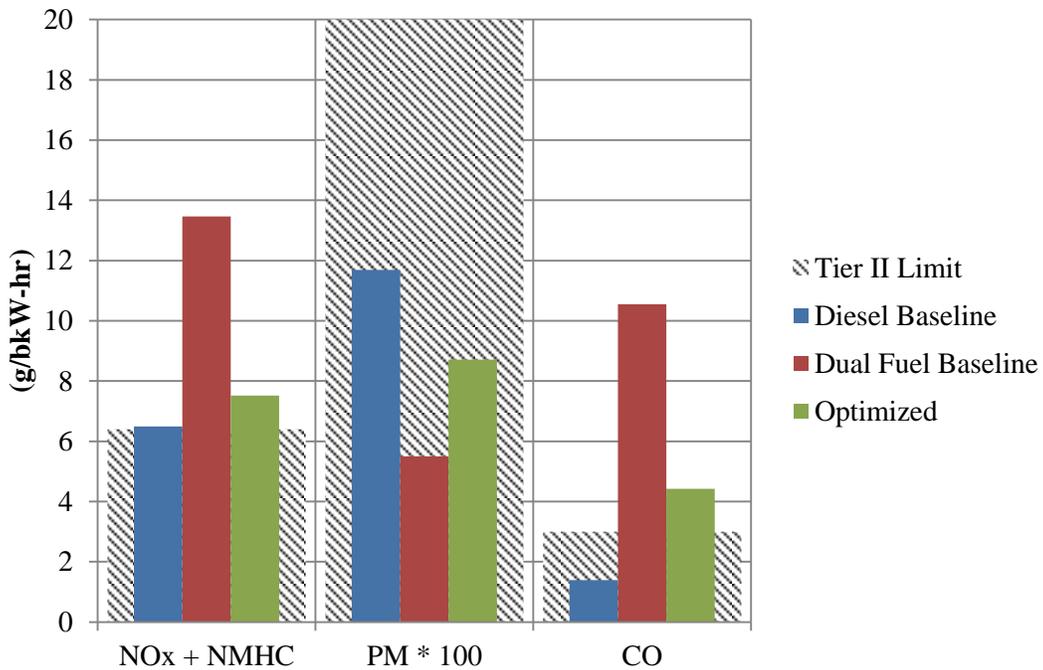
Figure 4.26: EPA regulated emissions for the diesel and dual fuel baselines and the optimized dual fuel map

5.0   CFD MODELING

CFD is an essential research tool for simulating engine combustion. It is able to provide information about combustion behavior and emissions formation in a cylinder with the help of mathematical equations. CFD is more reliable and accurate than before due to an increase in computer performance, advances in numerical algorithms, and the development of physical models. However, the physical and numerical processes involved are very complex. Therefore achieving accurate and reliable results with this tool requires extensive experience and skills in fluid dynamics and computation.

In this study, the CONVERGE CFD software is selected as the modeling tool for a number of numerical advantages in simulating flows in IC engines. For example, CONVERGE handles the moving boundaries in a completely automatic fashion and the deforming mesh issues typically associated with the moving parts are eliminated. Moreover, the true geometry is maintained during re-gridding. CONVERGE includes advanced numerical techniques and physical models describing processes of spray, turbulence and combustion, and the nonlinear interactions of such processes. . These models have been examined and extensively validated in IC engines. In this study, several models are included in order to improve the accuracy of diesel and dual fuel combustion using CONVERGE. The objective of modeling dual fuel combustion is to gain better understanding of the combustion behavior and the emission formation process in dual fuel engines. This modeling is performed in conjunction with experimental studies and the simulation results are validated by the experimental data.

5.1   Introduction

An investigation is performed on diesel and dual fuel combustion and emissions formation using CONVERGE. To reduce computational time, the computational domain is a

sector, 1/6 of the cylinder, with periodic boundaries. This sector includes one of the six nozzles of the diesel injector. To further reduce computational time, the compression, combustion, and expansion processes are simulated. The initial properties of residual gas, fuel, and air at intake valve closed (IVC) are specified using information from the experimental observations. The initial pressure, temperature, velocity and turbulence fields at IVC are iterated until it satisfies the motored pressure from experiments (the pressure was within 1%). A set of reduced kinetic mechanisms by Andrew et al. (54) are adopted to further reduce the computational effort. In this study, the gas phase of diesel is modeled as n-heptane because it has a Cetane number close to that of diesel fuel. However, diesel in its liquid state is modeled using the properties of diesel from the CONVERGE library. Natural gas is modeled as a mixture of methane, ethane and propane. The physical properties of the cylinder such as the dimension bore and stroke, injector nozzle diameter, and shape of the piston crown are obtained from John Deere. The Adaptive Mesh Refinement (AMR) is adopted based on temperature and velocity minimum cell size of 0.25mm. Near nozzle region, fixed embedding is used with cell size of 0.25mm. Two cases at low load and high load for each engine operating mode are modeled. Details about the physical models, fuel properties and mechanisms involved in this study are discussed in the following sections.

5.2   Spray Modeling

In a CI engine, liquid fuel spray is injected into the combustion chamber near the end of the compression stroke. After injection, the fuel spray undergoes atomization and vaporization processes, followed by fuel-air mixing. Ignition and combustion are integrated in time with those processes. Spray droplets are subject to several processes from the time of blob injection until the time of atomization. Table 5.1 shows a summary of selected spray models used in this study.

Table 5.1: Key spray processes used in this study using CONVERGE

Spray Model Physical Process	Models
Liquid injection	Blob injection
Spray breakup	Modified KH-RT
Liquid spray distance	0.99 x total liquid mass
Spray cone angle	25°
Drop drag	Dynamic drag models
Collision outcomes model	Post
Turbulent Dispersion	O'Rourke model
Drop/wall interaction	No Time Counter (NTC) collision

The primary breakup process of the liquid fuel is important as it influences downstream processes such as mixing, ignition and combustion. The spray model used in this study is based on the Lagrangian drop Eulerian type. The blob injection model is used to describe the initial injected droplet size (parent) where it is equal to the nozzle diameter. The hybrid Kelvin-Helmholtz Rayleigh-Taylor (KH-RT) description by Beala and Reitz is used in the droplet breakup model (55) . In this model, the primary atomization (child) process of the initial droplet is due to aerodynamically induced breakup using the KH instability analysis. This primary atomization is also encouraged by aerodynamics in the near-nozzle region and cavitation and turbulence from the injector nozzle. This is modeled using the Kelvin-Helmholtz-Aerodynamics Cavitation Turbulence (KH-ACT) by Som and Aggarwal (56). In addition to the KH breakup mechanism, RT instability is also believed to play an important role in droplet breakup mechanisms. The secondary breakup of these droplets is modeled as a competition between KH and RT mechanisms due to the rapid deceleration of the droplets. As seen in Figure 5.1, this hybrid KH-RT model allows the RT accelerative instabilities to affect all child droplets and does not use a breakup length to model primary breakup.

The droplet collision model is based on No Time Counter (NTC) model by Schmidt and Rutland (57). This model involves stochastic parcels sub-sampling within a cell, which result in faster and more accurate collision calculations. The spray-wall interaction (liquid drops with solid surfaces model used in this study is a hybrid wall film model. It includes the effect associated with a drop splash based on the Weber number.

Blob

KH and RT

KH
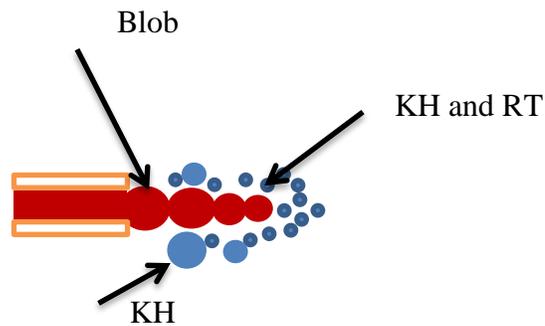
Figure 5.1: Schematic of the hybrid KH-RT breakup model

5.3 Combustion Modeling

The detailed chemistry or SAGE by Senecal (58) is used to model combustion. To solve chemical reactions, SAGE calculates the elementary reaction rate while CFD solves the transport equation. However, to reduce the computational expense, this detailed chemistry is only activated in cells that pass the minimum temperature and HC mole fraction specified in CONVERGE. In addition, to expedite the detailed chemistry calculations, the multizone chemistry model by Babajimopoulos (59) is also used. The multizone model groups cells that have similar thermodynamic states in zones. In this study, the variables of interest are temperature and reaction ratio. These zones are randomly distributed among different processors to balance the load, therefore reducing computation time.

Turbulence is modeled by the Renormalization Group (RNG) k-ε Reynolds Averaged Navier-Stokes (RANS) model. This RNG k-ε is more robust than the standard k-ε model. The model includes spray compressibility and the effect of turbulence interaction. It provides better predictions for streamline curvature, transitional flows, wall heat and mass transfer. The Turbulence Kinetic Energy (TKE) and Turbulent Dissipation (eps) initial values are provided accordingly. The heat transfer model by Han and Reitz (60) is considered and takes into account the effect of compressible flow. This model is developed from the assumption of one-dimensional energy conservation equation so that the analytical solution of the temperature profile can be obtained.

The shape of the injection rate for accurate combustion modeling is important. However, this information is unavailable; therefore, data is gathered from literature. The rate shape used in this study is based on the injector profile by Andrew et al. (54), which was taken originally from Perini et al. (61). In Perini's study, a set of injection rate shape at different injection pressure is published. Since the amount of the fuel injected and injection durations are different, the rate shape from Andrew et al. is modified according to the fuel amount and injection duration used in this study as seen in Figure 5.2.
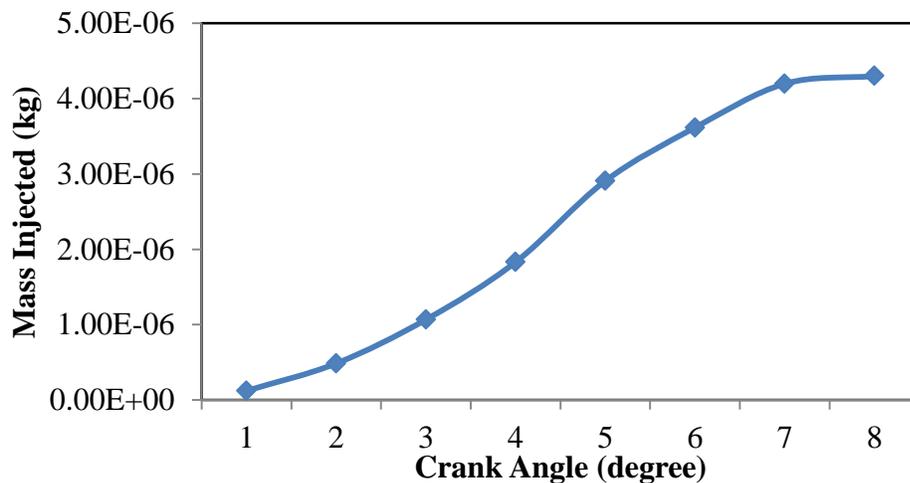
Figure 5.2: Injector rate shape used in this modeling

81

5.4   Reduced Mechanism

To make efficient calculations, the reduced primary reference fuel mechanism known as CSU86 is used. This reaction mechanism consists of 86 species and 393 reactions for n-heptane, methane, ethane and propane. This reduced mechanism is a combined version of the detailed mechanism from Healy et al. (62) and Yoo et al. (63). Healy et al. The detailed methane through n-pentane mechanism consists of 293 species and 1588 reactions. Yoo et al. n-heptane mechanism with 88 species is a reduced version from the detailed n-heptane mechanism from Curran et al. (64) with 561 species and 2539 reactions. Detailed description of the CSU86 mechanism is presented by Andrew et al. and will not be discussed in detail here.

5.5   Emissions Modeling

Emissions such as soot, NOx, HC and CO can be calculated in CONVERGE. The following section discusses the models of emissions used in this study.

5.5.1   Soot Modeling

The Hiroyasu-NSC model, proposed by Hiroyasu and Kadota is applied in the case of soot emissions (65). This model determines the production of soot mass, (M_s) by a single step competition between the soot mass formation rate ($\dot{M}_{sf}$) and soot mass oxidation rate ($\dot{M}_{so}$). According to

$$\frac{dMs}{dt} = \dot{M}_{sf} - \dot{M}_{so}$$

<div align="right">Equation 5.1</div>

the formation rate is proportional to the mass of soot formation species (M_{form}) given by

$$\dot{M}_{sf} = SF\ M_{form}$$

<div align="right">Equation 5.2</div>

and

$$SF = A_{sf}\, P^{0.5} \exp\left(\frac{-E_{sf}}{R_u T}\right)$$

Equation 5.3

P is the cell pressure in bar, R_u is the universal gas constant in *cal/Kgmol*, T is the cell temperature in *K*, E_{sf} is the activation energy in *cal/gmol*, and A_{sf} is the Arrhenius pre-exponential factor with units of $1/(s\ bar^{0.5})$.

The soot oxidation is modeled using the Nagle and Strickland-Constable (NSC) model (66). Based on the oxidation experiments of carbon graphite in an O_2 environment over a range of partial pressures, the oxidation rate is modeled by two mechanisms whose rates depend on the surface chemistry involving more reactive "A" sites and less reactive "B" sites. The oxidation rate of soot is given by

$$\dot{M}_{so} = SO\, M_s$$

Equation 5.4

where

$$SO = A_{so}\, \frac{6}{\rho_s D_s} R_{total} MW_c$$

Equation 5.5

A_{so} is the scaling factor, ρ_s is the soot density in g/cm^3, D_s is the nominal soot particle diameter in *cm*, and MW_c is the molecular weight of carbon.

5.5.2   NO$_x$ Modeling

In this study, NO formation is modeled using the extended Zel'dovich mechanism as presented by Heywood. This model consists of the following set of reactions:

$$O + N_2 \quad\longleftrightarrow\quad NO + N$$

$$N + O_2 \quad\longleftrightarrow\quad NO + O$$

$$N + OH \quad \leftrightarrow \quad NO + H$$
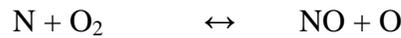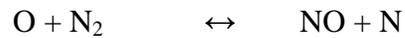
From the equations above and a steady state assumption for N, the NO formation rate is given as

$$\frac{d[NO]}{dt} = 2k_{R1,f}[O][N_2] \frac{1 - [NO]^2/(K[O_2][N_2])}{1 + k_{R1,r}[NO]/(k_{R2,f}[O_2] + k_{R3,f}[OH])}$$

Equation 5.6

where

$$K = (k_{R1,f}/k_{R1,r})(k_{R2,f}/k_{R2,r})$$

Equation 5.7

with rate constants for reaction

$$k_{R1,f} = 7.6 \text{ x } 10^{13} \exp(-38{,}000/T)$$

$$k_{R1,r} = 1.6 \text{ x } 10^{13}$$

$$k_{R2,f} = 6.4 \text{ x } 10^{9} \text{ T} \exp(-3150/T)$$

$$k_{R2,r} = 1.5 \text{ x } 10^{9} \text{ T} \exp(-19{,}500/T)$$

$$k_{R3,f} = 4.1 \text{ x} 10^{13}$$

$$k_{R3,r} = 2.0 \text{ x } 10^{14} \exp(-23{,}650/T)$$

Subscript "*f*" refers to forward reaction and subscript "*r*" denotes a reverse reaction.

6.0   CFD MODELING RESULTS AND DISCUSSION

The main objectives of CFD modeling are to understand dual fuel combustion and identify the locations of the formation of emissions in a cylinder. Ultimately, the purpose of this modeling is to prove the hypotheses made in the previous section. Test data is used to demonstrate the validity of the physical models adopted in the CFD simulations. Motored pressure, combustion pressure and net HRR resulted from of the simulations model are compared to the corresponding experimental results. This chapter discusses results from a set of simulation results for the 12% load and the 75% load, focusing on combustion behavior and emission formation in the dual fuel operations. Table 6.1 and Table 6.2 show some of the major results of the dual fuel experiments and modeling at 12% and 75% loads, respectively.

Table 6.1: A comparison of the main values in a dual fuel experiment and modeling at 12% load

Parameter	Experiment	Modeling
Start of Injection (°bTDC)	-6.5	-3.0
Injection Duration (°)	Not Measured	9.0
Peak Pressure (kPa)	4464	4379
Diesel Fuel Mass (kg)	1.89e-06	2.8e-06
Temperature at IVC (K)	314.6	398
Pressure at IVC (kPa)	178	92.5

Table 6.2: A comparison of the main values in a dual fuel experiment and modeling at 75% load

Parameter	Experiment	Modeling
Start of Injection (°bTDC)	-3.0	-5.5
Injection Duration (°)	Not Measured	10.0
Peak Pressure (kPa)	4382	4290
Diesel Fuel Mass (kg)	3.5e-06	4.5e-06
Temperature at IVC (K)	315	398
Pressure at IVC (kPa)	208	134.8

The mass injected is modified according to the injection rate shape and injection duration, as discussed in the previous section.

6.1   In-cylinder Pressure Comparison

The initial pressure is based on the experiment but carefully adjusted and iterated to obtain better results at peak motored pressure. The initial pressure values in Table 6.1 and Table 6.2 starts low, but the pressures rise to approach the experimental values. Figure 6.1 shows the comparison of motored pressure for experiment and simulation at 12% load, indicating that the experimental pressure profile is reproduced and matched in order to carry out the simulations at the same operating conditions.

Figure 6.2 compares the dual fuel experiment and simulation of motored pressure traces at 75% load. As can be seen, the initial pressure in a dual fuel simulation is set a little higher than the experiment to obtain a better peak pressure match.

Figure 6.3 depicts corresponding pressure variations as a function of crank position in a dual fuel experiment and simulation at 12% load. The dual fuel experiment curve represents an average of more than 100 cycles. While the motored peaks of both traces are matched, the simulation fails to reach a similar peak pressure as the experiment. The simulation pressure rises slightly earlier and falls lower than the experiment. The results show there is an approximately 2% error between simulation and experiment results. The predicted delay period from the simulation follows the experimental data.

Figure 6.4 shows the prediction of in-cylinder pressure with the corresponding data from the experiment at 75% load. The motoring pressure for both cases rise similarly. However, at 4° aTDC the simulation pressure decreases slightly. Then, at 11° aTDC the simulation pressure increases marginally higher than the experiment. This could be due to slightly high diesel mass

86

injection in the simulation. After 17°aTDC, the simulation pressure decreases earlier than experiment pressure. Despite this, the predicted results using the CSU86 mechanism is in good agreement to the experiment.

Figure 6.5 represents net HRR with a crank position at 12% load. The dual fuel simulation HRR shows slightly later development of combustion at 100 J/degree, while the experiment peaks at less than 80 J/degree. At this load, there is no significant mixing-controlled combustion. HRR continues at a lower rate for both conditions into the expansion stroke. At this point, a small amount of natural gas and n-heptane may have not yet burned as a result of incomplete combustion. Excess fuels end up in the exhaust as HC emission and a product of fuel-rich combustion such as CO. The results from the dual fuel experiment at this load show a higher amount of HC and CO emissions. The simulation goes beyond the predicted net HRR of a dual fuel in the experiment.
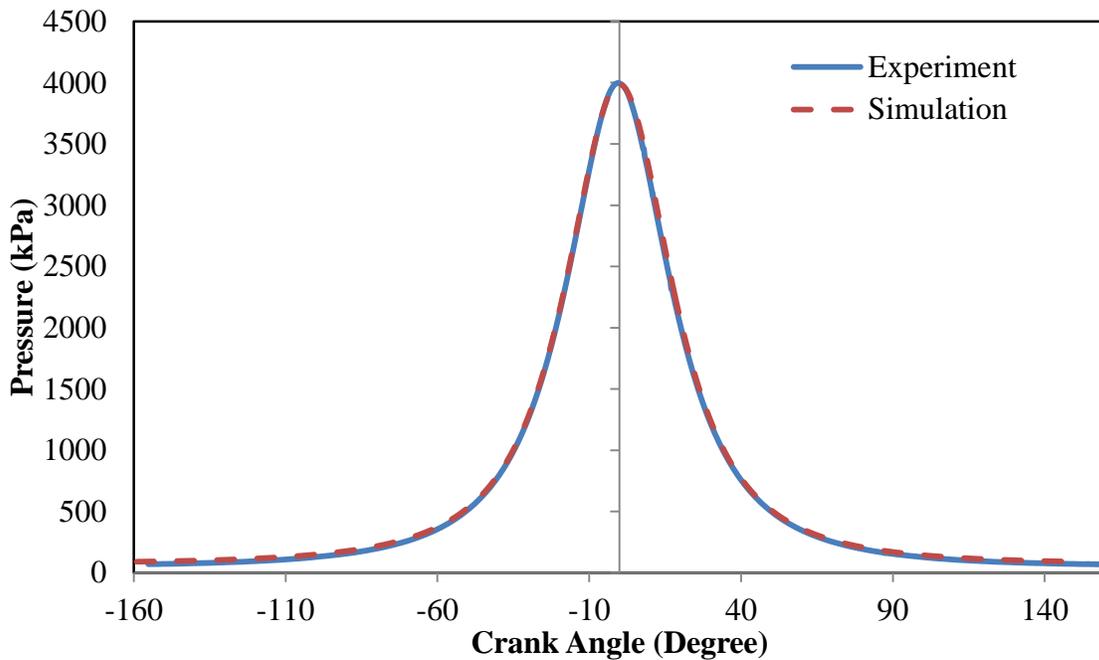
Figure 6.1: Motored pressure variations as a function of crank angle at 12% load
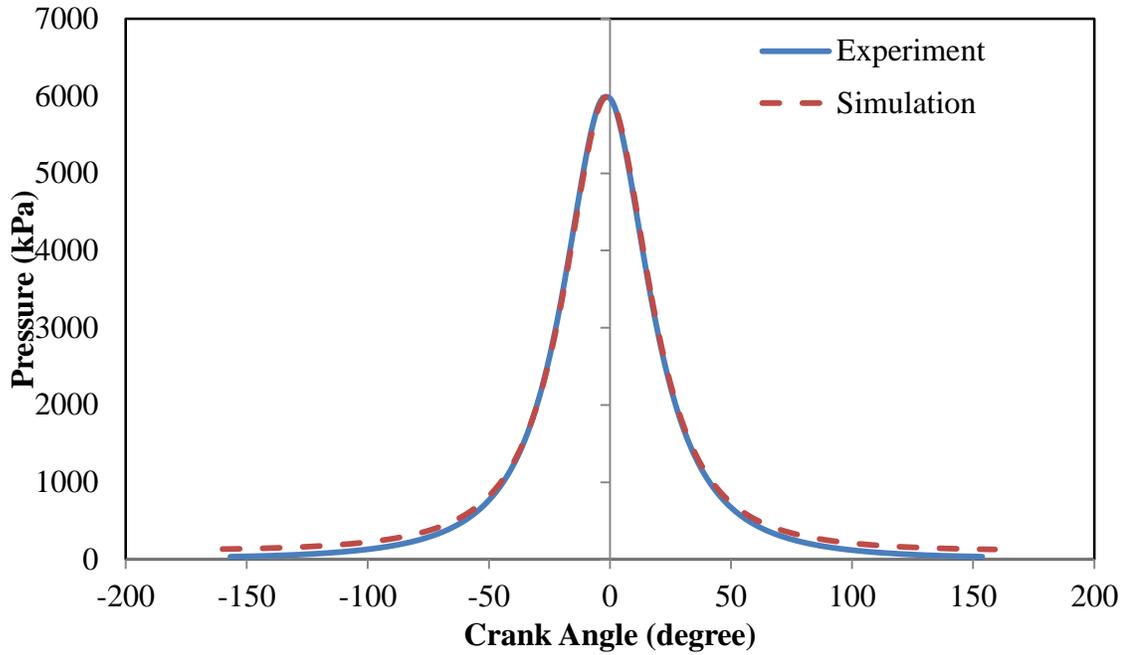
Figure 6.2: Motored pressure as a function of crank position at 75% load
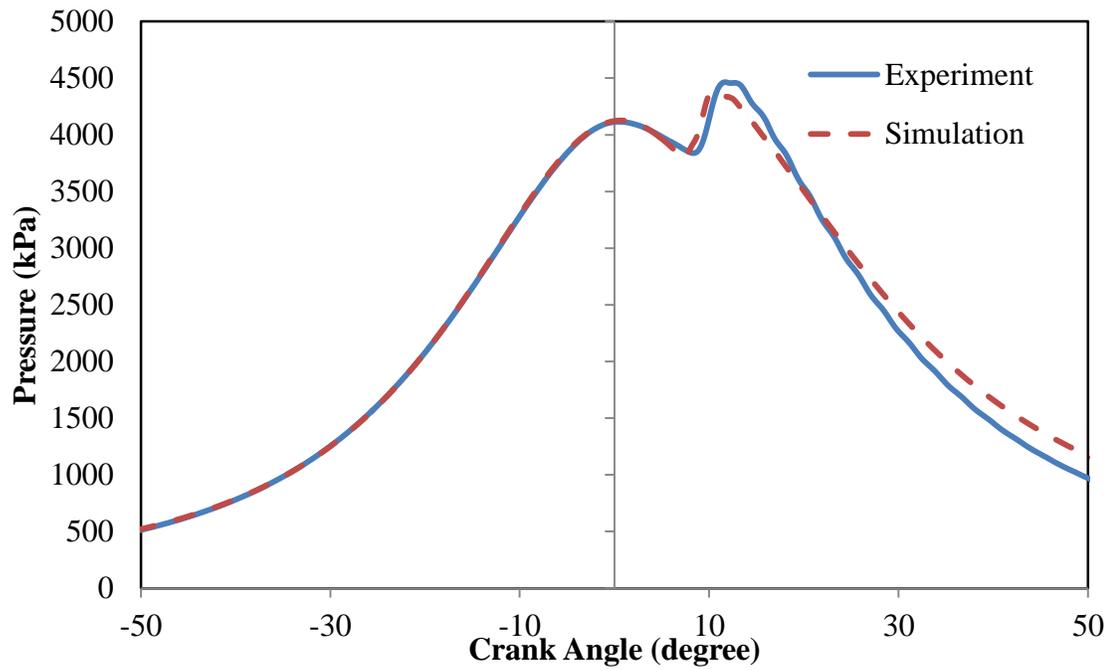
Figure 6.3: A comparison of pressure traces in a dual fuel experiment and simulation at 12% load
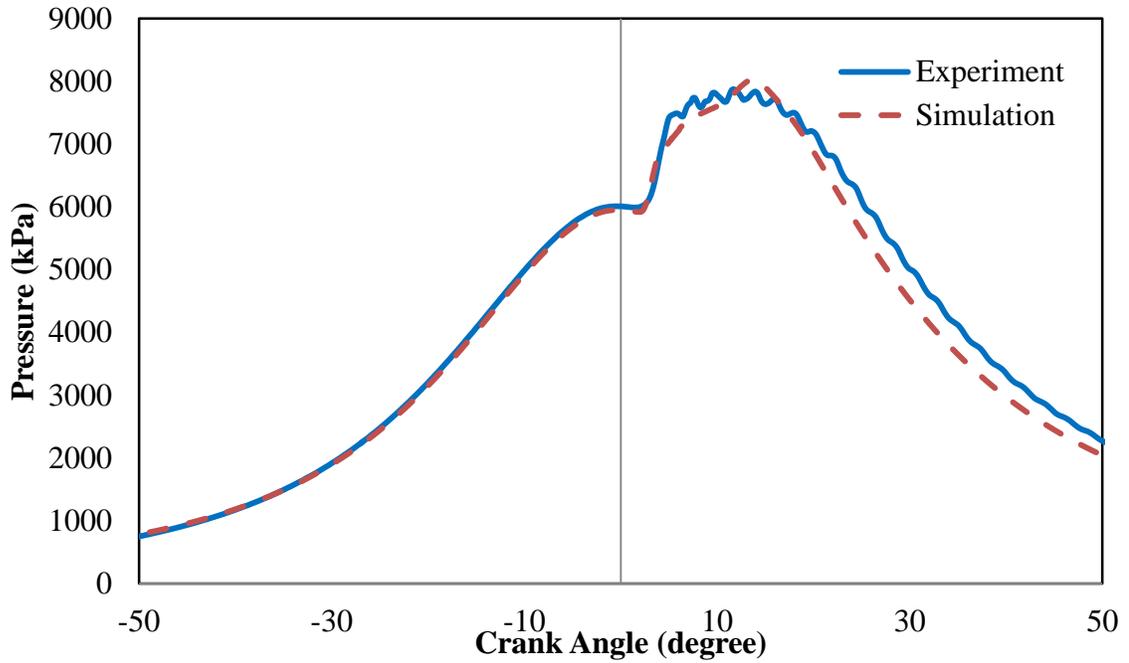
Figure 6.4: A comparison of pressure traces in a dual fuel experiment and simulation at 75% load
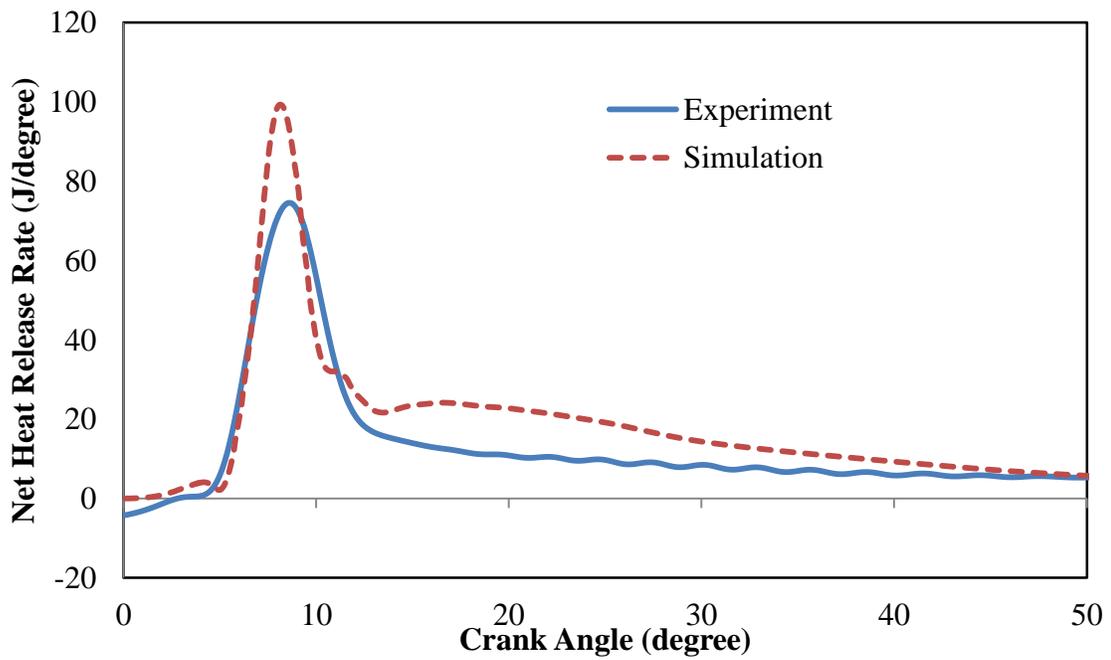
Figure 6.5: Net HRR for dual fuel experiment and simulation at 12% load

Figure 6.6 shows net HRR as a function of a crank angle at 75% load. At this load, both cases show two substantial phases. In diesel combustion, these peaks are identified as premixed and mixing-controlled combustion phases. However, in dual fuel combustion with natural gas as the primary fuel, these combustion phases should be reversed. The first peak is elevated shortly after diesel fuel injection. Since diesel combustion is primarily diffusion flame, therefore the combustion phase is described as mixing-controlled. The second peak rises due to natural gas combustion. Since natural gas is premixed, thus describes the second peak in Figure 6.6 as premixed combustion phase. In a dual fuel simulation, the heat release rises until it peaks at 170 J/degree. The experiment shows a steady increase of HRR which then peaks at 100 J/degree. After that, it decreases gradually into the lower rate of mixing controlled combustion phase. The more pronounced combustion during the premixed phase may result in high temperature which leads to a higher NO_x. As seen in Table 6.2, the injected diesel mass in simulation models is higher than the experiment. In this case, the HRR of the simulation goes beyond the values of the experiment. In dual fuel simulation, the heat release continues at a lower rate into late combustion phase at approximately 20° aTDC while, in dual fuel experiment the late combustion phase occurs at 25°aTDC. At approximately 30° aTDC both operations reach complete combustion.
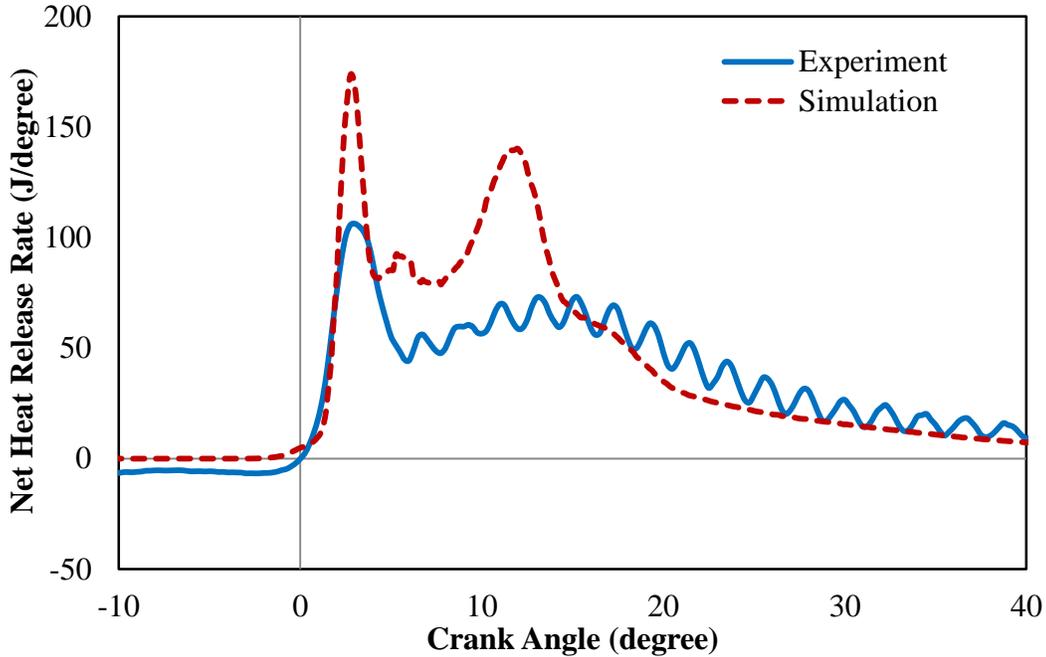
Figure 6.6: Net HRR as a function of a crank position at 75% load

6.2   Simulation Results

In this section, only dual fuel simulations at 12% and 75% loads are considered. As mentioned before, the purpose of this modeling study is to conduct an initial guide to better understand natural gas-diesel dual fuel combustion and emissions. Therefore, temperature contours, equivalence ratio, NO_x, soot, HC and CO emission mass fraction in dual fuel simulations at 12% and 75% loads are presented and discussed here.

6.2.1   Temperature Distributions

The temperature distributions in dual fuel engines at various crank positions are predicted using CONVERGE code as shown in Figure 6.7. The temperature profile is sliced through the spray axis. The temperature distribution at 12% load is presented on the left column, while the right column represents the distribution at 75% load. The green contours represent natural gas flame or premixed while diesel flames or non-premixed is illustrated by the red contours. The

data presented here is at odd crank starting at 5° until 27° aTDC. The 5° is chosen due to the significant temperature profile and emissions formation that occur in this stage. At crank angle of 27°aTDC, most dissociated product gases that appear at this crank position are assumed to exist in the exhaust as emissions.

The general flame structure in each load remains similar during the crank positions i.e. a flame is initially grow rapidly as a result of diesel fuel ignition and non-premixed combustion, then slows down as a result of natural gas premixed combustion. Comparing both loads at all crank positions, higher temperature flames are observed in 75% load than in 12% load. At 75% load, more diesel fuel mass is injected, therefore more volume charge is affected by diesel fuel combustion increasing the burning of natural gas and air mixture. At 12% load in contrast, many low temperature regions (blue contours) are observed as a result of incomplete combustion and fuel-rich combustion. Lower temperatures are expected in 12% load operation due to a leaner mixture and a smaller amount of diesel injected. This phenomenon is supported by lower net HRR at 12% load compared to 75% load, as shown in Figure 6.5 and Figure 6.6. At the end of the combustion at 29° aTDC, many regions are still unburned leading to higher HC and CO emissions in 12% load.

Crank Angle	12% Load	75% Load
5.0 °aTDC		

7.0 °aTDC	Crank angle = 7° Temp (K) 800 1250 1700 2150 2600	Crank angle = 7° Temp (K) 700 1175 1650 2125 2600
9.0 °aTDC	Crank angle = 9° Temp (K) 800 1250 1700 2150 2600	Crank angle = 9° Temp (K) 700 1175 1650 2125 2600
11.0 °aTDC	Crank angle = 11° Temp (K) 800 1250 1700 2150 2600	Crank angle = 11° Temp (K) 700 1175 1650 2125 2600
13.0 °aTDC	Crank angle = 13° Temp (K) 800 1250 1700 2150 2600	Crank angle = 13° Temp (K) 700 1175 1650 2125 2600

93

Figure 6.7: A set of temperature profiles at various crank angles at 12% and 75% loads

6.2.2 Equivalence Ratio Distributions

Φ is an important parameter that describes the formation of emissions inside the cylinder. HC, CO and NO_x emissions are affected by Φ. As the mixture goes richer, there is not enough oxygen to react with all the carbon and hydrogen, thus resulting in higher HC and CO emissions. HC is also high in very lean mixtures due to misfire and poor combustion. Peak NO_x is formed at Φ=0.95, which is a slightly leaner mixture. At this stage, the combustion temperature is high and not all O_2 reacts with N_2. Figure 6.8shows Φ distributions across the cylinder at crank angle 5° to 29° aTDC at 12% and 75% loads. In Figure 6.8, the rich region behavior is presented by red and green contours. It is clearly shown that the locations of rich region are different between the two cases. In 12% load, the rich region is identified mostly at piston bowl wall and near the clearance height wall. While, in 75% load the rich regions are located mostly at cylinder head. The Φ trend follows the diesel temperature flame propagations. For this reason, it is expected that the formations of HC and CO are high in these regions.

Crank Angle	12% Load	75% Load
5.0 °aTDC		

95

Crank angle = 7°	Crank angle = 7°
Crank angle = 9°	Crank angle = 9°
Crank angle = 11°	Crank angle = 11°
Crank angle = 13°	Crank angle = 13°

7.0 °aTDC

9.0 °aTDC

11.0 °aTDC

13.0 °aTDC

Equiv ratio
0.20   1.15   2.10   3.05   4.00

Equiv ratio
0.20   0.70   1.20   1.70   2.20
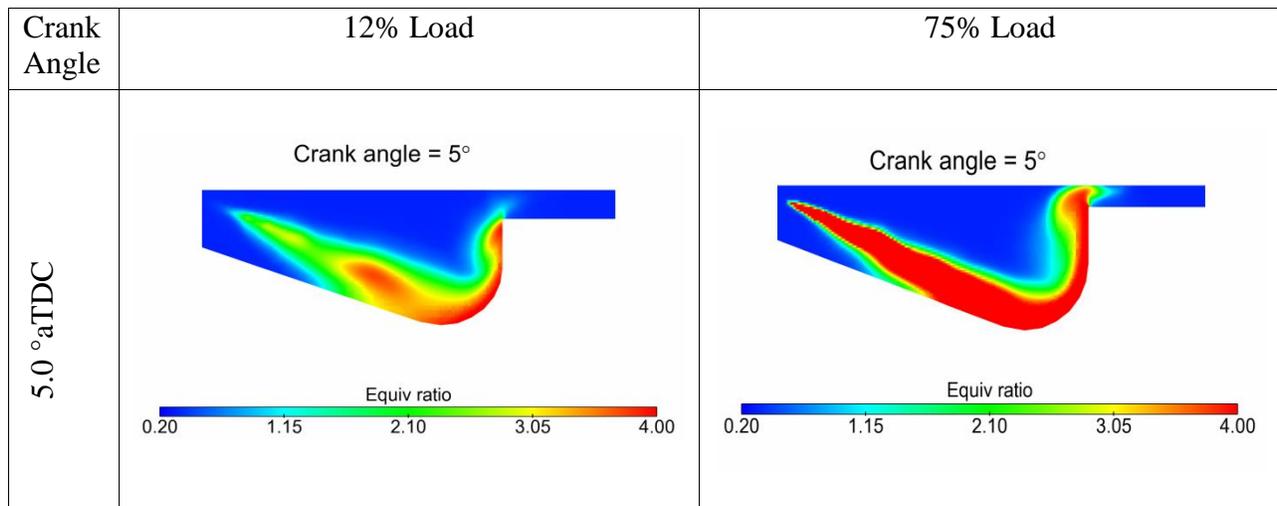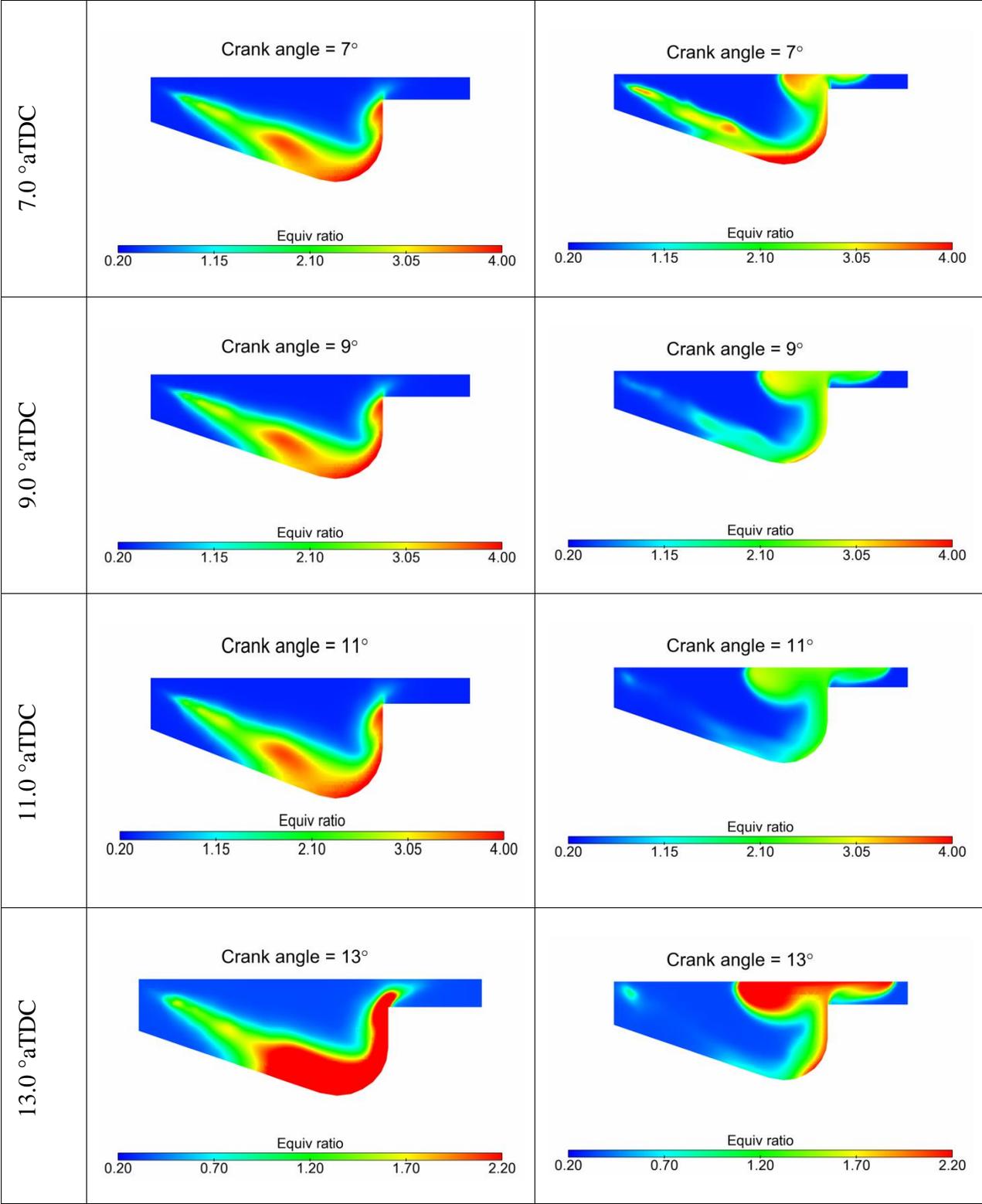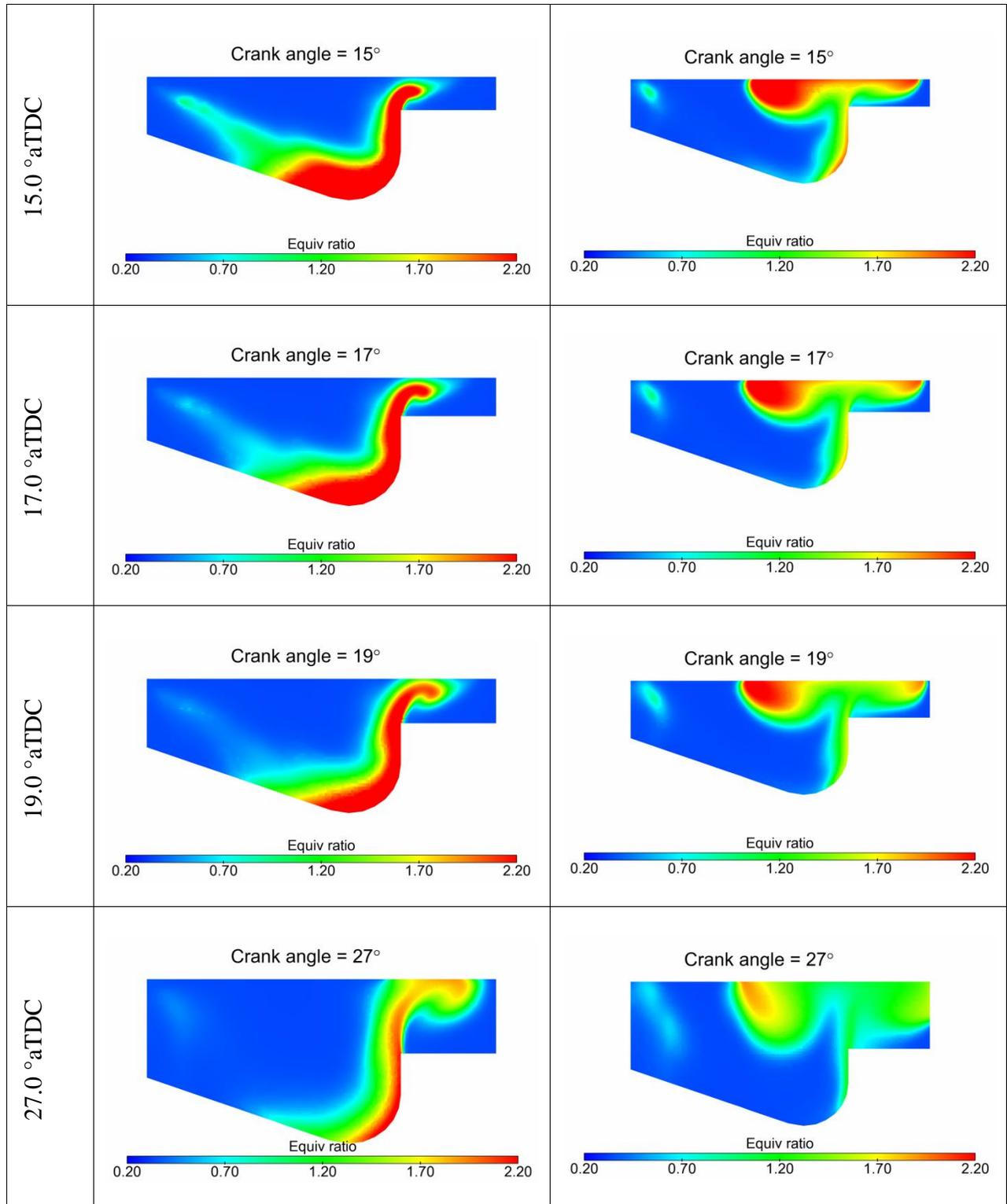
Figure 6.8: *Φ* distributions at 12% and 75% load.

6.2.3   CO Formations

The variations of CO emissions at various crank angles for 12% and 75% loads are presented in Figure 6.9. At 12% load, the formation of CO is mainly located near the piston bowl wall. At 75% load, CO emission is observed mostly at cylinder head. As presented in Figure 6.8, the locations of high CO is observed at high Φ, which explains the direct relationship of Φ and CO formation.

Crank Angle	12% Load	75% Load
5.0 °aTDC		
9.0 °aTDC		

11.0 °aTDC	Crank angle = 11° Mass Fraction CO 0.00 0.03 0.06 0.09 0.12	Crank angle = 11° Mass Fraction CO 0.00 0.03 0.06 0.09 0.12
13.0 °aTDC	Crank angle = 13° Mass Fraction CO 0.00 0.03 0.06 0.09 0.12	Crank angle = 13° Mass Fraction CO 0.00 0.03 0.06 0.09 0.12
15.0 °aTDC	Crank angle = 15° Mass Fraction CO 0.00 0.03 0.06 0.09 0.12	Crank angle = 15° Mass Fraction CO 0.00 0.03 0.06 0.09 0.12
17.0 °aTDC	Crank angle = 17° Mass Fraction CO 0.00 0.03 0.06 0.09 0.12	Crank angle = 17° Mass Fraction CO 0.00 0.03 0.06 0.09 0.12

Figure 6.9: Predicted CO mass fraction location at 12% and 75% loads

6.2.4 HC Formations

HC emissions are presented by unburned CH_4 fuel during the combustion process. Figure 6.10 shows the contours of CH_4 mass fraction for 12% and 75% load at various crank angle degrees. The view from on top of the Z- and spray axis is presented to illustrate HC emissions in a cylinder. At a crank position of 9° aTDC, a high amount of CH_4 is burned at 75% load, while some are left unburned near the cylinder and piston head. Compared to the 12% load, most of CH_4 is unburned during the combustion process at nozzle area, piston and cylinder head. Towards the end of the combustion phase at 27° aTDC, a very small amount of HC is observed in the 75% load while a large amount of CH_4 mass fraction is still unburned. At 75% load, two plane sections are shown to illustrate the location of HC emissions.

100

From the figure, it shows that the formation of HC in dual fuel combustion occurs due to the leaner mixture, and not the rich mixture. The effect is substantial in 12% load where the mixture is below the flammability limits. At 75% load, more diesel is injected even though the mixture is lean, thus promoting the combustion of the natural gas and air mixture.

Crank Angle	12% Load	75% Load
7.0 °aTDC		
9.0 °aTDC		
13.0 °aTDC		

15.0 °aTDC

Crank angle = 15°

Mass Fraction CH4
0.0000   0.0045   0.0090   0.0135   0.0180

Crank angle = 15°

Mass Fraction CH4
0.0000   0.0045   0.0090   0.0135   0.0180

17.0 °aTDC

Crank angle = 17°

Mass Fraction CH4
0.0000   0.0045   0.0090   0.0135   0.0180

Crank angle = 17°

Mass Fraction CH4
0.0000   0.0045   0.0090   0.0135   0.0180

19.0 °aTDC

Crank angle = 19°

Mass Fraction CH4
0.0000   0.0045   0.0090   0.0135   0.0180

Crank angle = 19°

Mass Fraction CH4
0.0000   0.0045   0.0090   0.0135   0.0180

Figure 6.10: Predicted HC emissions as CH_4 mass fraction across the cylinder at 12% and 75% loads

6.2.5   NOx Formations

The in-cylinder NO_x distribution in dual fuel is presented in Figure 6.11 at various crank positions starting at 11°aTDC. As seen, the NO_x locations are different between both cases. Both results depict that the NO_x location follows the temperature and Φ trends in Figure 6.7 and Figure 6.8. As discussed in Chapter 2.0, NO_x is mostly formed at maximum flame temperature, therefore high NO_x formation at these locations are expected. A very small mass fraction of NO_x (maximum of 0.002) is formed during the dual fuel combustion process as observed at 12% and 75% loads. The reason for the low formation of NO_x in dual fuel is due to the very lean mixture, with Φ ranging from 0.15 to 0.27. This statement is supported by the experimental values in Figure 4.11.

Crank Angle	12% Load	75% Load
11.0 °aTDC		
13.0 °aTDC		
15.0 °aTDC		
17.0 °aTDC		
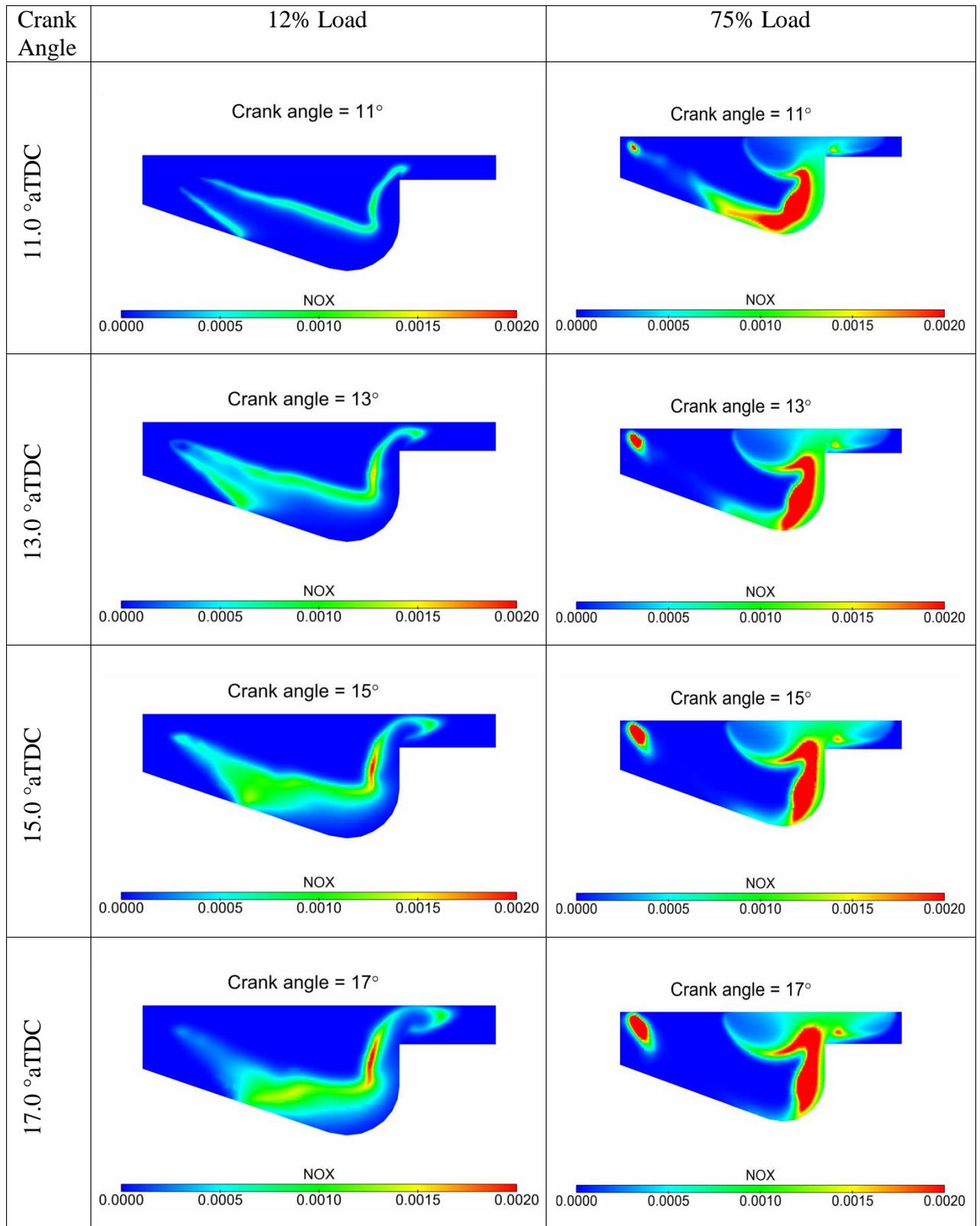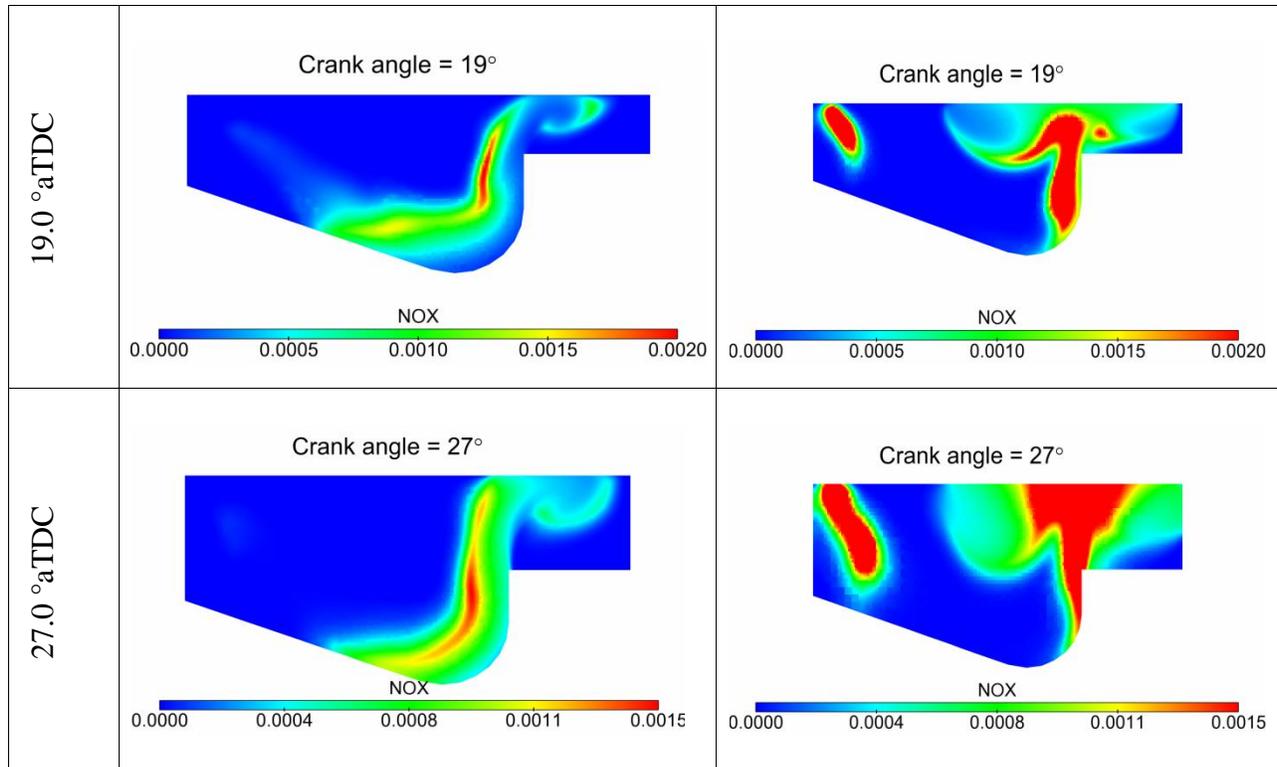
Figure 6.11: NO$_x$ formation as a function of crank positions at 12% and 75% loads

6.2.6 PM Formations

The location of PM formation for both 12% and 75% loads is illustrated in Figure 6.12. The PM formation in dual fuel simulation is modeled using Hiroyasu Soot models as described in Chapter 5.0. At 11° aTDC in 12% load, there is no significant PM is formed. High mass fraction of PM (red contours) is observed in the region where the Φ is more than 1.0. These richer regions are identified at the piston bowl rim, cylinder head and clearance height. Therefore, it is concluded that the soot is generated in the fuel-rich zone during the combustion where less oxygen is available to react with all carbons. Although the mass fraction of soot is high in this figure, the total soot formation is considered low with mass fraction of soot totaling less than 0.003.

105

Crank Angle	12% Load	75% Load
11.0 °aTDC	Crank angle = 11°	Crank angle = 11°
13.0 °aTDC	Crank angle = 13°	Crank angle = 13°
15.0 °aTDC	Crank angle = 15°	Crank angle = 15°
17.0 °aTDC	Crank angle = 17°	Crank angle = 17°
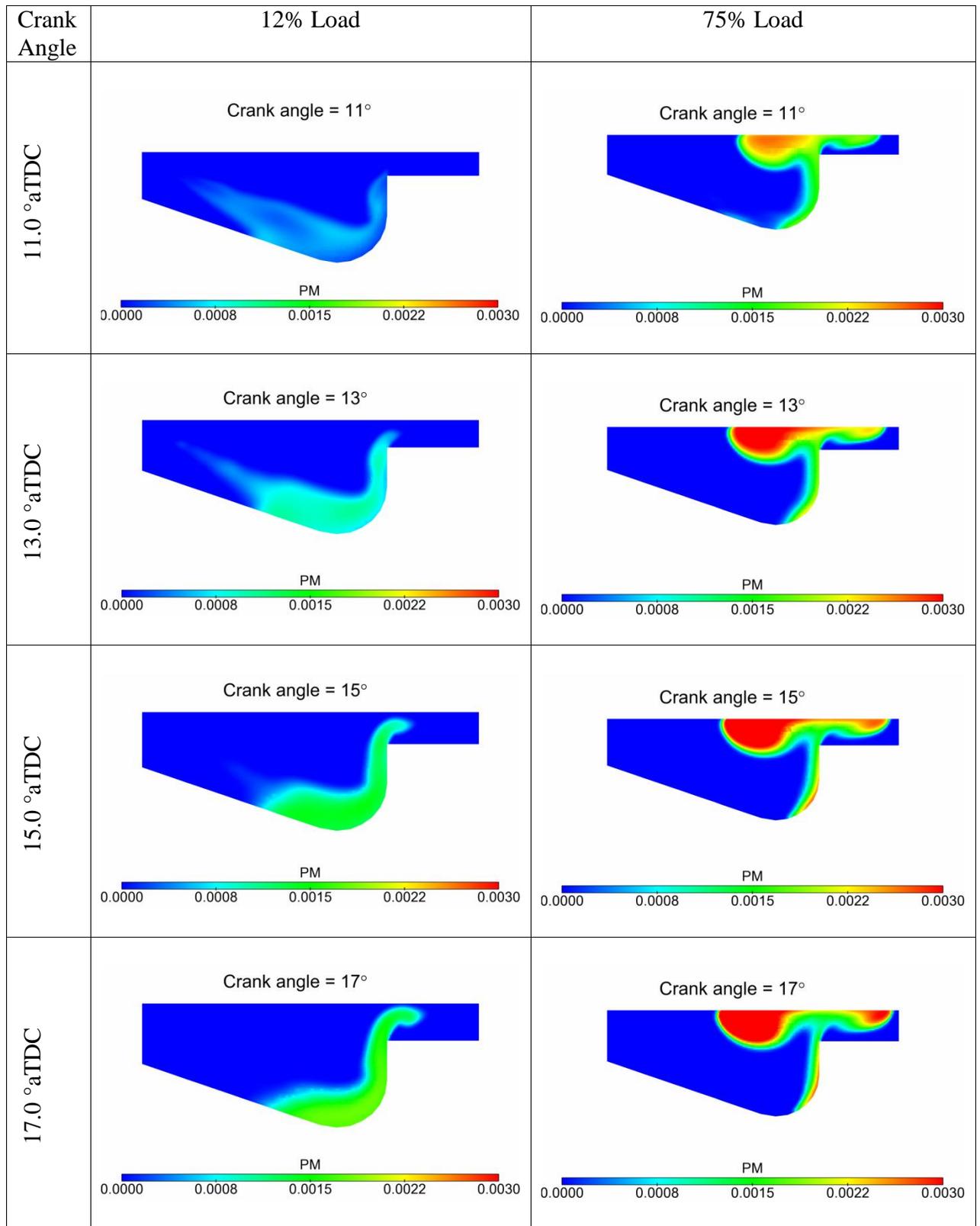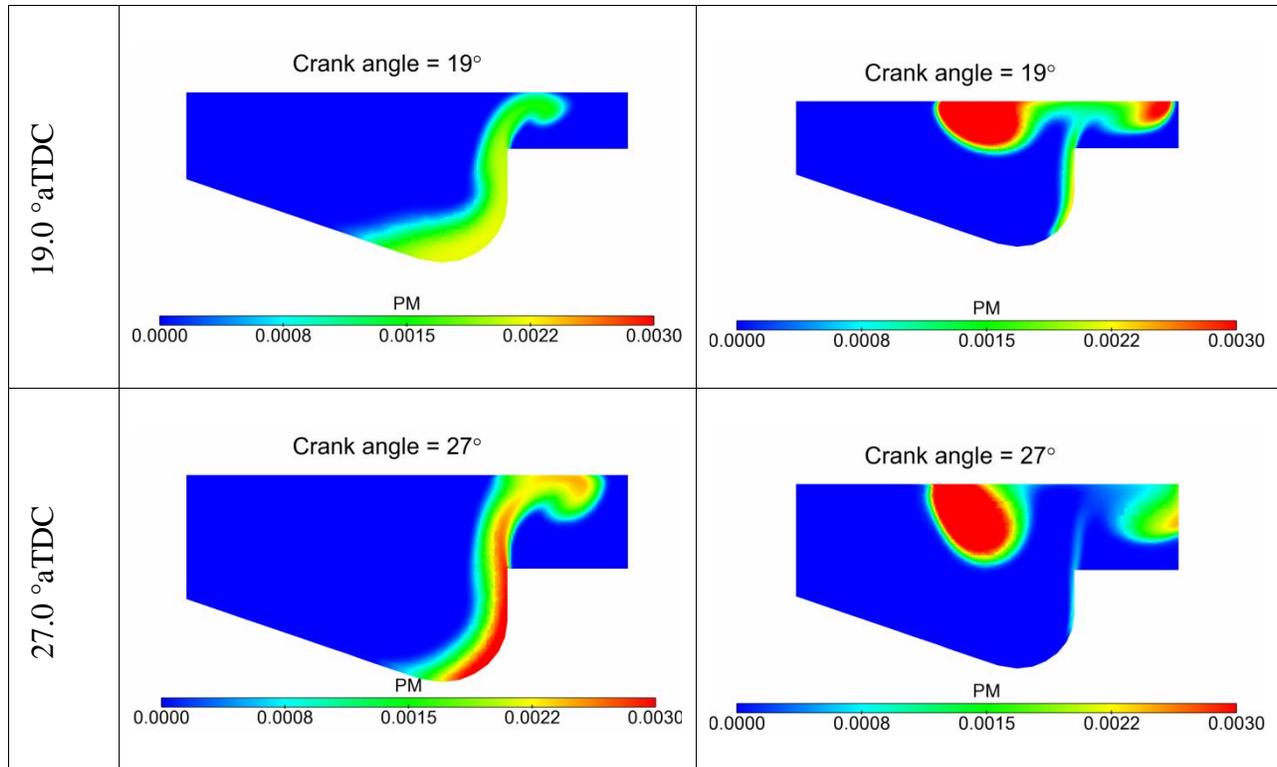
Figure 6.12: Predicted PM locations in a dual fuel combustion at 12% and 75% load

Figure 6.13: Emission comparisons in mg of experiment with simulation at 12% load

Emission	HC (mg)	CO (mg)	NO_x (mg)	PM (mg)
Dual Fuel Experiment	4.60	1.55	0.33	0.01
Dual Fuel Simulation	17.78	2.61	0.03	0.03

Figure 6.14: Emission comparisons in mg of experiment with simulation at 75% load

Emission	HC (mg)	CO (mg)	NO_x (mg)	PM (mg)
Dual Fuel Experiment	1.46	1.35	1.40	0.01
Dual Fuel Simulation	17.87	5.99	0.43	0.03

6.3 Conclusions

Findings from the CFD simulations using the CONVERGE software indicate that high CO and HC emissions in dual fuel operation at 12% and 75% loads. These formations are located mostly at the piston bowl wall, nozzle area, cylinder head and wall and piston head area. HC emissions are created where the mixture is lean. HC emission is significant at 12% load due to the excessive lean mixture and combustion flame from diesel fuel cannot propagate throughout the cylinder. For CO emission, it is observed high where the mixture is rich. In this region, less oxygen is available to combine with all the carbon. PM emission also increases with Φ. However, it is considered as low in dual fuel operation with 3 decimals mass fraction. On the other hand, NO_x is observed high in maximum flame temperature regions and stoichiometric mixture. These regions are illustrated as red contours in Figure 6.7 and green contours in Figure 6.8.

It is concluded that the CSU86 mechanism is able to predict pressure and HRR profiles in dual fuel combustion. The simulation pressure, HC, CO, NO_x and PM emissions are in good agreement with experiment. Although the simulation HRR is over predicted than in the experiment, it showed the same feature of a premixed and non-premixed combustion phase.

7.0   CONCLUSIONS AND FUTURE WORK

7.1   Overview

An experimental evaluation of the combustion characteristics, fuel cost savings through diesel displacement, efficiency and emissions benefits of a natural gas-diesel dual fuel engine have been performed. This research provides solution for high fuel cost and a high NO_x and PM emission associated with diesel engine as well as addresses the key challenges related to natural gas-diesel dual fuel engines.

The findings have addressed the research objectives:

1) Evaluate the emissions and performance of a dual fuel engine and compare the results with the diesel equivalent.

2) Develop an emissions control methodology in order to maintain applicable regulatory standards on emissions levels.

3) Investigate in-cylinder combustion by implementing the CFD simulation using CONVERGE code with a reduced chemical-kinetic mechanism for time saving. The location where the emission is formed will be investigated as well.

The completed work supports the earlier hypotheses:

1) Dual fuel operation saves cost compared to diesel operation through diesel displacement. Natural gas fuel prices have remained well below that of diesel fuel and have been more consistent compared to diesel fuel. Therefore, when natural gas is introduced in diesel engine, it displaces some of the diesel fuel in compression ignition engine.

2) Dual fuel engines reduce NO_x and PM emission compared to diesel engines. Natural gas combustion with methane as a lowest member in paraffin family is expected to produce less PM. In addition, the premixed combustion in dual fuel engine reduces the formation of locally rich mixtures. Therefore, with lean conditions, the flame temperature is lower, thus reduces the NO_x formation in dual fuel engine.

3) Dual fuel engines emit excessive HC and CO. The Φ for the natural gas and air entering the cylinder is below the flammability limit and the penetration of the diesel fuel jet does not extend across the cylinder. In addition, the flame temperature does not propagate through the lean mixture. Consequently, regions near the edge of the combustion chamber with natural gas and air mixtures below the flammability limit are either unburned (HC emission) or partially burned (CO emission).

7.2   Conclusions

An experimental evaluation of the cost, performance and emissions benefits of a diesel-dual fuel engine has been performed. Significant diesel displacement is achieved at all loads, with the maximum of 70% at 50% load and 61% cost reduction associated with dual fuel engine. Dual fuel reductions in NO_x and PM emissions are demonstrated but considerably higher CO and THC emissions results from dual fuel operations especially at low loads. It is observed that HC emission is formed where the mixture ratio is lean at low loads. On the other hand, CO emission is formed where the mixture is rich. EPA regulated NOx + NMHC and CO emissions are exceeded for dual fuel operation.

Conclusions from the experimental work comparing diesel and dual fuel baseline and optimization testing are given below:

1) Significant diesel displacement is achieved at all loads with a maximum of 70% at 50% and 75% loads. The maximum fuel cost saving with up to 61% of cost reduction can be achieved when the dual fuel engine operates at 50% load. Maximum 58% cost saving can be accomplished when running in optimized dual fuel mode at 75% load.

2) The natural gas and air Φ obtained ranges from 0.15 to 0.27, which is well below the limit of laminar flammability (0.46 for methane).

3) Higher levels of COV of peak pressure are observed at intermediate and high loads with maximum of 3.08 for dual fuel engine.

4) The dual fuel engine exhibits higher COV of IMEP compared to diesel at all loads. Maximum COV of IMEP is observed at 25% load with COV is 8.9 for dual fuel engine.

5) The ignition delay in dual fuel engine based on 0-10% burn duration analysis is higher at all loads. The primary phase of combustion which is presented as 10-90% burn duration is also higher in dual fuel engine than diesel at all loads.

6) At 12% and 25% loads, the dual fuel engine in-cylinder pressure is lower than diesel baseline. At 12% load, the peak HRR reduction in dual fuel engine is 17% while at 25% load, the reduction of peak HRR is approximately 40%.

7) At 50%, 75% and 100% loads, the in-cylinder pressure for dual fuel operation is improved with a slightly higher than the diesel engine. The HRR profiles showed two peaks in both operations except at 50% load where one peak is observed in dual fuel engine. The dual fuel HRR rising earlier than diesel at these loads.

8) Diesel operation produces higher brake thermal efficiency at low load whereas dual fuel achieves higher brake thermal efficiency at intermediate and high loads.

9) NO_x and PM emissions are demonstrated in dual fuel operation, while considerably higher CO and HC emissions were resulted from dual fuel operation.

10) EPA regulated NO_x + NMHC and CO emissions are exceeded for dual fuel operations. In dual fuel baseline, the EPA regulated NO_x + NMHC emission is doubled than in diesel baseline. This was due to the NMHC increasing by 97% while NO_x was reduced by 34%. The dual fuel engine also produces EPA regulated CO emission seven times higher than in diesel engine. On the contrary, the EPA regulated PM emission in dual fuel engine shows 50% reduction than diesel engine.

11) In order to optimize dual fuel performance and emission, a diesel displacement and injection timing sweep were conducted. Taking these factors into account, it is suggested to turn off dual fuel at low loads and increasing the diesel displacement at intermediate and high loads.

Conclusions for the investigation into dual fuel combustion and emissions using CONVERGE and CSU86 reduced mechanism at 12% and 75% loads are as follows:

1) Overall, the peak pressure in dual fuel simulation is slightly higher than dual fuel experiment. The HRR is over predicted compared to the experiments.

2) Findings showed that CO formation in 12% load of dual fuel engine is mainly located at the piston bowl rim. While in 75% load, the formation of CO is observed mostly at cylinder head.

3) At low load, HC emission is observed higher than at high load especially around the injector. From the simulation results, it is revealed that HC formation in dual fuel operation occurs due to lean mixture of natural gas and air.

4) From the CFD results, low PM and NO_x mass fraction is observed in dual fuel engine.

5) The CSU86 reduced mechanism is able to predict experimental pressure and HRR in dual fuel engine for two different loads and injection timings.

7.3 Research Recommendations

In order to develop general overview of dual fuel engine combustion and emission, additional work on simulation at 25%, 50% and 100% is recommended. The effort should include the injection timing and diesel displacement variations, and the effects of these parameters on combustion and emission in dual fuel engine. To reduce and control further the CO and HC emissions in dual fuel engine, the use of oxidation catalyst is recommended. Engine testing incorporating the use of oxidation catalyst would allow further optimization of the dual fuel system.

REFERENCES

1. **Pulkrabek, Willard W.** *Engineering Fundamentals of the Internal Combustion Engine.* Upper Saddle River (New Jersey) : Pearson Prentice-Hall, 2004 .

2. **Gupta, H. N.** *Fundamentals of Internal Combustion Engines.* Delhi : PHI Learning Private Limited, 2013.

3. **Heywood, John B.** *Internal Combustion Engine Fundamentals.* New York : Tata McGraw-Hill, 1988.

4. **Moore, Malcolm.** *China considers introducing carbon emission targets .* Shanghai : The Telegraph, 2009.

5. **NACS.** The Association for Convenience & Fuel Retailing. [Online] 2013. www.nacsonline.com.

6. U.S. Department of Energy. [Online] 2014. www.eia.gov.

7. **Doane, Seth.** *Beijing pollution forces students to play under dome.* Beijing : CBN News, 2013.

8. *Sensitivity of dual fuel engine combustion and knocking limits to gaseous fuel composition.* **Selim, Mohamed Y.E.** 2004, Energy Conversion and Management, pp. 411-425.

9. *Effect of engine parameters and type of gaseous fuel on the performance of dual-fuel gas diesel engines—A critical review.* **Sahoo, B.B., Sahoo, N. and Saha, U.K.** 2009, Renewable and Sustainable Energy Reviews, pp. 1151–1184.

10. *Effect of compression ratio on performance, combustion and emission characteristics of a dual fuel diesel engine run on raw biogas.* **Bhaskor J. Bora,Ujjwal K. Saha, Soumya Chatterjee and Vijay Veerb.** 2014, Energy Conversion and Management, pp. 1000–1009.

11. *Effects of chemical compositions and ensiling on the biogas productivity and degradation rates of agricultural and food processing by-products.* **Kafle, Gopi Krishna and Kim, Sang Hun.** 2013, Bioresource Technology, pp. 553-561.

12. *Effects of mixing system and pilot fuel quality on diesel-biogas dual fuel engine performance.* **Bedoya, Iván Darío, Arrieta, Andrés Amell and Cadavid, Francisco Javier.** 2009, Bioresource Technology, pp. 6624-6629.

13. *Effect of carbon dioxide on the performance of biogas/diesel duel-fuel engine.* **Bari, Saiful.** 1996, Renewable Energy, pp. 1007-1010.

14. Wikipedia. [Online] 2014. http://en.wikipedia.org/wiki/Biogas.

15. *Performance and emission comparison of a supercharged dual-fuel engine fueled by producer gases with varying hydrogen content.* **Murari Mohon Roy, Eiji Tomita, Nobuyuki Kawaraha, Yuji Hadara and Atsushi Sakane.** 2009, International Journal of Hydrogen Energy, pp. 7811–7822.

16. *Comparative performance studies of a 4-stroke CI engine operated on dual fuel mode with producer gas and Honge oil and its methyl ester (HOME) with and without carburetor.* **Banapurmath, N.R. and Tewari, P.G.** 2009, Renewable Energy, pp. 1009-0015.

17. *Effect of Pilot Fuel Quantity on the Performance and Emission of a Dual Producer Gas– Diesel Engine.* **Sombatwong, Pisarn, Thaiyasuit, Prachasanti and Pianthong, Kulachate.** 2013, Energy Procedia, pp. 218-227.

18. *Experimental Investigation on Attenuation of Emission with Optimized LPG Jet Induction in a Dual Fuel Diesel Engine and Prediction by ANN Model.* **Renald, C.J. Thomas and Somasundaram, P.** 2012, Energy Procedia, pp. 1427-1438.

19. *Experimental studies on homogeneous charge CI engine fueled with LPG using DEE as an ignition enhancer.* **Jothi, N.K. Miller, Nagarajan, G. and Renganarayanan, S.** 2007, Renewable Energy, pp. 1581–1593.

20. **Shinichi Goto, Daeyup Lee, Joseph Shakal, Naoya Harayama, Fumitaka Honyo and Hiroki Ueno.** *Performance and Emissions of an LPG Lean-Burn Engine for Heavy Duty Vehicles.* s.l. : SAE Technical Paper, 1999. 1999–01-1513.

21. *Effect of variation in LPG composition on emissions and performance in a dual fuel diesel engine.* **Saleh, H.E.** 2008, Fuel, pp. 3031-3039.

22. *Performance and gaseous and particle emissions from a liquefied petroleum gas (LPG) fumigated compression ignition engine.* **N.C.Surawski, B.Miljevica,T.A. Bodisco, R.Situ, Z.D.Ristovski and R.J. Brown.** 2014, Fuel, pp. 17-25.

23. *Effect of hydrogen and LPG addition on the efficiency and emissions of a dual fuel diesel engine.* **Lata, D.B., Misra, Ashok and Medhekar, S.** 2012, International Journal of Hydrogen Energy, pp. 6084–6096.

24. *Investigations on the combustion parameters of a dual fuel diesel engine with hydrogen and LPG as secondary fuels.* **Lata, D.B., Misra, Ashok and Medhekar, S.** 2011, International Journal of Hydrogen Energy, pp. 13808–13819.

25. *Towards improvement of natural gas-diesel dual fuel mode: An experimental investigation on performance and exhaust emissions.* **Mohand Said Lounici,Khaled Loubar, Lyes Tarabet, Mourad Balistrou, Dan-Catalin Niculescu and Mohand Tazerout.** 2014, Energy, pp. 200-211.

26. *Combustion and exhaust emission characteristics of a dual fuel compression ignition engine operated with pilot Diesel fuel and natural gas.* **Papagiannakis, R.G and Hountalas, D.T.** 2004, Energy Conversion and Management, pp. 2971–2987.

27. *Experimental investigation concerning the effect of natural gas percentage on performance and emissions of a DI dual fuel diesel engine.* **Papagiannakis, R.G and Hountalas, D.T.** 2003, Applied Thermal Engineering, pp. 353–365.

28. *Emission characteristics of high speed, dual fuel, compression ignition engine operating in a wide range of natural gas/diesel fuel proportion.* **Papagiannakis, R.G., et al., et al.** 2010, Fuel, pp. 1397–1406.

29. *Experimental study of the effects of natural gas injection timing on the combustion performance and emissions of a turbocharged common rail dual-fuel engine.* **Bo Yang, Xing Wei, Chengxun Xi, Yifu Liu, Ke Zheng and Ming-Chia Lai.** 2014, Energy Conversion and Management, pp. 297–304.

30. *Emissions and efficiency evaluations of a 6.8 liter diesel derivative dual fuel engine.* **Wan Mansor, Wan Nurdiyana, Vaughn, Jennifer S. and Olsen, Daniel B.** Toronto : s.n., 2014. Proceedings of The Canadian Society for Mechanical Engineering International Congress.

31. **Laboratory, National Energy Technology and Energy, U.S. Department of.** U.S. Department of Energy. [Online] 2005. http://energy.gov/sites/prod/files/2013/04/f0/LNG_primerupd.pdf.

32. *The Expansion of Unconventional Production of Natural Gas (Tight Gas, Gas Shale and Coal Bed Methane).* **Alonso, Alejandro Suarez.** s.l. : Intech, 2012, Advances in Natural Gas Technology, pp. 123-146.

33. **Perry, Kent F.** *Hydraulic Fracturing – A Historical and Impact Perspective.* Texas : Gas Technology Institute, 2010. Slide 33.

34. *Combustion and emissions characteristics of a dual fuel engine operated on alternative gaseous fuels.* **Mustafi, Nirendra N., Raine, Robert R. and Verhelst, Sebastian.** 2013, Fuel, pp. 669–678.

35. System, ComAp. *DWPPON Elektric.* [Online] 2009. http://www.dwppon.com/bifuel.pdf.

36. **Association, American Public Gas.** *A Brief History of Natural Gas.* Washington DC : American Public Gas Association, 2012.

37. **Liu, Zhigang.** *An examination of the combustion characteristics of compression ignition engines fuelled with gaseous fuels.* Calgary, Canada : University of Calgary, 1995. PhD Thesis.

38. *The Dual-Fuel Engine and Its Application to Sewage Treatment Plants.* **Crooks, W. R.** 1949, Sewage Works Journa, pp. 957-961.

39. *Steel Reheat Furnaces - Use of Oxy-Fuel in Steel Reheat Furnaces.* **Brown, A., Ekman, T. and Axelsson, C.L.** 2002, Steel Times International, pp. 30-32.

40. *Towards improvement of natural gas-diesel dual fuel mode: An experimental investigation on performance and exhaust emissions.* **Lounici, Mohand Said, et al., et al.** 2014, Energy, pp. 200-211.

41. *Assessment of combustion in natural gas fuelled compression ignition engines with DME and RME pilot ignition.* **Namasivayam, A.M., et al., et al.** s.l. : International Journal of Engine Research, 2009, International Journal of Engine Research, pp. 165-174.

42. **Weaver, Christopher S. and Turner, Sean H.** *Dual Fuel Natural Gas/Diesel Engines: Technology, Performance, and Emissions.* Sacramento : Engine, Fuel, and Emission Enginerring, Inc, 1994. SAE Technical Paper 940548.

43. *Effect of injection timing on the exhaust emissions of a diesel engine using diesel–methanol blends.* **Sayin, Cenk, et al., et al.** 2009, Renewable Energy , pp. 1261-1269.

44. *Effect of Pilot Fuel Quantity on the Performance and Emission of a Dual Producer Gas–Diesel Engine.* **Sombatwong, Pisarn, Thaiyasuit, Prachasanti and Pianthong, Kulachate.** 2013, Energy Procedia, pp. 218–227.

45. *An Examination the Maximum Possible Natural Gas Substitution Diesel Fuel in a Direct injected Diesel Engine.* **Mbarawa, M. and Milton, B.E.** 2005, R&D Journal.

46. **OGJ.** *Micropilot tests progress, durability an issue.* Texas : Oil and Gas Journal, 2006. Article.

47. **Power, CAP Clean Air.** Dual Fuel R&D. [Online] 2013. http://www.cleanairpower.com/rd.html.

48. **Cannon, Shane.** *Cummins QSK50 Dual Fuel Engine.* s.l. : Cummins, 2013.

49. **Kistler Group.** Type 6056A PiezoStar Pressure Sensor for Combustion Engines. [Online] 2013. [Cited: Feb 19, 2014.] http://www.kistler.com/us/en/product/pressure/6056A.

50. AVL. *AVL Fuel Balance Product Description.* [Online] January 21, 2009. https://www.avl.com/c/document_library/get_file?uuid=19cf6064-ca5b-42f7-8607-3f9cd06acf4e&groupId=10138. AVL_PD_733S_Fuel_Balance_ENG.doc.

51. **K2BW.** Signal USA. *K2BW.* [Online] K2BW Environmental Equipment Co., 2013. http://www.k2bw.com/chemiluminescence.htm.

52. *A dilution stack sampler for collection of organic aerosol emissions - design, characterization and field tests.* **Hildemann, L. M., Cass, G. R. and Markowski, G. R.** 1, 1989, Aerosol Science and Technology, Vol. 10, pp. 193-204.

53. *Heat release analysis of engine pressure data.* **Gatowski, J. A., et al., et al.** 1984, SAE 841359.

54. *An Experimental and Multidimensional Computational Study on Uncontrolled Combustion Rates in a Light Duty Natural Gas/Diesel Dual Fuel Engine.* **Hockett, Andrew G., et al., et al.** s.l. : Submitted, 2014, Journal Submission for Combustion Science and Technology.

55. *Modeling Spray Atomization with the Kelvin-Helmholtz/Rayleigh-Taylor Hybrid Model.* **Beale, J. and Reitz, R.** s.l. : Atomization and Sprays, 9 (1999) 623-650, 1999, Atomization and Sprays, pp. 623-650.

56. *Effect of primary breakup modeling on spray and combustion characteristics of compression ignition engines.* **Som, S. and Aggarwal, S. K.** 2010, Combustion and Flame, pp. 1179-1193.

57. *A New Droplet Collision Algorithm.* **Schmidt, D. P. and Rutland, C. J.** 2000, J. Comp. Phys, p. 62.

58. *Multi-Dimensional Modeling of Direct-Injection Spray Liquid Length and Flame Lift-off Lenght using CFD and Parallel Detailed Chemistry.* **Senecal, P.K., Pomraning, E. and K.J.Richards.** 2003, SAE Paper.

59. *A coupled computational fluid dynamics and multi-zone model with detailed chemical kinetics for the simulation of premixed charge compression ignition engins.* **Babajimopoulos, A., et al., et al.** 2005, International Journal of Engine Research, p. 497.

60. *A Temperature Wall Function Formulation for Variable Density zturbulence Flow with Application to Engine Convective Heat Transfer Modeling.* **Han, Z. and Reitz, R.D.** 1997, Int. J. Heat and Mass Transfer.

61. *A Computational Investigation of the Effects of Swirl Ratio and Injection Pressure on Mixture Preparation and Wall Heat Transfer in a Light-Duty Diesel Engine.* **Perini, F., et al., et al.** s.l. : SAE Technical Paper, 2013, SAE Technical Paper.

62. *Oxidation of C1-C5 Alkane Quinternary Natural Gas Mixtures at High Pressures.* **Healy, D., et al., et al.** 2010, Energy and Fuels, pp. 1521-1528.

63. *Direct numerical simulations of ignition of a lean n-heptane/air mixture with temperature inhomogeneities at constant volume: Parametric study.* **Yoo, C. S., Lu, T. and J. H. Chen and C. K. Law.** 2011, Combustion and Flame, pp. 1727-1741.

64. *A Comprehensive Modeling Study of n-Heptane Oxidation.* **Curran, H. J., Gaffuri, P. and Westbrook, W. J. Pitz and C. K.** s.l. : Combustion and Flame, 1998, Combustion and Flame, pp. 149-177.

65. *Models for Combustion and Formation of Nitric Oxide and Soot in DI Diesel Engines.* **H.Hiroyasu and T.Kadota.** 760129, s.l. : SAE Paper, 1976.

66. *Oxidation of Carbon Betweem 1000-2000 C.* **J.Nagle and Strickland-Constable, R.F.** 1962, Proc. of the Fifth Carbon Conf., p. 154.

67. Chevron. [Online] 2014. http://www.chevron.com/deliveringenergy/naturalgas/shalegas.

68. **C2ES.org.** Center for Climate and Energy Solutions. [Online] http://www.c2es.org/technology/factsheet/natural-gas.

69. **Wikipedia.** United States Department of Energy. [Online] http://en.wikipedia.org/wiki/List_of_countries_by_carbon_dioxide_emissions.

70. *Knock characteristics of dual-fuel combustion in diesel.* **Nwafor, O.M.I.** 2001, Sadhana, pp. 375–382.

71. *Prediction of stratified charge divided chamber engine performance.* **Mozafari, M Tiourad and A.** 2009, Sci. Iran. Trans. B, pp. 92–100.

72. **Rajput, R. K.** *Internal Combustion Engines.* New Delhi, India : Laxmi Publications, 2005.

73. **Bueno, André V., Velásquez, José A. and Milanez, Luiz F.** *Internal Combustion Engine Indicating Measurements Federal University of Ceara, UFC,2012.* Brazil : Intechopen, 2012.

74. *Combustion and emission characteristics of a natural gas-fueled diesel engine with EGR.* **Abdelaal, M.M. and Hegab, AH.H.** 2012, Energy Conversion and Management, pp. 301-312.

75. *Natural Gas Fueled Spark-Ignition (SI) and Compression-Ignition (CI) Engine Performance and Emission.* **Korakianitis, T., Namasivayam, A.M. and Crookes, R.J.** 2011, Prog. Energy Combust. Sci, pp. 89-112.

76. *Strategies for reduced NOx emissions in pilot-ignited natural gas engines.* **Krishnan, S.R., et al., et al.** s.l. : Proc. ICEF, 2004, J. Eng. Gas Turbines Power , pp. 665-671.

77. *Effect of exhaust gas recirculation on some combustion characteristics of dual fuel engine.* **Selim, Mohamed YE.** 2003, Energy conversion and management, pp. 707-721.

78. *Effect of Exhaust Gas Recirculation (EGR) on Performance and Emission characteristics of a Three Cylinder Direct Injection Compression Ignition Engine.* **Hussain, Jaffar, et al., et al.** 2012, Alexandria Engineering Journal, pp. 241–247.

79. *Experimental Investigation of the Factors Affecting the Performance of a LPG - Diesel Dual Fuel Engine.* **Poonia, M.P., Ramesh, A. and Gaur, R.R.** s.l. : SAE Technical Paper, 1999. International Congress & Exposiiton.

80. *Emission characteristics of an electricity generation system in diesel alone and dual fuel modes.* **Uma, R., Kandpal, T.C. and Kishore, V.V.N.** 2004, Biomass Energy, pp. 195-203.

81. *Effects of pilot fuel quantity on the emissions characteristics of a CNG/diesel dual fuel engine with optimized pilot injection timing.* **Liu, Jie, et al., et al.** 2013, Applied Energy, pp. 201–206.

82. **Bennett, Maren R.** *Emissions from a Diesel Engine Operating with Soy-Based Biodiesel Fuel.* Fort Collins : MS Thesis, Colorado State University, 2007.

83. **Andrew H., Barta G, Hampson J and Anthony M.** *An Experimental and Multidimensional Computational Study on Uncontrolled Combustion Rates in a Light Duty Natural Gas/Diesel Dual Fuel Engine.* s.l. : Submitted, 2014.

APPENDIX A   TEST PROCEDURES

Diesel Testing Procedure

Engine setpoints:

- Intake Manifold Temperature = 43°C

- Block Coolant Temperature   = 88°C

- Engine governor should be set to Gen-set mode and isochronous

    o Switch 2 and 3 should be turned on

- Engine speed should be 1800rpm

- Fuel return temperature post fuel cooler should be maintained as close to fuel inlet temperature as possible

- Engine Load Points

    o 100% = 164kW

    o 75%   = 123kW

    o 50%   = 82kW

    o 25%   = 41kW

    o 12%   = 20kW

- Dual fuel system turned off and powered down

- Dilution Tunnel dilution ratio = 15:1

Steady State Engine Testing:

- Startup and warm-up of emissions analyzers and engine [Time = 1.5 – 2hr]

- 100% load point

    o Take engine to 100% load [164kW] and allow to stabilize [Time = 15 min]

        ▪ During this time take 2 – 2 min diesel fuel flow measurements and average the results [Units = kg/hr]

        ▪ Input the averaged diesel fuel flow measurement into the JD6068 DAQ VI in the plant control tab (this measurement is used to calculate the space velocity through the catalyst)

    o Record a 10 min data point

        ▪ Analyzers – DAQ, FTIR, Dilution Tunnel, and Dev-X data

        ▪ Combustion

- Record 3 – 1000 cycle data points. Each 1000 cycle data point should be about 2 min in length
    - Fuel flow data
        - Record 3 – 2 min data points during this time, be mindful that the fuel flow meters balance volume is small so a refill period during the 10 min data point is likely

- 75% load point
    - Take engine to 75% load [123kW] and allow to stabilize [Time = 15 min]
        - During this time take 2 – 2 min diesel fuel flow measurements and average the results [Units = kg/hr]
        - Input the averaged diesel fuel flow measurement into the JD6068 DAQ VI in the plant control tab (this measurement is used to calculate the space velocity through the catalyst)
    - Record a 10 min data point
        - Analyzers – DAQ, FTIR, Dilution Tunnel, and Dev-X data
        - Combustion
            - Record 3 – 1000 cycle data points. Each 1000 cycle data point should be about 2 min in length
        - Fuel flow data
            - Record 3 – 2 min data points during this time, be mindful that the fuel flow meters balance volume is small so a refill period during the 10 min data point is likely

- 50% load point
    - Take engine to 50% load [82kW] and allow to stabilize [Time = 15 min]
        - During this time take 2 – 2 min diesel fuel flow measurements and average the results [Units = kg/hr]
        - Input the averaged diesel fuel flow measurement into the JD6068 DAQ VI in the plant control tab (this measurement is used to calculate the space velocity through the catalyst)
    - Record a 10 min data point
        - Analyzers – DAQ, FTIR, Dilution Tunnel, and Dev-X data

- ▪ Combustion
    - • Record 3 – 1000 cycle data points. Each 1000 cycle data point should be about 2 min in length
- ▪ Fuel flow data
    - • Record 3 – 2 min data points during this time, be mindful that the fuel flow meters balance volume is small so a refill period during the 10 min data point is likely

- • 25% load point
    - o Take engine to 25% load [41kW] and allow to stabilize [Time = 15 min]
        - ▪ During this time take 2 – 2 min diesel fuel flow measurements and average the results [Units = kg/hr]
        - ▪ Input the averaged diesel fuel flow measurement into the JD6068 DAQ VI in the plant control tab (this measurement is used to calculate the space velocity through the catalyst)
    - o Record a 10 min data point
        - ▪ Analyzers – DAQ, FTIR, Dilution Tunnel, and Dev-X data
        - ▪ Combustion
            - • Record 3 – 1000 cycle data points. Each 1000 cycle data point should be about 2 min in length
        - ▪ Fuel flow data
            - • Record 3 – 2 min data points during this time, be mindful that the fuel flow meters balance volume is small so a refill period during the 10 min data point is likely

- • 12% load point
    - o Take engine to 12% load [20kW] and allow to stabilize [Time = 15 min]
        - ▪ During this time take 2 – 2 min diesel fuel flow measurements and average the results [Units = kg/hr]
        - ▪ Input the averaged diesel fuel flow measurement into the JD6068 DAQ VI in the plant control tab (this measurement is used to calculate the space velocity through the catalyst)
    - o Record a 10 min data point

123

- Analyzers – DAQ, FTIR, Dilution Tunnel, and Dev-X data
- Combustion
  - Record 3 – 1000 cycle data points. Each 1000 cycle data point should be about 2 min in length
- Fuel flow data
  - Record 3 – 2 min data points during this time, be mindful that the fuel flow meters balance volume is small so a refill period during the 10 min data point is likely

Dual Fuel Testing Procedure

Engine Setpoints:

- Intake Manifold Temperature = 43°C
- Block Coolant Temperature   = 88°C
- Engine governor should be set to Gen-set mode and isochronous
  - Switch 2 and 3 should be turned on
- Engine speed should be 1800rpm
- Fuel return temperature post fuel cooler should be maintained as close to fuel inlet temperature as possible
- Engine Load Points
  - 100% = 164kW
  - 75%   = 123kW
  - 50%   = 82kW
  - 25%   = 41kW
  - 12%   = 20kW
- Dual fuel system turned on and powered up
- Dilution Tunnel dilution ratio = 15:1
- During this round of testing the combustion data should be monitored closely noting any interesting results

Steady State Engine Testing:

- Startup and warm-up of emissions analyzers and engine [Time = 1.5 – 2hr]

- 100% load point
  - Take engine to 100% load [164kW] and allow to stabilize [Time = 15 min]
    - During this time take 2 – 2 min diesel fuel flow measurements and average the results [Units = kg/hr]
    - Input the averaged diesel fuel flow measurement into the JD6068 DAQ VI in the plant control tab (this measurement is used to calculate the space velocity through the catalyst)
  - Record a 10 min data point
    - Analyzers – DAQ, FTIR, Dilution Tunnel, and Dev-X data
    - Combustion
      - Record 3 – 1000 cycle data points. Each 1000 cycle data point should be about 2 min in length
    - Fuel flow data
      - Record 3 – 2 min data points during this time, be mindful that the fuel flow meters balance volume is small so a refill period during the 10 min data point is likely
- 75% load point
  - Take engine to 75% load [123kW] and allow to stabilize [Time = 15 min]
    - During this time take 2 – 2 min diesel fuel flow measurements and average the results [Units = kg/hr]
    - Input the averaged diesel fuel flow measurement into the JD6068 DAQ VI in the plant control tab (this measurement is used to calculate the space velocity through the catalyst)
  - Record a 10 min data point
    - Analyzers – DAQ, FTIR, Dilution Tunnel, and Dev-X data
    - Combustion
      - Record 3 – 1000 cycle data points. Each 1000 cycle data point should be about 2 min in length
    - Fuel flow data

- Record 3 – 2 min data points during this time, be mindful that the fuel flow meters balance volume is small so a refill period during the 10 min data point is likely
- 50% load point
  - Take engine to 50% load [82kW] and allow to stabilize [Time = 15 min]
    - During this time take 2 – 2 min diesel fuel flow measurements and average the results [Units = kg/hr]
    - Input the averaged diesel fuel flow measurement into the JD6068 DAQ VI in the plant control tab (this measurement is used to calculate the space velocity through the catalyst)
  - Record a 10 min data point
    - Analyzers – DAQ, FTIR, Dilution Tunnel, and Dev-X data
    - Combustion
      - Record 3 – 1000 cycle data points. Each 1000 cycle data point should be about 2 min in length
    - Fuel flow data
      - Record 3 – 2 min data points during this time, be mindful that the fuel flow meters balance volume is small so a refill period during the 10 min data point is likely
- 25% load point
  - Take engine to 25% load [41kW] and allow to stabilize [Time = 15 min]
    - During this time take 2 – 2 min diesel fuel flow measurements and average the results [Units = kg/hr]
    - Input the averaged diesel fuel flow measurement into the JD6068 DAQ VI in the plant control tab (this measurement is used to calculate the space velocity through the catalyst)
  - Record a 10 min data point
    - Analyzers – DAQ, FTIR, Dilution Tunnel, and Dev-X data
    - Combustion
      - Record 3 – 1000 cycle data points. Each 1000 cycle data point should be about 2 min in length

126

- Fuel flow data
  - Record 3 – 2 min data points during this time, be mindful that the fuel flow meters balance volume is small so a refill period during the 10 min data point is likely
- 12% load point
  - Take engine to 12% load [20kW] and allow to stabilize [Time = 15 min]
    - During this time take 2 – 2 min diesel fuel flow measurements and average the results [Units = kg/hr]
    - Input the averaged diesel fuel flow measurement into the JD6068 DAQ VI in the plant control tab (this measurement is used to calculate the space velocity through the catalyst)
  - Record a 10 min data point
    - Analyzers – DAQ, FTIR, Dilution Tunnel, and Dev-X data
    - Combustion
      - Record 3 – 1000 cycle data points. Each 1000 cycle data point should be about 2 min in length
    - Fuel flow data
      - Record 3 – 2 min data points during this time, be mindful that the fuel flow meters balance volume is small so a refill period during the 10 min data point is likely

Dual Fuel Systems Optimization

Testing Plan

- Baseline Diesel Testing
  - Initial shakedown of entire skid. The dual fuel system OFF. ISO 8178 Cycle D2 5-mode load map plus transient engine testing.
    - Cycle D2:
      - Engine Speed   1800 RPM
      - % Torque   Modes:
        1- 100%
        2- 75%
        3- 50%

4-   25%

                                                        5-   10%

                                            Each mode held for >10 minutes.

- o Decision whether 1800 RPM will produce exhaust temperatures high enough for light off and emissions reductions within catalyst.
- Dual Fuel Testing with Standard Tuning
  - o Allow dual fuel system to autotune throttle map. Repeat ISO 8178 Cycle D2 and transient testing.
    - Cycle D2:
      - Engine Speed   1800 RPM
      - % Torque   Modes:

                            1-   100%

                            2-   75%

                            3-   50%

                            4-   25%

                            5-   10%

                            Each mode held for >10 minutes.
      - Catalyst Sample   : 5 min pre-catalyst, 5 min post-catalyst @ each mode
- Dual Fuel System Optimization for low CO and CH_4 emissions
  - o % Natural Gas substitution sweep. Observe CO, CH_4 emissions real time as substitution levels are swept at constant load. Continue until knock index reaches
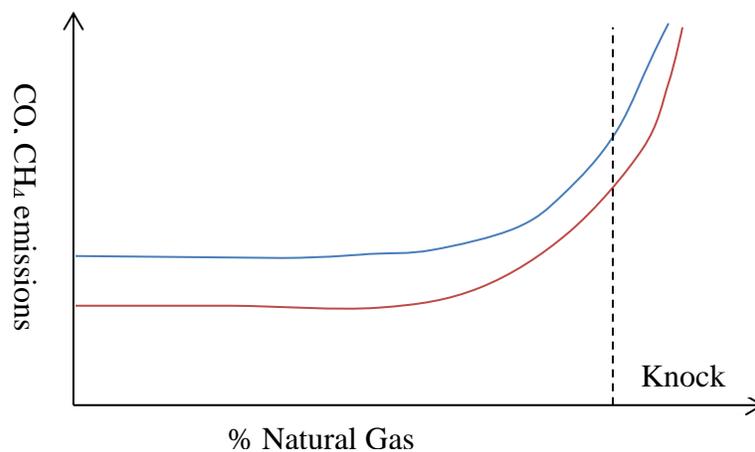
a pre-determined (arbitrary) factor. Approx. 30 min data point.

- Engine Parameters
  - Engine Speed   1800 RPM
  - % Torque   50%

                                  100%

- Injection timing alterations. With access to ECU, advance injection timing in 2° increments. Repeat %NG sweep above at each increment to observe knock onset and emissions response.

APPENDIX B   CSU86 REDUCED MECHANISM

ELEMENTS
C H N O AR HE
END

SPECIES
H   H2   O   O2   OH   H2O   N2   HO2
H2O2   CO   CO2   CH2O   HCO   HOCHO   CH3O
DIL
CH3O2H   CH3O2   CH4   CH3   CH   C2H6   C2H5
C2H4   C2H3   C2H2   CH3CHO   CH3CO   CH2CHO
HCCO   CH2
HCCOH   C2H5O   C2H5O2H   C2H5O2   C2H3CHO   C3H8
IC3H7
NC3H7   C3H6   C3H6OOH1-3   C3H6OOH2-1   C3H6OOH1-3O2
C3H6OOH2-1O2   NC3H7O2
IC3H7O2   C3KET13   C3KET21   IC3H6CHO
 !
 !from 68 species nhept skeletel mech reduced via DRGEP from 88
 !spec uconn mech, which was a reduction of LLNL nc7 mech
 !
CH3COCH2 C3H5O C2H5COCH2 C7H15-4 C7H14OOH3-5 NC7KET24
C2H5CHO C4H7O NC3H7COCH2 C7H14-3 C7H14OOH4-2 NC7KET35
C3H4-A C5H10-1 C3H5-A NC4H9CO C7H15O2-1 C7H14OOH2-4O2
NC7KET42 C3H3 NC7H16 C7H15O2-2 C7H14OOH3-5O2 CH2CO
C3H2 C7H15-1 C7H15O2-3 C7H14OOH4-2O2 C4H8-1 NC3H7CHO
C7H15-2 C7H15O2-4 C7H14O1-3 PC4H9 NC3H7CO C7H15-3 C7H14OOH2-4
C7H14O2-4
END

REACTIONS
 H+O2=O+OH   3.54700E+15 -4.06000E-01 1.66000E+04
    REV/1.02700E+13 -1.50000E-02 -1.33000E+02/
 O+H2=H+OH   5.08000E+04 2.67000E+00 6.29200E+03
    REV/2.63700E+04 2.65100E+00 4.88000E+03/
 OH+H2=H+H2O   2.16000E+08 1.51000E+00 3.43000E+03
    REV/2.29000E+09 1.40400E+00 1.83200E+04/
 O+H2O=OH+OH   2.97000E+06 2.02000E+00 1.34000E+04
    REV/1.45400E+05 2.10700E+00 -2.90400E+03/
 H2+M=H+H+M   4.57700E+19 -1.40000E+00 1.04400E+05
       H2/2.5000E+00/ H2O/1.2000E+01/ CO/1.9000E+00/ CO2/3.8000E+00/
    REV/1.14500E+20 -1.67600E+00 8.20000E+02/

130

O2+M=O+O+M   4.42000E+17 -6.34000E-01 1.18900E+05
      H2/2.5000E+00/ H2O/1.2000E+01/ CO/1.9000E+00/ CO2/3.8000E+00/
CH4/2.0000E+00/ C2H6/3.0000E+00/
      REV/6.16500E+15 -5.00000E-01 0.00000E+00/
OH+M=O+H+M   9.78000E+17 -7.43000E-01 1.02100E+05
      H2/2.5000E+00/ H2O/1.2000E+01/ CO/1.5000E+00/ CO2/2.0000E+00/
CH4/2.0000E+00/ C2H6/3.0000E+00/
      REV/4.71400E+18 -1.00000E+00 0.00000E+00/
H2O+M=H+OH+M   1.90700E+23 -1.83000E+00 1.18500E+05
      H2/7.3000E-01/ H2O/1.2000E+01/ CH4/2.0000E+00/ C2H6/3.0000E+00/
      REV/4.50000E+22 -2.00000E+00 0.00000E+00/
H+O2(+M)=HO2(+M)   1.47500E+12 6.00000E-01 0.00000E+00
      LOW /3.48200E+16 -4.11000E-01 -1.11500E+03/
      TROE/   5.00000E-01   1.00000E-30   1.00000E+30   1.00000E+10 /
      H2/1.3000E+00/ H2O/1.4000E+01/ CO/1.9000E+00/ CO2/3.8000E+00/
CH4/2.0000E+00/ C2H6/3.0000E+00/
HO2+H=H2+O2   1.66000E+13 0.00000E+00 8.23000E+02
      REV/3.16600E+12 3.48000E-01 5.55100E+04/
HO2+H=OH+OH   7.07900E+13 0.00000E+00 2.95000E+02
      REV/2.02800E+10 7.20000E-01 3.68400E+04/
HO2+O=OH+O2   3.25000E+13 0.00000E+00 0.00000E+00
      REV/3.21700E+12 3.29000E-01 5.32800E+04/
HO2+OH=H2O+O2   2.89000E+13 0.00000E+00 -4.97000E+02
      REV/5.84400E+13 2.42000E-01 6.90800E+04/
H2O2+O2=HO2+HO2   1.13600E+16 -3.47000E-01 4.97300E+04
      REV/1.03000E+14 0.00000E+00 1.10400E+04/
          DUPLICATE
H2O2+O2=HO2+HO2   2.14100E+13 -3.47000E-01 3.72800E+04
      REV/1.94000E+11 0.00000E+00 -1.40900E+03/
          DUPLICATE
 !
 !Bumped up per Patel et al. SAE2004-01-0558
 !increased A from 2.95100E+14 to 8E+14
 !increased Ea from 4.84300E+04 to
 !
H2O2(+M)=OH+OH(+M)   9.00000E+16 0.00000E+00 5.80000E+04
      LOW /1.20200E+17 0.00000E+00 4.55000E+04/
      TROE/   5.00000E-01   1.00000E-30   1.00000E+30   1.00000E+10 /
      H2/2.5000E+00/ H2O/1.2000E+01/ CO/1.9000E+00/ CO2/3.8000E+00/
CH4/2.0000E+00/ C2H6/3.0000E+00/
H2O2+H=H2O+OH   2.41000E+13 0.00000E+00 3.97000E+03
      REV/1.26500E+08 1.31000E+00 7.14100E+04/
H2O2+H=H2+HO2   2.15000E+10 1.00000E+00 6.00000E+03

REV/3.71600E+07 1.69500E+00 2.20000E+04/
H2O2+O=OH+HO2   9.55000E+06 2.00000E+00 3.97000E+03
    REV/8.56800E+03 2.67600E+00 1.85600E+04/
H2O2+OH=H2O+HO2   2.00000E+12 0.00000E+00 4.27200E+02
    REV/3.66500E+10 5.89000E-01 3.13200E+04/
         DUPLICATE
H2O2+OH=H2O+HO2   1.70000E+18 0.00000E+00 2.94100E+04
    REV/3.11500E+16 5.89000E-01 6.03000E+04/
         DUPLICATE
CO+O(+M)=CO2(+M)   1.80000E+10 0.00000E+00 2.38400E+03
    LOW /1.35000E+24 -2.78800E+00 4.19100E+03/
     H2/2.0000E+00/ O2/6.0000E+00/ H2O/6.0000E+00/ CO/1.5000E+00/ CO2/3.5000E+00/
CH4/2.0000E+00/ C2H6/3.0000E+00/
CO+O2=CO2+O   1.05000E+12 0.00000E+00 4.25400E+04
    REV/8.03500E+15 -8.00000E-01 5.12300E+04/
CO+OH=CO2+H   1.78400E+05 1.89000E+00 -1.15800E+03
    REV/4.71700E+11 6.99000E-01 2.42600E+04/
CO+HO2=CO2+OH   1.57000E+05 2.18000E+00 1.79400E+04
    REV/1.18900E+08 1.71000E+00 7.99100E+04/
HCO+M=H+CO+M   4.75000E+11 6.60000E-01 1.48700E+04
     H2/2.0000E+00/ H2O/1.2000E+01/ CO/1.5000E+00/ CO2/2.0000E+00/
CH4/2.0000E+00/ C2H6/3.0000E+00/
    REV/3.58200E+10 1.04100E+00 -4.57300E+02/
HCO+O2=CO+HO2   7.58000E+12 0.00000E+00 4.10000E+02
    REV/1.19800E+12 3.09000E-01 3.39500E+04/
HCO+H=CO+H2   7.34000E+13 0.00000E+00 0.00000E+00
    REV/2.21200E+12 6.56000E-01 8.82300E+04/
HCO+O=CO+OH   3.02000E+13 0.00000E+00 0.00000E+00
    REV/4.72500E+11 6.38000E-01 8.68200E+04/
 HCO+O=CO2+H   3.00000E+13 0.00000E+00 0.00000E+00
    REV/1.24100E+18 -5.53000E-01 1.12200E+05/
 HCO+OH=CO+H2O   1.02000E+14 0.00000E+00 0.00000E+00
    REV/3.25900E+13 5.51000E-01 1.03100E+05/
 HCO+CH3=CH4+CO   2.65000E+13 0.00000E+00 0.00000E+00
    REV/7.28600E+14 2.11000E-01 8.97700E+04/
 HCO+HO2=CH2O+O2   2.49900E+14 -6.10000E-02 1.39200E+04
    REV/8.07000E+15 0.00000E+00 5.34200E+04/
 HCO+HO2=CO2+H+OH   3.00000E+13 0.00000E+00 0.00000E+00
    REV/0.00000E+00 0.00000E+00 0.00000E+00/
CH2O+CO=HCO+HCO   9.18600E+13 3.70000E-01 7.30400E+04
    REV/1.80000E+13 0.00000E+00 0.00000E+00/
 HCO+HCO=H2+CO+CO   3.00000E+12 0.00000E+00 0.00000E+00
    REV/0.00000E+00 0.00000E+00 0.00000E+00/

HCO+H(+M)=CH2O(+M)   1.09000E+12 4.80000E-01 -2.60000E+02
    LOW /1.35000E+24 -2.57000E+00 1.42500E+03/
    TROE/   7.82400E-01   2.71000E+02   2.75500E+03   6.57000E+03 /
    H2/2.0000E+00/ H2O/6.0000E+00/ CO/1.5000E+00/ CO2/2.0000E+00/
CH4/2.0000E+00/ C2H6/3.0000E+00/
CO+H2(+M)=CH2O(+M)   4.30000E+07 1.50000E+00 7.96000E+04
    LOW /5.07000E+27 -3.42000E+00 8.43480E+04/
    TROE/   9.32000E-01   1.97000E+02   1.54000E+03   1.03000E+04 /
    H2/2.0000E+00/ H2O/6.0000E+00/ CO/1.5000E+00/ CO2/2.0000E+00/
CH4/2.0000E+00/ C2H6/3.0000E+00/
CH2O+OH=HCO+H2O   7.82000E+07 1.63000E+00 -1.05500E+03
    REV/4.89600E+06 1.81100E+00 2.90300E+04/
CH2O+H=HCO+H2   5.74000E+07 1.90000E+00 2.74000E+03
    REV/3.39000E+05 2.18700E+00 1.79300E+04/
CH2O+O=HCO+OH   6.26000E+09 1.15000E+00 2.26000E+03
    REV/1.91900E+07 1.41800E+00 1.60400E+04/
CH2O+CH3=HCO+CH4   3.83000E+01 3.36000E+00 4.31200E+03
    REV/2.06300E+02 3.20100E+00 2.10400E+04/
CH2O+HO2=HCO+H2O2   7.10000E-03 4.51700E+00 6.58000E+03
    REV/2.42600E-02 4.10800E+00 5.76900E+03/
HOCHO=CO+H2O   2.45000E+12 0.00000E+00 6.04700E+04
    REV/2.25500E+03 2.09300E+00 5.28900E+04/
HOCHO=CO2+H2   2.95000E+09 0.00000E+00 4.85200E+04
    REV/6.77200E+05 1.00800E+00 5.14700E+04/
HOCHO=HCO+OH   3.47100E+22 -1.54200E+00 1.10700E+05
    REV/1.00000E+14 0.00000E+00 0.00000E+00/
HOCHO+OH=H2O+CO2+H   2.62000E+06 2.06000E+00 9.16000E+02
    REV/0.00000E+00 0.00000E+00 0.00000E+00/
HOCHO+OH=H2O+CO+OH   1.85000E+07 1.51000E+00 -9.62000E+02
    REV/0.00000E+00 0.00000E+00 0.00000E+00/
HOCHO+H=H2+CO2+H   4.24000E+06 2.10000E+00 4.86800E+03
    REV/0.00000E+00 0.00000E+00 0.00000E+00/
HOCHO+H=H2+CO+OH   6.03000E+13 -3.50000E-01 2.98800E+03
    REV/0.00000E+00 0.00000E+00 0.00000E+00/
HOCHO+CH3=CH4+CO+OH   3.90000E-07 5.80000E+00 2.20000E+03
    REV/0.00000E+00 0.00000E+00 0.00000E+00/
HOCHO+HO2=H2O2+CO+OH   1.00000E+12 0.00000E+00 1.19200E+04
    REV/0.00000E+00 0.00000E+00 0.00000E+00/
HOCHO+O=CO+OH+OH   1.77000E+18 -1.90000E+00 2.97500E+03
    REV/0.00000E+00 0.00000E+00 0.00000E+00/
CH3O(+M)=CH2O+H(+M)   6.80000E+13 0.00000E+00 2.61700E+04
    LOW /1.86700E+25 -3.00000E+00 2.43070E+04/
    TROE/   9.00000E-01   2.50000E+03   1.30000E+03   1.00000E+99 /

133

H2/2.0000E+00/ H2O/6.0000E+00/ CO/1.5000E+00/ CO2/2.0000E+00/
CH4/2.0000E+00/ C2H6/3.0000E+00/
CH3O+O2=CH2O+HO2   4.38000E-19 9.50000E+00 -5.50100E+03
    REV/1.41600E-20 9.81600E+00 2.10800E+04/
CH3O+CH3=CH2O+CH4   1.20000E+13 0.00000E+00 0.00000E+00
    REV/6.74900E+13 2.18000E-01 8.28100E+04/
CH3O+H=CH2O+H2   2.00000E+13 0.00000E+00 0.00000E+00
    REV/1.23300E+11 6.64000E-01 8.12700E+04/
CH3O+HO2=CH2O+H2O2   3.01000E+11 0.00000E+00 0.00000E+00
    REV/1.07400E+12 -3.10000E-02 6.52700E+04/
CH3+H(+M)=CH4(+M)   1.27000E+16 -6.00000E-01 3.83000E+02
      LOW /1.98160E+33 -4.76000E+00 2.44400E+03/
      TROE/   7.83000E-01   7.40000E+01   2.94000E+03   6.96000E+03 /
      H2/2.0000E+00/ H2O/6.0000E+00/ CO/1.5000E+00/ CO2/2.0000E+00/
CH4/2.0000E+00/ C2H6/3.0000E+00/
CH4+H=CH3+H2   6.14000E+05 2.50000E+00 9.58700E+03
    REV/6.73000E+02 2.94600E+00 8.04700E+03/
CH4+OH=CH3+H2O   5.83000E+04 2.60000E+00 2.19000E+03
    REV/6.77600E+02 2.94000E+00 1.55400E+04/
CH4+O=CH3+OH   1.02000E+09 1.50000E+00 8.60000E+03
    REV/5.80400E+05 1.92700E+00 5.64800E+03/
CH4+HO2=CH3+H2O2   1.13000E+01 3.74000E+00 2.10100E+04
    REV/7.16600E+00 3.49100E+00 3.46800E+03/
CH3+OH=CH2O+H2   8.00000E+09 5.00000E-01 -1.75500E+03
    REV/1.06600E+12 3.22000E-01 6.82100E+04/
CH3+OH=CH3O+H   6.94300E+07 1.34300E+00 1.12000E+04
    REV/1.50000E+12 5.00000E-01 -1.10000E+02/
CH3+HO2=CH3O+OH   1.00000E+12 2.69000E-01 -6.87500E+02
    REV/6.19000E+12 1.47000E-01 2.45500E+04/
CH3+HO2=CH4+O2   1.16000E+05 2.23000E+00 -3.02200E+03
    REV/2.01800E+07 2.13200E+00 5.32100E+04/
CH3+O=CH2O+H   5.54000E+13 5.00000E-02 -1.36000E+02
    REV/3.83000E+15 -1.47000E-01 6.84100E+04/
CH3+O2=CH3O+O   7.54600E+12 0.00000E+00 2.83200E+04
    REV/4.71800E+14 -4.51000E-01 2.88000E+02/
CH3+O2=CH2O+OH   2.64100E+00 3.28300E+00 8.10500E+03
    REV/5.28500E-01 3.47700E+00 5.99200E+04/
CH3O2+M=CH3+O2+M   4.34E+27   -3.42E+00   3.05E+04
      REV/5.44E+25   -3.30E+00   0.00000E+00/
!CH3+O2(+M)=CH3O2(+M)   7.81200E+09 !9.00000E-01 0.00000E+00
!   LOW /6.85000E+24 -3.00000E+00 0.00000E+00/
!   TROE/   6.00000E-01   1.00000E+03   !7.00000E+01   1.70000E+03 /
CH3O2+CH2O=CH3O2H+HCO   1.99000E+12 0.00000E+00 1.16600E+04

134

REV/1.32300E+14 -8.53000E-01 9.25900E+03/
CH4+CH3O2=CH3+CH3O2H   1.81000E+11 0.00000E+00 1.84800E+04
    REV/2.23300E+12 -6.94000E-01 -6.55000E+02/
CH3O2+CH3=CH3O+CH3O   5.08000E+12 0.00000E+00 -1.41100E+03
    REV/1.96700E+12 1.76000E-01 2.80700E+04/
CH3O2+HO2=CH3O2H+O2   2.47000E+11 0.00000E+00 -1.57000E+03
    REV/5.30200E+14 -7.92000E-01 3.55200E+04/
CH3O2+CH3O2=O2+CH3O+CH3O   1.40000E+16 -1.61000E+00
1.86000E+03
    REV/0.00000E+00 0.00000E+00 0.00000E+00/
CH3O2+H=CH3O+OH   9.60000E+13 0.00000E+00 0.00000E+00
    REV/1.72000E+09 1.01900E+00 4.07800E+04/
CH3O2+O=CH3O+O2   3.60000E+13 0.00000E+00 0.00000E+00
    REV/2.22900E+11 6.28000E-01 5.75200E+04/
CH3O2H=CH3O+OH   6.31000E+14 0.00000E+00 4.23000E+04
    REV/2.51400E+06 1.88300E+00 -2.87500E+03/
CH+O2=HCO+O   3.30000E+13 0.00000E+00 0.00000E+00
    REV/9.37100E+12 1.61000E-01 7.12100E+04/
CH+O=CO+H   5.70000E+13 0.00000E+00 0.00000E+00
    REV/2.77400E+15 0.00000E+00 1.76000E+05/
CH+OH=HCO+H   3.00000E+13 0.00000E+00 0.00000E+00
    REV/5.06900E+14 0.00000E+00 8.81100E+04/
CH+H2O=H+CH2O   1.71300E+13 0.00000E+00 -7.55000E+02
    REV/8.37200E+14 0.00000E+00 5.75200E+04/
CH+CO2=HCO+CO   1.70000E+12 0.00000E+00 6.85000E+02
    REV/2.56500E+11 0.00000E+00 6.64600E+04/
CH3+CH3(+M)=C2H6(+M)   9.21400E+16 -1.17000E+00 6.35800E+02
    LOW /1.13500E+36 -5.24600E+00 1.70500E+03/
    TROE/   4.05000E-01   1.12000E+03   6.96000E+01   1.00000E+10 /
    H2/2.0000E+00/ H2O/6.0000E+00/ CO/1.5000E+00/ CO2/2.0000E+00/
CH4/2.0000E+00/ C2H6/3.0000E+00/
C2H5+H(+M)=C2H6(+M)   5.21000E+17 -9.90000E-01 1.58000E+03
    LOW /1.99000E+41 -7.08000E+00 6.68500E+03/
    TROE/   8.42000E-01   1.25000E+02   2.21900E+03   6.88200E+03 /
    H2/2.0000E+00/ H2O/6.0000E+00/ CO/1.5000E+00/ CO2/2.0000E+00/
CH4/2.0000E+00/ C2H6/3.0000E+00/
C2H6+H=C2H5+H2   1.15000E+08 1.90000E+00 7.53000E+03
    REV/1.06200E+04 2.58200E+00 9.76000E+03/
C2H6+O=C2H5+OH   3.55000E+06 2.40000E+00 5.83000E+03
    REV/1.70200E+02 3.06300E+00 6.64800E+03/
C2H6+OH=C2H5+H2O   1.48000E+07 1.90000E+00 9.50000E+02
    REV/1.45000E+04 2.47600E+00 1.80700E+04/
C2H6+O2=C2H5+HO2   6.03000E+13 0.00000E+00 5.18700E+04

REV/2.92100E+10 3.34000E-01 -5.93000E+02/
C2H6+CH3=C2H5+CH4   5.48000E-01 4.00000E+00 8.28000E+03
REV/4.61800E-02 4.23600E+00 1.20500E+04/
C2H6+HO2=C2H5+H2O2   6.92000E+01 3.61000E+00 1.69200E+04
REV/3.69900E+00 3.59700E+00 3.15100E+03/
C2H6+CH3O2=C2H5+CH3O2H   1.94000E+01 3.64000E+00 1.71000E+04
REV/2.01700E+01 3.18200E+00 1.73400E+03/
C2H4+H(+M)=C2H5(+M)   1.08100E+12 4.54000E-01 1.82200E+03
LOW /1.20000E+42 -7.62000E+00 6.97000E+03/
TROE/   9.75000E-01   2.10000E+02   9.84000E+02   4.37400E+03 /
H2/2.0000E+00/ H2O/6.0000E+00/ CO/1.5000E+00/ CO2/2.0000E+00/
CH4/2.0000E+00/ C2H6/3.0000E+00/
H2+CH3O2=H+CH3O2H   1.50000E+14 0.00000E+00 2.60300E+04
REV/1.68800E+18 -1.14000E+00 8.43400E+03/
H2+C2H5O2=H+C2H5O2H   1.50000E+14 0.00000E+00 2.60300E+04
REV/1.69100E+18 -1.14000E+00 8.43800E+03/
C2H5+C2H3=C2H4+C2H4   6.85900E+11 1.10000E-01 -4.30000E+03
REV/4.82000E+14 0.00000E+00 7.15300E+04/
CH3+C2H5=CH4+C2H4   1.18000E+04 2.45000E+00 -2.92100E+03
REV/2.39000E+06 2.40000E+00 6.66900E+04/
C2H5+H=CH3+CH3   9.69000E+13 0.00000E+00 2.20000E+02
REV/2.02900E+09 1.02800E+00 1.05100E+04/
C2H5+H=C2H4+H2   2.00000E+12 0.00000E+00 0.00000E+00
REV/4.44000E+11 3.96000E-01 6.80700E+04/
C2H5+O=CH3CHO+H   1.10000E+14 0.00000E+00 0.00000E+00
REV/1.03300E+17 -5.00000E-01 7.74200E+04/
C2H5+HO2=C2H5O+OH   1.10000E+13 0.00000E+00 0.00000E+00
REV/9.68000E+15 -7.23000E-01 2.76500E+04/
CH3O2+C2H5=CH3O+C2H5O   8.00000E+12 0.00000E+00 -1.00000E+03
REV/4.40400E+14 -4.25000E-01 3.08900E+04/
C2H5O+O2=CH3CHO+HO2   4.28000E+10 0.00000E+00 1.09700E+03
REV/1.32200E+08 6.15000E-01 3.41300E+04/
C2H5O=CH3+CH2O   1.32100E+20 -2.01800E+00 2.07500E+04
REV/3.00000E+11 0.00000E+00 6.33600E+03/
C2H5O=CH3CHO+H   5.42800E+15 -6.87000E-01 2.22300E+04
REV/8.00000E+12 0.00000E+00 6.40000E+03/
C2H5O2=C2H5+O2   1.31200E+62 -1.47840E+01 4.91800E+04
REV/2.87600E+56 -1.38200E+01 1.46200E+04/
C2H5O2+CH2O=C2H5O2H+HCO   1.99000E+12 0.00000E+00
1.16600E+04
REV/1.32500E+14 -8.53000E-01 9.26300E+03/
CH4+C2H5O2=CH3+C2H5O2H   1.81000E+11 0.00000E+00 1.84800E+04
REV/2.23700E+12 -6.94000E-01 -6.51000E+02/

```
C2H5O2+HO2=C2H5O2H+O2                    1.75000E+10 0.00000E+00 -3.27500E+03
    REV/3.76300E+13 -7.92000E-01 3.38200E+04/
C2H6+C2H5O2=C2H5+C2H5O2H                 8.60000E+00 3.76000E+00
1.72000E+04
    REV/8.95700E+00 3.30200E+00 1.83800E+03/
C2H5O2H=C2H5O+OH                        6.31000E+14 0.00000E+00 4.23000E+04
    REV/5.66100E+08 1.03300E+00 -1.70500E+03/
C2H5+O2=C2H4+HO2                        3.78000E+14 -1.01000E+00 4.74900E+03
    REV/4.40100E+14 -9.62000E-01 1.81300E+04/
        DUPLICATE
C2H5+O2=C2H4+HO2                        4.00000E-01 3.88000E+00 1.36200E+04
    REV/4.65600E-01 3.92800E+00 2.70000E+04/
        DUPLICATE
C2H5+O2=CH3CHO+OH                       8.26500E+02 2.41000E+00 5.28500E+03
    REV/2.24700E+03 2.30100E+00 6.59700E+04/
C2H5O2=CH3CHO+OH                        2.52000E+41 -1.02000E+01 4.37100E+04
    REV/1.50200E+36 -9.34500E+00 6.98400E+04/
C2H5O2=C2H4+HO2                         1.81500E+38 -8.45000E+00 3.78900E+04
    REV/4.63200E+32 -7.43800E+00 1.67000E+04/
CH3CHO=CH3+HCO                          7.68700E+20 -1.34200E+00 8.69500E+04
    REV/1.75000E+13 0.00000E+00 0.00000E+00/
CH3CHO+H=CH3CO+H2                       2.37000E+13 0.00000E+00 3.64200E+03
    REV/1.63900E+10 6.33000E-01 1.76000E+04/
CH3CHO+O=CH3CO+OH                       5.94000E+12 0.00000E+00 1.86800E+03
    REV/2.13300E+09 6.14000E-01 1.44100E+04/
CH3CHO+OH=CH3CO+H2O                     3.37000E+12 0.00000E+00 -6.19000E+02
    REV/2.47200E+10 5.27000E-01 2.82300E+04/
CH3CHO+O2=CH3CO+HO2                     3.01000E+13 0.00000E+00 3.91500E+04
    REV/1.09200E+11 2.85000E-01 -1.58800E+03/
CH3CHO+CH3=CH3CO+CH4                    7.08000E-04 4.58000E+00 1.96600E+03
    REV/4.46800E-04 4.76700E+00 1.74600E+04/
CH3CHO+HO2=CH3CO+H2O2                   3.01000E+12 0.00000E+00 1.19200E+04
    REV/1.20500E+12 -6.20000E-02 9.87700E+03/
CH3O2+CH3CHO=CH3O2H+CH3CO              3.01000E+12 0.00000E+00
1.19200E+04
    REV/2.34400E+13 -5.07000E-01 8.28200E+03/
CH3CHO+OH=CH3+HOCHO                     3.00000E+15 -1.07600E+00 0.00000E+00
    REV/2.37100E+16 -1.27700E+00 2.37500E+04/
CH3CHO+OH=CH2CHO+H2O                    1.72000E+05 2.40000E+00 8.15000E+02
    REV/1.33200E+05 2.51100E+00 2.49500E+04/
CH3CO(+M)=CH3+CO(+M)                    3.00000E+12 0.00000E+00 1.67200E+04
     LOW /1.20000E+15 0.00000E+00 1.25180E+04/
CH2CHO+O2=CH2O+CO+OH                    8.95000E+13 -6.00000E-01 1.01200E+04
```

REV/0.00000E+00 0.00000E+00 0.00000E+00/
HCCO+OH=H2+CO+CO   1.00000E+14 0.00000E+00 0.00000E+00
    REV/0.00000E+00 0.00000E+00 0.00000E+00/
HCCO+O=H+CO+CO   8.00000E+13 0.00000E+00 0.00000E+00
    REV/0.00000E+00 0.00000E+00 0.00000E+00/
HCCO+O2=OH+CO+CO   4.20000E+10 0.00000E+00 8.50000E+02
    REV/0.00000E+00 0.00000E+00 0.00000E+00/
HCCO+M=CH+CO+M   6.50000E+15 0.00000E+00 5.88200E+04
    REV/1.39100E+11 1.03300E+00 -1.37200E+04/
CH+HCCO=CO+C2H2   5.00000E+13 0.00000E+00 0.00000E+00
    REV/1.72100E+17 0.00000E+00 1.64600E+05/
C2H3+H(+M)=C2H4(+M)   6.08000E+12 2.70000E-01 2.80000E+02
    LOW /1.40000E+30 -3.86000E+00 3.32000E+03/
    TROE/   7.82000E-01   2.07500E+02   2.66300E+03   6.09500E+03 /
    H2/2.0000E+00/ H2O/6.0000E+00/ CO/1.5000E+00/ CO2/2.0000E+00/
CH4/2.0000E+00/ C2H6/3.0000E+00/
C2H4(+M)=C2H2+H2(+M)   8.00000E+12 4.40000E-01 8.87700E+04
    LOW /7.00000E+50 -9.31000E+00 9.98600E+04/
    TROE/   7.34500E-01   1.80000E+02   1.03500E+03   5.41700E+03 /
    H2/2.0000E+00/ H2O/6.0000E+00/ CO/1.5000E+00/ CO2/2.0000E+00/
CH4/2.0000E+00/ C2H6/3.0000E+00/
C2H4+H=C2H3+H2   5.07000E+07 1.93000E+00 1.29500E+04
    REV/1.60200E+04 2.43600E+00 5.19000E+03/
C2H4+O=CH3+HCO   8.56400E+06 1.88000E+00 1.83000E+02
    REV/3.29700E+02 2.60200E+00 2.61400E+04/
C2H4+O=CH2CHO+H   4.98600E+06 1.88000E+00 1.83000E+02
    REV/1.54100E+09 1.20100E+00 1.87800E+04/
C2H4+OH=C2H3+H2O   1.80000E+06 2.00000E+00 2.50000E+03
    REV/6.02900E+03 2.40000E+00 9.63200E+03/
C2H4+CH3=C2H3+CH4   6.62000E+00 3.70000E+00 9.50000E+03
    REV/1.90800E+00 3.76000E+00 3.28000E+03/
C2H4+O2=C2H3+HO2   4.00000E+13 0.00000E+00 5.82000E+04
    REV/6.62600E+10 1.58000E-01 -4.24900E+03/
C2H4+CH3O2=C2H3+CH3O2H   2.23000E+12 0.00000E+00 1.71900E+04
    REV/7.92900E+12 -6.34000E-01 -8.16700E+03/
C2H4+C2H5O2=C2H3+C2H5O2H   2.23000E+12 0.00000E+00
1.71900E+04
    REV/7.94300E+12 -6.34000E-01 -8.16300E+03/
CH+CH4=C2H4+H   6.00000E+13 0.00000E+00 0.00000E+00
    REV/3.57300E+14 0.00000E+00 5.54800E+04/
C2H3(+M)=C2H2+H(+M)   3.86000E+08 1.62000E+00 3.70500E+04
    LOW /2.56500E+27 -3.40000E+00 3.57990E+04/
    TROE/   1.98160E+00   5.38370E+03   4.29320E+00   -7.95000E-02 /

138

H2/2.0000E+00/ H2O/6.0000E+00/ CO/1.5000E+00/ CO2/2.0000E+00/
CH4/2.0000E+00/ C2H6/3.0000E+00/
 C2H3+O2=C2H2+HO2   5.19000E+15 -1.20000E+00 3.31000E+03
    REV/2.66100E+16 -1.29500E+00 1.78600E+04/
 C2H3+O2=CH2O+HCO   8.50000E+28 -5.31200E+00 6.50000E+03
    REV/3.99400E+27 -4.88300E+00 9.34500E+04/
 C2H3+O2=CH2CHO+O   5.50000E+14 -6.11000E-01 5.26000E+03
    REV/3.00000E+18 -1.38600E+00 1.63000E+04/
 CH3+C2H3=CH4+C2H2   3.92000E+11 0.00000E+00 0.00000E+00
    REV/3.49700E+14 -1.93000E-01 7.07800E+04/
 C2H3+H=C2H2+H2   9.64000E+13 0.00000E+00 0.00000E+00
    REV/9.42700E+13 2.53000E-01 6.92400E+04/
 C2H3+OH=C2H2+H2O   3.01100E+13 0.00000E+00 0.00000E+00
    REV/3.12200E+14 1.47000E-01 8.41300E+04/
 C2H2+O2=HCCO+OH   2.00000E+08 1.50000E+00 3.01000E+04
    REV/2.03900E+06 1.54100E+00 3.22700E+04/
 C2H2+O=HCCO+H   5.30000E+04 2.68000E+00 2.36000E+03
    REV/1.86700E+05 2.33000E+00 2.12600E+04/
 C2H2+OH=CH3+CO   4.83000E-04 4.00000E+00 -2.00000E+03
    REV/3.49500E-06 4.63800E+00 5.21200E+04/
 OH+C2H2=H+HCCOH   5.04000E+05 2.30000E+00 1.35000E+04
    REV/3.85200E+09 1.43600E+00 4.38200E+03/
 C2H3CHO=C2H3+HCO   2.00300E+24 -2.13500E+00 1.03400E+05
    REV/1.81000E+13 0.00000E+00 0.00000E+00/
 C3H8(+M)=CH3+C2H5(+M)   1.29000E+37 -5.84000E+00 9.73800E+04
     LOW /5.64000E+74 -1.57400E+01 9.87140E+04/
     TROE/   3.10000E-01   5.00000E+01   3.00000E+03   9.00000E+03 /
    H2/2.0000E+00/ H2O/6.0000E+00/ CO/1.5000E+00/ CO2/2.0000E+00/
CH4/2.0000E+00/ C2H6/3.0000E+00/
 C3H8=NC3H7+H   3.75000E+17 -3.57000E-01 1.01200E+05
    REV/1.00000E+14 0.00000E+00 0.00000E+00/
 C3H8=IC3H7+H   2.37700E+18 -6.71000E-01 9.86800E+04
    REV/1.00000E+14 0.00000E+00 0.00000E+00/
 C3H8+O2=IC3H7+HO2   2.00000E+13 0.00000E+00 4.96400E+04
    REV/1.76400E+09 5.99000E-01 -1.69000E+02/
 C3H8+O2=NC3H7+HO2   6.00000E+13 0.00000E+00 5.22900E+04
    REV/3.35400E+10 2.85000E-01 -5.90000E+01/
 H+C3H8=H2+IC3H7   1.30000E+06 2.40000E+00 4.47100E+03
    REV/2.18600E+01 3.34700E+00 9.35100E+03/
 H+C3H8=H2+NC3H7   3.49000E+05 2.69000E+00 6.45000E+03
    REV/3.72000E+01 3.32300E+00 8.79000E+03/
 C3H8+O=IC3H7+OH   5.49000E+05 2.50000E+00 3.14000E+03
    REV/4.79300E+00 3.42800E+00 6.60800E+03/

C3H8+O=NC3H7+OH   3.71000E+06 2.40000E+00 5.50500E+03
    REV/2.05300E+02 3.01400E+00 6.43300E+03/
C3H8+OH=NC3H7+H2O   1.05400E+10 9.70000E-01 1.58600E+03
    REV/1.19100E+07 1.49700E+00 1.88200E+04/
C3H8+OH=IC3H7+H2O   4.67000E+07 1.61000E+00 -3.50000E+01
    REV/8.32700E+03 2.45100E+00 1.97400E+04/
C3H8+HO2=IC3H7+H2O2   6.32000E+01 3.37000E+00 1.37200E+04
    REV/6.14900E-01 3.62200E+00 2.59800E+03/
C3H8+HO2=NC3H7+H2O2   4.08000E+01 3.59000E+00 1.71600E+04
    REV/2.51600E+00 3.52800E+00 3.50000E+03/
CH3+C3H8=CH4+IC3H7   6.40000E+04 2.17000E+00 7.52000E+03
    REV/9.81900E+02 2.67100E+00 1.39400E+04/
CH3+C3H8=CH4+NC3H7   9.04000E-01 3.65000E+00 7.15400E+03
    REV/8.79100E-02 3.83700E+00 1.10300E+04/
IC3H7+C3H8=NC3H7+C3H8   3.00000E+10 0.00000E+00 1.29000E+04
    REV/3.00000E+10 0.00000E+00 1.29000E+04/
C2H3+C3H8=C2H4+IC3H7   1.00000E+11 0.00000E+00 1.04000E+04
    REV/1.31000E+11 0.00000E+00 1.78000E+04/
C2H3+C3H8=C2H4+NC3H7   1.00000E+11 0.00000E+00 1.04000E+04
    REV/1.31000E+11 0.00000E+00 1.78000E+04/
C2H5+C3H8=C2H6+IC3H7   1.00000E+11 0.00000E+00 1.04000E+04
    REV/3.63000E+10 0.00000E+00 9.93400E+03/
C2H5+C3H8=C2H6+NC3H7   1.00000E+11 0.00000E+00 1.04000E+04
    REV/3.63000E+10 0.00000E+00 9.93400E+03/
CH3O2+C3H8=CH3O2H+NC3H7   1.38600E+00 3.97000E+00
1.82800E+04
    REV/1.66300E+00 3.46300E+00 3.02400E+03/
CH3O2+C3H8=CH3O2H+IC3H7   1.01900E+01 3.58000E+00 1.48100E+04
    REV/1.92800E+00 3.38700E+00 2.09000E+03/
C2H5O2+C3H8=C2H5O2H+NC3H7   1.38600E+00 3.97000E+00
1.82800E+04
    REV/1.66600E+00 3.46300E+00 3.02800E+03/
C2H5O2+C3H8=C2H5O2H+IC3H7   1.01900E+01 3.58000E+00
1.48100E+04
    REV/1.93100E+00 3.38700E+00 2.09400E+03/
IC3H7=H+C3H6   6.91900E+13 -2.50000E-02 3.76900E+04
    REV/2.64000E+13 0.00000E+00 2.16000E+03/
IC3H7+H=C2H5+CH3   2.00000E+13 0.00000E+00 0.00000E+00
    REV/4.34400E+07 1.17600E+00 8.62000E+03/
IC3H7+O2=C3H6+HO2   4.50000E-19 0.00000E+00 5.02000E+03
    REV/2.00000E-19 0.00000E+00 1.75000E+04/
IC3H7+OH=C3H6+H2O   2.41000E+13 0.00000E+00 0.00000E+00
    REV/2.98500E+12 5.70000E-01 8.38200E+04/

IC3H7+O=CH3CHO+CH3   4.81800E+13 0.00000E+00 0.00000E+00
    REV/1.27900E+11 8.00000E-01 8.64800E+04/
NC3H7=CH3+C2H4   9.97000E+40 -8.60000E+00 4.14300E+04
    REV/1.89800E+34 -6.99000E+00 1.71000E+04/
NC3H7=H+C3H6   8.78000E+39 -8.10000E+00 4.65800E+04
    REV/2.07000E+37 -7.39000E+00 1.20200E+04/
NC3H7+O2=C3H6+HO2   3.00000E-19 0.00000E+00 3.00000E+03
    REV/2.00000E-19 0.00000E+00 1.75000E+04/
C2H3+CH3(+M)=C3H6(+M)   2.50000E+13 0.00000E+00 0.00000E+00
    LOW /4.27000E+58 -1.19400E+01 9.76980E+03/
    TROE/   1.75000E-01   1.34060E+03   6.00000E+04   1.01400E+04 /
C3H6+O=C2H5+HCO   1.58000E+07 1.76000E+00 -1.21600E+03
    REV/9.18800E+01 2.72500E+00 2.31100E+04/
C3H6+H=C2H4+CH3   2.30000E+13 0.00000E+00 2.54700E+03
    REV/7.27200E+07 1.27100E+00 1.12000E+04/
NC3H7O2=NC3H7+O2   2.40000E+20 -1.61600E+00 3.59600E+04
    REV/4.52000E+12 0.00000E+00 0.00000E+00/
IC3H7O2=IC3H7+O2   3.13200E+22 -2.16700E+00 3.81600E+04
    REV/7.54000E+12 0.00000E+00 0.00000E+00/
NC3H7O2=C3H6OOH1-3   1.12500E+11 0.00000E+00 2.44000E+04
    REV/2.71600E+11 -5.07000E-01 8.93600E+03/
IC3H7O2=C3H6OOH2-1   1.80000E+12 0.00000E+00 2.94000E+04
    REV/1.12200E+10 1.19000E-01 1.18100E+04/
C3H6OOH2-1=C3H6+HO2   3.23900E+18 -2.00000E+00 1.89700E+04
    REV/1.00000E+11 0.00000E+00 1.17500E+04/
C3H6OOH1-3=OH+CH2O+C2H4   3.03500E+15 -7.90000E-01
2.74000E+04
    REV/0.00000E+00 0.00000E+00 0.00000E+00/
C3H6OOH1-3O2=C3H6OOH1-3+O2   2.85300E+20 -1.62600E+00
3.56900E+04
    REV/4.52000E+12 0.00000E+00 0.00000E+00/
C3H6OOH2-1O2=C3H6OOH2-1+O2   5.22700E+22 -2.24400E+00
3.78200E+04
    REV/4.52000E+12 0.00000E+00 0.00000E+00/
C3H6OOH1-3O2=C3KET13+OH   7.50000E+10 0.00000E+00 2.14000E+04
    REV/4.10100E+03 1.49600E+00 4.47400E+04/
C3H6OOH2-1O2=C3KET21+OH   3.00000E+11 0.00000E+00 2.38500E+04
    REV/1.39700E+03 1.83400E+00 4.97500E+04/
C3KET13=CH2O+CH2CHO+OH   1.00000E+16 0.00000E+00
4.30000E+04
    REV/0.00000E+00 0.00000E+00 0.00000E+00/
C3KET21=CH2O+CH3CO+OH   1.00000E+16 0.00000E+00 4.30000E+04
    REV/0.00000E+00 0.00000E+00 0.00000E+00/

IC3H7O2=C3H6+HO2   1.19600E+43 -9.43000E+00 4.15300E+04
    REV/2.30200E+33 -7.31000E+00 1.67100E+04/
NC3H7O2=C3H6+HO2   4.30800E+36 -7.50000E+00 3.95100E+04
    REV/1.02300E+28 -5.61700E+00 1.94400E+04/
IC3H6CHO=C3H6+HCO   1.03100E+15 -6.20000E-01 2.31700E+04
    REV/1.00000E+11 0.00000E+00 7.80000E+03/
IC3H6CHO=C2H3CHO+CH3   2.42500E+13 -2.70000E-01 2.24700E+04
    REV/1.00000E+11 0.00000E+00 7.80000E+03/
!
!
!!!
!CH2 reactions added to improve CO predictions
!!!
!
!
CH4+CH2=CH3+CH3   2.46000E+06 2.00000E+00 8.27000E+03
    REV/1.73600E+06 1.86800E+00 1.29800E+04/
CH3+OH=CH2+H2O   5.60000E+07 1.60000E+00 5.42000E+03
    REV/9.22400E+05 2.07200E+00 1.40600E+04/
CH2+H(+M)=CH3(+M)   2.50000E+16 -8.00000E-01 0.00000E+00
    LOW /3.20000E+27 -3.14000E+00 1.23000E+03/
    TROE/   6.80000E-01   7.80000E+01   1.99500E+03   5.59000E+03 /
    H2/2.0000E+00/ H2O/6.0000E+00/ CO/1.5000E+00/ CO2/2.0000E+00/
CH4/2.0000E+00/ C2H6/3.0000E+00/
CH2+O2=CH2O+O   2.40000E+12 0.00000E+00 1.50000E+03
    REV/5.95500E+14 -3.65000E-01 6.09800E+04/
CH2+O2=CO2+H+H   5.80000E+12 0.00000E+00 1.50000E+03
    REV/0.00000E+00 0.00000E+00 0.00000E+00/
CH2+O2=CO+OH+H   5.00000E+12 0.00000E+00 1.50000E+03
    REV/0.00000E+00 0.00000E+00 0.00000E+00/
CH2+O=CO+H+H   5.00000E+13 0.00000E+00 0.00000E+00
    REV/0.00000E+00 0.00000E+00 0.00000E+00/
CH2+H=CH+H2   1.00000E+18 -1.56000E+00 0.00000E+00
    REV/5.16000E+18 -1.80000E+00 3.46000E+03/
        DUPLICATE
CH2+OH=CH+H2O   1.13000E+07 2.00000E+00 3.00000E+03
    REV/6.18300E+08 1.65500E+00 2.13500E+04/
CH2+H=CH+H2   2.70000E+11 6.70000E-01 2.57000E+04
    REV/1.89700E+11 6.70000E-01 2.87300E+04/
        DUPLICATE
C2H6+CH=C2H5+CH2   1.10000E+14 0.00000E+00 -2.60000E+02
    REV/1.96900E+09 9.21000E-01 -1.49000E+03/
C2H2+O=CH2+CO   8.20000E+09 1.10000E+00 2.37000E+03

REV/4.78600E+04 2.29800E+00 4.88300E+04/
!
!
!!!
!rxns added from 68 spec skeletal nhept mech (reduced from 88
!spec skeletelal uconn mech)
!!!
!
!
CH2CO+H=CH3+CO   1.10E+13   0.00E+00   3.40E+03
   REV/2.40E+12   0.00E+00   4.02000E+04/
CH2CO+O=HCCO+OH   1.00E+13   0.00E+00   8.00E+03
   REV/1.43E+10   0.00E+00   -1.25500E+03/
CH2CO+OH=HCCO+H2O   1.00E+13   0.00E+00   2.00E+03
   REV/1.41E+11   0.00E+00   9.99500E+03/
CH2CO+H=HCCO+H2   2.00E+14   0.00E+00   8.00E+03
   REV/6.52E+11   0.00E+00   8.40000E+02/
HCCO+OH=HCO+HCO   1.00E+13   0.00E+00   0.00E+00
   REV/2.41E+14   0.00E+00   4.03600E+04/
C2H6=C2H5+H   2.78E+21   -1.56E+00   1.04E+05
   REV/3.61E+13   0.00E+00   0.00000E+00/
C3H6=C2H3+CH3   2.73E+62   -1.33E+01   1.23E+05
   REV/4.71E+59   -1.32E+01   2.95400E+04/
C3H6=C3H5-A+H   2.01E+61   -1.33E+01   1.19E+05
   REV/4.89E+56   -1.23E+01   2.80800E+04/
C3H6+O=CH2CO+CH3+H   2.50E+07   1.76E+00   7.60E+01
   REV/1.00E+00   0.00E+00   0.00000E+00/
C3H6+HO2=C3H5-A+H2O2   1.50E+11   0.00E+00   1.42E+04
   REV/5.87E+05   1.33E+00   9.75900E+03/
C3H6+OH=C3H5-A+H2O   3.12E+06   2.00E+00   -2.98E+02
   REV/6.19E+06   2.01E+00   3.18800E+04/
C3H6+O=C3H5-A+OH   5.24E+11   7.00E-01   5.88E+03
   REV/1.06E+11   7.10E-01   2.08200E+04/
C3H6+H=C3H5-A+H2   1.73E+05   2.50E+00   2.49E+03
   REV/7.93E+04   2.51E+00   1.95200E+04/
C4H8-1=C3H5-A+CH3   5.00E+15   0.00E+00   7.10E+04
   REV/5.00E+12   0.00E+00   0.00000E+00/
C4H8-1=C2H3+C2H5   1.00E+19   -1.00E+00   9.68E+04
   REV/9.00E+12   0.00E+00   0.00000E+00/
PC4H9=C2H5+C2H4   7.50E+17   -1.41E+00   2.96E+04
   REV/3.30E+11   0.00E+00   7.20000E+03/
PC4H9=C4H8-1+H   1.16E+17   -1.17E+00   3.82E+04
   REV/1.00E+13   0.00E+00   2.90000E+03/

PC4H9+O2=C4H8-1+HO2   3.00E-19   0.00E+00   3.00E+03
   REV/2.00E-19   0.00E+00   1.75000E+04/
CH3COCH2=CH2CO+CH3   1.00E+14   0.00E+00   3.10E+04
   REV/1.00E+11   0.00E+00   6.00000E+03/
C2H5CHO=C2H5+HCO   9.85E+18   -7.30E-01   8.17E+04
   REV/1.81E+13   0.00E+00   0.00000E+00/
C5H10-1=C2H5+C3H5-A   9.17E+20   -1.63E+00   7.40E+04
   REV/4.00E+12   0.00E+00   -5.96000E+02/
C5H10-1+O=PC4H9+HCO   1.00E+11   0.00E+00   0.00E+00
   REV/0.00E+00   0.00E+00   0.00000E+00/
C5H10-1+O=NC3H7+CH3CO   1.00E+11   0.00E+00   0.00E+00
   REV/0.00E+00   0.00E+00   0.00000E+00/
C5H10-1+OH=PC4H9+CH2O   1.00E+11   0.00E+00   0.00E+00
   REV/0.00E+00   0.00E+00   0.00000E+00/
C5H10-1+OH=NC3H7+CH3CHO   1.00E+11   0.00E+00   0.00E+00
   REV/0.00E+00   0.00E+00   0.00000E+00/
CH3CO+H=CH2CO+H2   2.00E+13   0.00E+00   0.00E+00
   REV/5.63E+17   -1.13E+00   6.37000E+04/
CH3CO+O=CH2CO+OH   2.00E+13   0.00E+00   0.00E+00
   REV/5.95E+18   -1.13E+00   1.20700E+05/
CH3CO+CH3=CH2CO+CH4   5.00E+13   0.00E+00   0.00E+00
   REV/8.20E+17   -6.70E-01   7.98300E+04/
C2H5O+M=CH3+CH2O+M   1.35E+38   -6.96E+00   2.38E+04
   REV/6.44E+36   -6.99E+00   1.68500E+04/
C3H2+O2=HCCO+CO+H   5.00E+13   0.00E+00   0.00E+00
   REV/0.00E+00   0.00E+00   0.00000E+00/
C2H5O+M=CH3CHO+H+M   1.16E+35   -5.89E+00   2.53E+04
   REV/3.06E+30   -4.78E+00   6.10000E+03/
C3H5O=C2H3CHO+H   1.00E+14   0.00E+00   2.91E+04
   REV/7.71E+11   4.80E-01   1.77500E+04/
C3H5O=C2H3+CH2O   2.03E+12   9.00E-02   2.36E+04
   REV/1.50E+11   0.00E+00   1.06000E+04/
C3H5O+O2=C2H3CHO+HO2   1.00E+12   0.00E+00   6.00E+03
   REV/1.29E+11   0.00E+00   3.20000E+04/
C3H5-A+HO2=C3H5O+OH   7.00E+12   0.00E+00   -1.00E+03
   REV/2.04E+13   -1.60E-01   1.22600E+04/
C3H5-A+CH3O2=C3H5O+CH3O   7.00E+12   0.00E+00   -1.00E+03
   REV/1.99E+15   -7.40E-01   1.70200E+04/
C3H6+CH3O2=C3H5-A+CH3O2H   3.24E+11   0.00E+00   1.49E+04
   REV/2.00E+10   0.00E+00   1.50000E+04/
C4H7O=CH3CHO+C2H3   7.94E+14   0.00E+00   1.90E+04
   REV/1.00E+10   0.00E+00   2.00000E+04/
C4H7O=C2H3CHO+CH3   7.94E+14   0.00E+00   1.90E+04

```
    REV/1.00E+10   0.00E+00   2.00000E+04/
C4H8-1+OH=NC3H7+CH2O   1.00E+12   0.00E+00   0.00E+00
    REV/1.62E+12   0.00E+00   1.32300E+04/
C4H8-1+O=C3H6+CH2O   7.23E+05   2.34E+00   -1.05E+03
    REV/2.00E+05   2.34E+00   8.02800E+04/
C4H8-1+O=CH3CHO+C2H4   1.30E+13   0.00E+00   8.50E+02
    REV/2.07E+12   0.00E+00   8.51000E+04/
C4H8-1+O=CH3CO+C2H5   1.30E+13   0.00E+00   8.50E+02
    REV/2.35E+12   0.00E+00   3.81500E+04/
C4H8-1+OH=CH3CHO+C2H5   1.00E+12   0.00E+00   0.00E+00
    REV/9.33E+12   0.00E+00   1.99300E+04/
C4H8-1+OH=CH3CO+C2H6   5.00E+11   0.00E+00   0.00E+00
    REV/9.83E+12   0.00E+00   3.24300E+04/
C4H8-1+OH=C2H5CHO+CH3   1.00E+12   0.00E+00   0.00E+00
    REV/4.95E+10   0.00E+00   1.69400E+04/
C3H4-A+HO2=C2H4+CO+OH   1.00E+12   0.00E+00   1.40E+04
    REV/1.00E+00   0.00E+00   0.00000E+00/
C3H4-A+HO2=C3H3+H2O2   3.00E+13   0.00E+00   1.40E+04
    REV/1.55E+16   -1.38E+00   4.40000E+04/
C3H6+O2=C3H5-A+HO2   4.00E+12   0.00E+00   3.99E+04
    REV/3.33E+10   3.40E-01   -5.56000E+02/
C3H6+CH3=C3H5-A+CH4   2.21E+00   3.50E+00   5.68E+03
    REV/2.65E+01   3.51E+00   2.31800E+04/
C3H6+C2H5=C3H5-A+C2H6   1.00E+11   0.00E+00   9.80E+03
    REV/5.37E+05   1.33E+00   1.64400E+04/
C3H5-A+HO2=C2H3+CH2O+OH   1.00E-18   0.00E+00   0.00E+00
    REV/1.00E-30   0.00E+00   0.00000E+00/
C3H5-A+H=C3H4-A+H2   1.81E+13   0.00E+00   0.00E+00
    REV/1.23E+13   1.20E-01   4.72300E+04/
C3H5-A+CH3=C3H4-A+CH4   1.00E+11   0.00E+00   0.00E+00
    REV/4.92E+12   5.00E-02   4.77800E+04/
C3H5-A+C2H5=C2H6+C3H4-A   4.00E+11   0.00E+00   0.00E+00
    REV/1.80E+12   5.00E-02   4.03300E+04/
C3H5-A+C2H5=C2H4+C3H6   4.00E+11   0.00E+00   0.00E+00
    REV/6.94E+16   -1.33E+00   5.28000E+04/
C3H5-A+C2H3=C2H4+C3H4-A   1.00E+12   0.00E+00   0.00E+00
    REV/1.62E+13   5.00E-02   4.81900E+04/
C3H4-A+C3H6=C3H5-A+C3H5-A   8.39E+17   -1.29E+00   3.37E+04
    REV/1.00E+12   0.00E+00   0.00000E+00/
C3H5-A+O2=C2H3CHO+OH   2.47E+13   -4.40E-01   2.30E+04
    REV/1.90E+14   -8.00E-01   7.48800E+04/
C3H4-A+M=C3H3+H+M   1.14E+17   0.00E+00   7.00E+04
    REV/1.80E+15   -3.80E-01   1.06100E+04/
```

145

C3H4-A+O2=C3H3+HO2   4.00E+13   0.00E+00   3.92E+04
  REV/1.18E+11   3.00E-01   3.80000E+01/
C3H3+H=C3H2+H2   5.00E+13   0.00E+00   0.00E+00
  REV/3.85E+10   3.80E-01   4.60000E+03/
C3H4-A+OH=C3H3+H2O   1.00E+07   2.00E+00   1.00E+03
  REV/7.00E+06   1.97E+00   3.45200E+04/
C3H4-A+O=C2H4+CO   7.80E+12   0.00E+00   1.60E+03
  REV/8.28E+13   -2.10E-01   1.24800E+05/
C3H5-A=C3H4-A+H   6.66E+15   -4.30E-01   6.32E+04
  REV/2.40E+11   6.90E-01   3.00700E+03/
C3H4-A+H=C3H3+H2   2.00E+07   2.00E+00   5.00E+03
  REV/3.24E+06   1.97E+00   2.33600E+04/
C3H4-A+CH3=C3H3+CH4   3.67E-02   4.01E+00   6.83E+03
  REV/1.55E-01   3.98E+00   2.56700E+04/
C3H4-A+C3H5-A=C3H3+C3H6   2.00E+11   0.00E+00   7.70E+03
  REV/2.64E+19   -2.71E+00   4.21400E+04/
C3H3+OH=C3H2+H2O   1.00E+13   0.00E+00   0.00E+00
  REV/1.34E+15   0.00E+00   1.56800E+04/
C3H3+O2=CH2CO+HCO   3.01E+10   0.00E+00   2.87E+03
  REV/4.88E+11   0.00E+00   5.94700E+04/
CH2CHO=CH2CO+H   3.09E+15   -2.60E-01   5.08E+04
  REV/5.00E+13   0.00E+00   1.23000E+04/
C3H5-A+O2=C3H4-A+HO2   2.18E+21   -2.85E+00   3.08E+04
  REV/2.69E+19   -2.40E+00   2.05000E+04/
C3H5-A+O2=CH2CHO+CH2O   7.14E+15   -1.21E+00   2.11E+04
  REV/4.94E+16   -1.40E+00   8.86200E+04/
HCCO+O2=CO2+HCO   2.40E+11   0.00E+00   -8.54E+02
  REV/1.47E+14   0.00E+00   1.33600E+05/
C2H4+H2=CH3+CH3   3.77E+12   8.30E-01   8.47E+04
  REV/1.00E+14   0.00E+00   3.20000E+04/
NC3H7CHO+O2=NC3H7CO+HO2   2.00E+13   5.00E-01   4.22E+04
  REV/1.00E+07   5.00E-01   4.00000E+03/
NC3H7CHO+OH=NC3H7CO+H2O   2.69E+10   7.60E-01   -3.40E+02
  REV/1.85E+10   7.50E-01   3.12200E+04/
NC3H7CHO+H=NC3H7CO+H2   4.00E+13   0.00E+00   4.20E+03
  REV/1.80E+13   0.00E+00   2.40000E+04/
NC3H7CHO+O=NC3H7CO+OH   5.00E+12   0.00E+00   1.79E+03
  REV/1.00E+12   0.00E+00   1.90000E+04/
NC3H7CHO+HO2=NC3H7CO+H2O2   2.80E+12   0.00E+00   1.36E+04
  REV/1.00E+12   0.00E+00   1.00000E+04/
NC3H7CHO+CH3=NC3H7CO+CH4   1.70E+12   0.00E+00   8.44E+03
  REV/1.50E+13   0.00E+00   2.80000E+04/
NC3H7CHO+CH3O2=NC3H7CO+CH3O2H   1.00E+12   0.00E+00   9.50E+03

REV/2.50E+10   0.00E+00   1.00000E+04/
NC3H7CO=NC3H7+CO   5.33E+15   -8.60E-01   1.34E+04
    REV/1.50E+11   0.00E+00   4.80000E+03/
C2H5COCH2=CH2CO+C2H5   1.57E+13   0.00E+00   3.00E+04
    REV/2.11E+11   0.00E+00   7.35000E+03/
NC3H7COCH2=NC3H7+CH2CO   1.23E+18   -1.40E+00   4.35E+04
    REV/1.00E+11   0.00E+00   1.16000E+04/
NC4H9CO=PC4H9+CO   1.00E+11   0.00E+00   9.60E+03
    REV/1.00E+11   0.00E+00   0.00000E+00/
!!
!n-hept destruct - small rxn rates
NC7H16=H+C7H15-1   1.34E+88   -2.12E+01   1.43E+05
    REV/3.37E+82   -2.02E+01   3.96100E+04/
NC7H16=H+C7H15-2   6.50E+87   -2.10E+01   1.40E+05
    REV/5.21E+80   -1.97E+01   3.88900E+04/
NC7H16=H+C7H15-3   6.50E+87   -2.10E+01   1.40E+05
    REV/5.21E+80   -1.97E+01   3.88900E+04/
NC7H16=H+C7H15-4   3.25E+87   -2.10E+01   1.40E+05
    REV/5.19E+80   -1.97E+01   3.88900E+04/
NC7H16=PC4H9+NC3H7   1.42E+78   -1.77E+01   1.21E+05
    REV/1.36E+68   -1.61E+01   3.24600E+04/
!!
!n-hept destruct - large rxn rates; attack by h and o
!
!!!!!!!!!!! largest of h attack
!
NC7H16+H=C7H15-2+H2   2.60E+06   2.40E+00   4.47E+03
    REV/3.93E+03   2.7E+00   1.12600E+04/
NC7H16+H=C7H15-3+H2   2.60E+06   2.40E+00   4.47E+03
    REV/3.93E+03   2.74E+00   1.12600E+04/
!
NC7H16+H=C7H15-4+H2   1.30E+06   2.40E+00   4.47E+03
    REV/3.91E+03   2.74E+00   1.12600E+04/
!
NC7H16+H=C7H15-1+H2   1.88E+05   2.75E+00   6.28E+03
    REV/8.93E+03   2.70E+00   1.05500E+04/
!
!
!!!!!!!!!!! largest of o attack
!
NC7H16+O=C7H15-1+OH   1.93E+05   2.68E+00   3.72E+03
    REV/4.03E+03   2.63E+00   5.89300E+03/
!

NC7H16+O=C7H15-2+OH   9.54E+04   2.71E+00   2.11E+03
    REV/6.33E+01   3.05E+00   6.79800E+03/
NC7H16+O=C7H15-3+OH   9.54E+04   2.71E+00   2.11E+03
    REV/6.33E+01   3.05E+00   6.79800E+03/
!
NC7H16+O=C7H15-4+OH   4.77E+04   2.71E+00   2.11E+03
    REV/6.31E+01   3.05E+00   6.79800E+03/
!!!
!n-hept attack by oh radical
!
NC7H16+OH=C7H15-1+H2O   1.05E+10   0.97E+00   1.59E+03
    REV/1.50E+10   1.05E+00   2.33300E+04/
!
!raised A from 9.4E+07 to 1.00E+10
!lowered n from 1.61 to 1.00
!lowered Ea from -3.50E+01 to -5.0E+02
!
NC7H16+OH=C7H15-2+H2O   9.40E+07   1.61E+00   -3.50E+01
    REV/6.15E+05   1.95E+00   2.19100E+04/
!
!raised A from 9.4E+07 to 1.00E+10
!lowered n from 1.61 to 1.00
!lowered Ea from -3.50E+01 to -5.0E+02
!
NC7H16+OH=C7H15-3+H2O   9.40E+07   1.61E+00   -3.50E+01
    REV/6.15E+05   1.95E+00   2.19100E+04/
!
!
NC7H16+OH=C7H15-4+H2O   4.70E+07   1.61E+00   -3.50E+01
    REV/6.13E+05   1.95E+00   2.19100E+04/
!!!
NC7H16+HO2=C7H15-1+H2O2   1.68E+13   0.00E+00   2.04E+04
    REV/2.05E+13   -3.80E-01   8.39900E+03/
NC7H16+HO2=C7H15-2+H2O2   1.12E+13   0.00E+00   1.77E+04
    REV/4.35E+11   1.00E-02   8.16500E+03/
NC7H16+HO2=C7H15-3+H2O2   1.12E+13   0.00E+00   1.77E+04
    REV/4.35E+11   1.00E-02   8.16500E+03/
NC7H16+HO2=C7H15-4+H2O2   5.60E+12   0.00E+00   1.77E+04
    REV/4.33E+11   1.00E-02   8.16500E+03/
NC7H16+CH3=C7H15-1+CH4   9.04E-01   3.65E+00   7.15E+03
    REV/1.12E+00   3.60E+00   1.19100E+04/
NC7H16+CH3=C7H15-2+CH4   5.41E+04   2.26E+00   7.29E+03
    REV/2.14E+03   2.60E+00   1.45500E+04/

148

```
NC7H16+CH3=C7H15-3+CH4   5.41E+04   2.26E+00   7.29E+03
    REV/2.14E+03   2.60E+00   1.45500E+04/
NC7H16+CH3=C7H15-4+CH4   2.71E+04   2.26E+00   7.29E+03
    REV/2.13E+03   2.60E+00   1.45500E+04/
NC7H16+O2=C7H15-1+HO2   6.00E+13   0.00E+00   5.28E+04
    REV/5.18E+10   2.80E-01   -4.06000E+02/
NC7H16+O2=C7H15-2+HO2   4.00E+13   0.00E+00   5.02E+04
    REV/1.10E+09   6.70E-01   -5.41000E+02/
NC7H16+O2=C7H15-3+HO2   4.00E+13   0.00E+00   5.02E+04
    REV/1.10E+09   6.70E-01   -5.41000E+02/
NC7H16+O2=C7H15-4+HO2   2.00E+13   0.00E+00   5.02E+04
    REV/1.09E+09   6.70E-01   -5.41000E+02/
NC7H16+C2H5=C7H15-1+C2H6   1.00E+11   0.00E+00   1.34E+04
    REV/3.20E+11   0.00E+00   1.23000E+04/
NC7H16+C2H5=C7H15-2+C2H6   1.00E+11   0.00E+00   1.04E+04
    REV/1.00E+11   0.00E+00   1.29000E+04/
NC7H16+C2H5=C7H15-3+C2H6   1.00E+11   0.00E+00   1.04E+04
    REV/1.00E+11   0.00E+00   1.29000E+04/
NC7H16+C2H5=C7H15-4+C2H6   5.00E+10   0.00E+00   1.04E+04
    REV/1.00E+11   0.00E+00   1.29000E+04/
NC7H16+C2H3=C7H15-1+C2H4   1.00E+12   0.00E+00   1.80E+04
    REV/2.57E+12   0.00E+00   2.54000E+04/
NC7H16+C2H3=C7H15-2+C2H4   8.00E+11   0.00E+00   1.68E+04
    REV/2.00E+12   0.00E+00   2.42000E+04/
NC7H16+C2H3=C7H15-3+C2H4   8.00E+11   0.00E+00   1.68E+04
    REV/2.00E+12   0.00E+00   2.42000E+04/
NC7H16+C2H3=C7H15-4+C2H4   4.00E+11   0.00E+00   1.68E+04
    REV/2.00E+12   0.00E+00   2.42000E+04/
NC7H16+CH3O2=C7H15-1+CH3O2H   1.21E+13   0.00E+00   2.04E+04
    REV/3.60E+12   0.00E+00   9.80000E+03/
NC7H16+CH3O2=C7H15-2+CH3O2H   8.06E+12   0.00E+00   1.77E+04
    REV/2.38E+11   0.00E+00   3.70000E+03/
NC7H16+CH3O2=C7H15-3+CH3O2H   8.06E+12   0.00E+00   1.77E+04
    REV/2.38E+11   0.00E+00   3.70000E+03/
NC7H16+CH3O2=C7H15-4+CH3O2H   4.03E+12   0.00E+00   1.77E+04
    REV/2.38E+11   0.00E+00   3.70000E+03/
NC7H16+C7H15-1=C7H15-2+NC7H16   1.00E+11   0.00E+00   1.04E+04
    REV/1.50E+11   0.00E+00   1.23000E+04/
NC7H16+C7H15-1=C7H15-3+NC7H16   1.00E+11   0.00E+00   1.04E+04
    REV/1.50E+11   0.00E+00   1.23000E+04/
NC7H16+C7H15-1=C7H15-4+NC7H16   5.00E+10   0.00E+00   1.04E+04
    REV/1.50E+11   0.00E+00   1.23000E+04/
NC7H16+C7H15-2=C7H15-3+NC7H16   1.00E+11   0.00E+00   1.04E+04
```

```
     REV/1.00E+11    0.00E+00    1.04000E+04/
NC7H16+C7H15-2=C7H15-4+NC7H16    5.00E+10    0.00E+00    1.04E+04
     REV/1.00E+11    0.00E+00    1.04000E+04/
NC7H16+C7H15-3=C7H15-4+NC7H16    5.00E+10    0.00E+00    1.04E+04
     REV/1.00E+11    0.00E+00    1.04000E+04/
!!!!!!!!!!!!!!!!!!!!!!!!!!!!!!!!!!!!!!!!!!!!!!!!!!!!!!!!!!!!!!!!!!!!!!!!!!!!!!!
!n-hept breakup to smaller species
!lower rxn rates than n-hept + h and o
!
!
!raised A from 2.22E+16 to
!lowered n from -0.89 to
!lowered Ea from 3.01E+04 to
!
C7H15-2=PC4H9+C3H6    2.22E+16    -8.90E-01    3.01E+04
     REV/1.00E+11    0.00E+00    8.20000E+03/
!
!raised A from 9.63E+17 to
!lowered n from -1.42 to
!lowered Ea from 3.06E+04 to
!
C7H15-3=C4H8-1+NC3H7    9.63E+17    -1.42E+00    3.06E+04
     REV/1.00E+11    0.00E+00    7.70000E+03/
!
!raised A from 5.43E+16 to
!lowered n from -0.89 to
!lowered Ea from 3.06E+04 to
!
C7H15-4=C2H5+C5H10-1    5.43E+16    -8.90E-01    3.06E+04
     REV/1.00E+11    0.00E+00    8.20000E+03/
!!!!!!!!!!!!!!!!!!!!!!!!!!!!!!!!!!!
!
!raised A from 1.0E+11 to
!lowered n from 0.0 to
!lowered Ea from -4.00E+03 to
!
C7H14-3+OH=C2H5CHO+PC4H9    1.00E+11    0.00E+00    -4.00E+03
     REV/0.00E+00    0.00E+00    0.00000E+00/
!
!raised A from 1.0E+11 to
!lowered n from 0.0 to
!lowered Ea from -1.05E+03 to
!
```

C7H14-3+O=CH3CHO+C5H10-1   1.00E+11   0.00E+00   -1.05E+03
    REV/0.00E+00   0.00E+00   0.00000E+00/
!!!
C7H15-3=C7H14-3+H   2.02E+15   -6.60E-01   3.77E+04
    REV/1.00E+13   0.00E+00   2.90000E+03/
C7H15-4=C7H14-3+H   4.02E+15   -6.60E-01   3.77E+04
    REV/1.00E+13   0.00E+00   2.90000E+03/
C7H15-3+O2=C7H14-3+HO2   3.00E-09   0.00E+00   3.00E+03
    REV/5.09E-09   -1.00E-02   1.81800E+04/
C7H15-4+O2=C7H14-3+HO2   6.00E-09   0.00E+00   3.00E+03
    REV/5.11E-09   -1.00E-02   1.81800E+04/
C7H15-1=C7H15-3   1.39E+09   9.80E-01   3.38E+04
    REV/4.41E+07   1.38E+00   3.62800E+04/
C7H15-1=C7H15-4   2.54E+09   3.50E-01   1.98E+04
    REV/1.61E+08   7.40E-01   2.22800E+04/
C7H15-2=C7H15-3   9.59E+08   1.39E+00   3.97E+04
    REV/9.59E+08   1.39E+00   3.97000E+04/
C7H15-1=C7H15-2   5.48E+08   1.62E+00   3.88E+04
    REV/1.74E+07   2.01E+00   4.12800E+04/
!!!
!!!
!start of qooh ltc reactions
C7H15O2-1=C7H15-1+O2   2.66E+20   -1.67E+00   3.54E+04
    REV/4.52E+12   0.00E+00   0.00000E+00/
C7H15O2-2=C7H15-2+O2   1.36E+23   -2.36E+00   3.77E+04
    REV/7.54E+12   0.00E+00   0.00000E+00/
C7H15O2-3=C7H15-3+O2   9.88E+21   -1.97E+00   3.79E+04
    REV/7.54E+12   0.00E+00   0.00000E+00/
C7H15O2-4=C7H15-4+O2   1.36E+23   -2.36E+00   3.77E+04
    REV/7.54E+12   0.00E+00   0.00000E+00/
!!!
!
!
!lowered A from 2.5E+10 to 3.0E+18
!lowered n from 0 to -3.0
!lowered Ea from 2.09E+4 to -3.0E+3
!
C7H15O2-2=C7H14OOH2-4   2.5E+10   0.00E+00   2.09E+04
    REV/2.83E+09   -1.10E-01   8.27000E+03/
!
!
!lowered A from 2.5E+10 to 1.0E+13
!lowered n from 0 to -3.0

!lowered Ea from 2.09E+4 to -3.0E+3
!
C7H15O2-3=C7H14OOH3-5   2.5E+10   0.00E+00   2.09E+04
   REV/3.88E+10   -5.10E-01   8.08000E+03/
!
!lowered A from 5.0E+10 to
!lowered n from 0 to
!lowered Ea from 2.09E+4 to
!
C7H15O2-4=C7H14OOH4-2   5.0E+10   0.00E+00   2.09E+04
   REV/5.66E+09   -1.10E-01   8.27000E+03/
!!!
C7H14OOH2-4=C7H14O2-4+OH   7.50E+10   0.00E+00   1.53E+04
   REV/0.00E+00   0.00E+00   0.00000E+00/
C7H14OOH4-2=C7H14O2-4+OH   7.50E+10   0.00E+00   1.53E+04
   REV/0.00E+00   0.00E+00   0.00000E+00/
C7H14OOH2-4=OH+CH3CHO+C5H10-1   5.36E+17   -1.40E+00   2.68E+04
   REV/0.00E+00   0.00E+00   0.00000E+00/
C7H14OOH3-5=OH+C2H5CHO+C4H8-1   2.47E+18   -1.55E+00   2.70E+04
   REV/0.00E+00   0.00E+00   0.00000E+00/
C7H14OOH4-2=OH+NC3H7CHO+C3H6   1.30E+18   -1.49E+00   2.68E+04
   REV/0.00E+00   0.00E+00   0.00000E+00/
C7H14OOH2-4O2=C7H14OOH2-4+O2   1.39E+23   -2.38E+00   3.76E+04
   REV/7.54E+12   0.00E+00   0.00000E+00/
C7H14OOH3-5O2=C7H14OOH3-5+O2   1.39E+23   -2.38E+00   3.76E+04
   REV/7.54E+12   0.00E+00   0.00000E+00/
C7H14OOH4-2O2=C7H14OOH4-2+O2   6.97E+22   -2.38E+00   3.76E+04
   REV/7.54E+12   0.00E+00   0.00000E+00/
C7H14OOH2-4O2=NC7KET24+OH   1.25E+10   0.00E+00   1.79E+04
   REV/1.62E+02   1.83E+00   4.42000E+04/
C7H14OOH3-5O2=NC7KET35+OH   1.25E+10   0.00E+00   1.79E+04
   REV/1.62E+02   1.83E+00   4.42000E+04/
C7H14OOH4-2O2=NC7KET42+OH   1.25E+10   0.00E+00   1.79E+04
   REV/1.62E+02   1.83E+00   4.42000E+04/
NC7KET24=NC3H7CHO+CH3COCH2+OH   1.05E+16   0.00E+00   4.16E+04
   REV/0.00E+00   0.00E+00   0.00000E+00/
NC7KET35=C2H5CHO+C2H5COCH2+OH   1.05E+16   0.00E+00   4.16E+04
   REV/0.00E+00   0.00E+00   0.00000E+00/
NC7KET42=CH3CHO+NC3H7COCH2+OH   1.05E+16   0.00E+00   4.16E+04
   REV/0.00E+00   0.00E+00   0.00000E+00/
C7H14O2-4+OH=CH3CO+C5H10-1+H2O   2.50E+12   0.00E+00   0.00E+00
   REV/0.00E+00   0.00E+00   0.00000E+00/
C7H14O1-3+OH=C2H4+NC4H9CO+H2O   2.50E+12   0.00E+00   0.00E+00

```
  REV/0.00E+00   0.00E+00   0.00000E+00/
C7H14O2-4+OH=C3H6+NC3H7CO+H2O   2.50E+12   0.00E+00   0.00E+00
  REV/0.00E+00   0.00E+00   0.00000E+00/
C7H14O2-4+HO2=CH3CO+C5H10-1+H2O2   5.00E+12   0.00E+00   1.77E+04
  REV/0.00E+00   0.00E+00   0.00000E+00/
C7H14O1-3+HO2=C2H4+NC4H9CO+H2O2   5.00E+12   0.00E+00   1.77E+04
  REV/0.00E+00   0.00E+00   0.00000E+00/
C7H14O2-4+HO2=C3H6+NC3H7CO+H2O2   5.00E+12   0.00E+00   1.77E+04
  REV/0.00E+00   0.00E+00   0.00000E+00/
END
```

APPENDIX C CFD RESULTS FOR DIESEL OPERATION

Figure C.1 through Figure C.5 show temperature, ϕ, CO, PM and viscosity distributions in diesel operation at 12% load. The mechanism used in this study is from CONVERGE library.
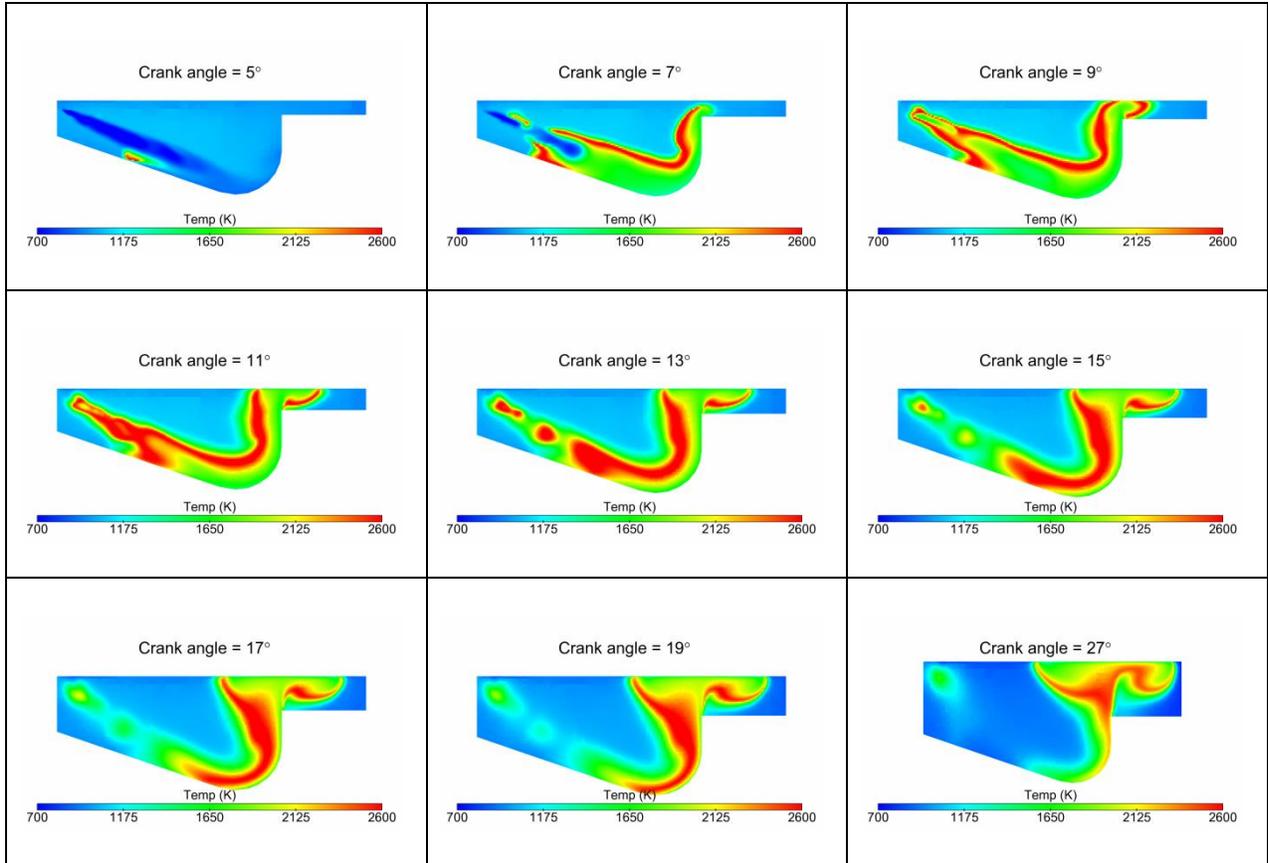
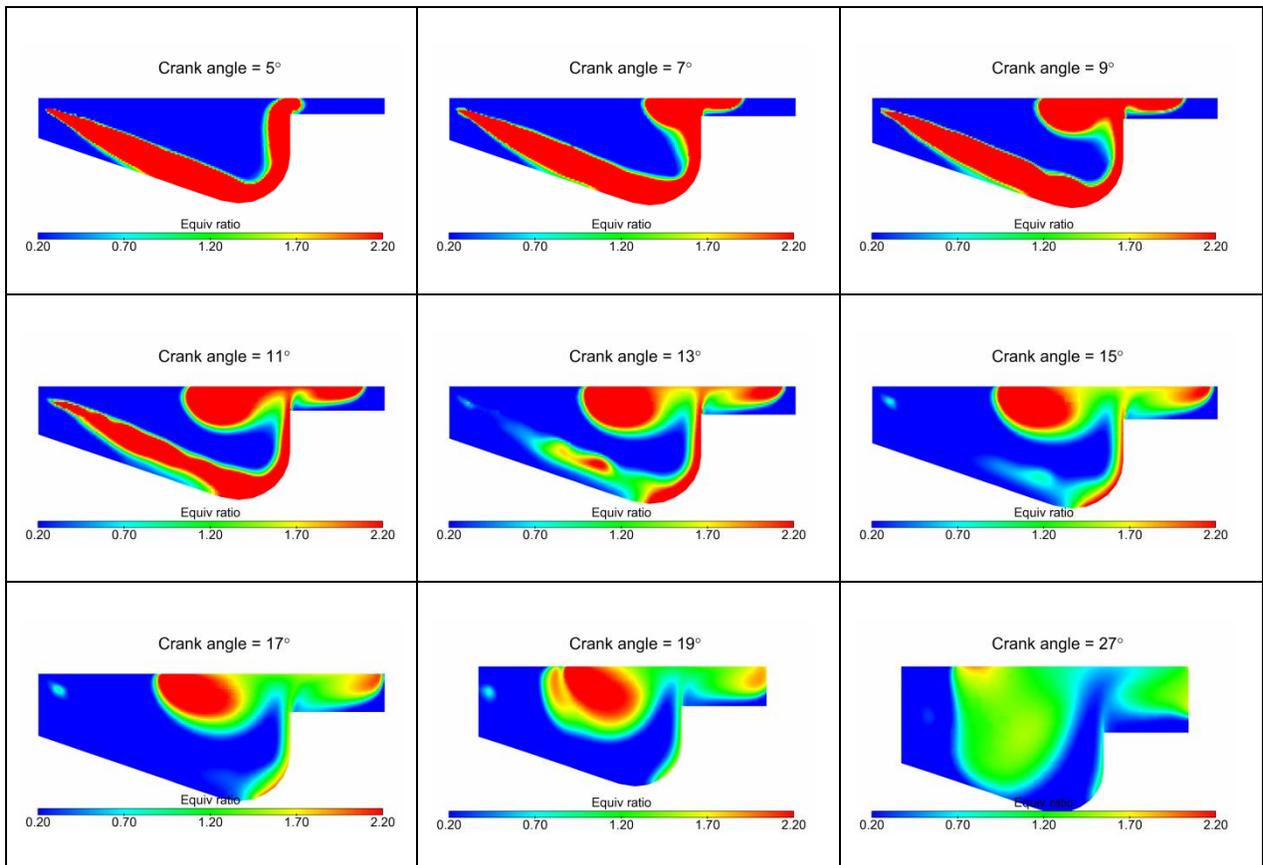Figure C.1: Temperature distributions in diesel engine at 12% load at crank angles
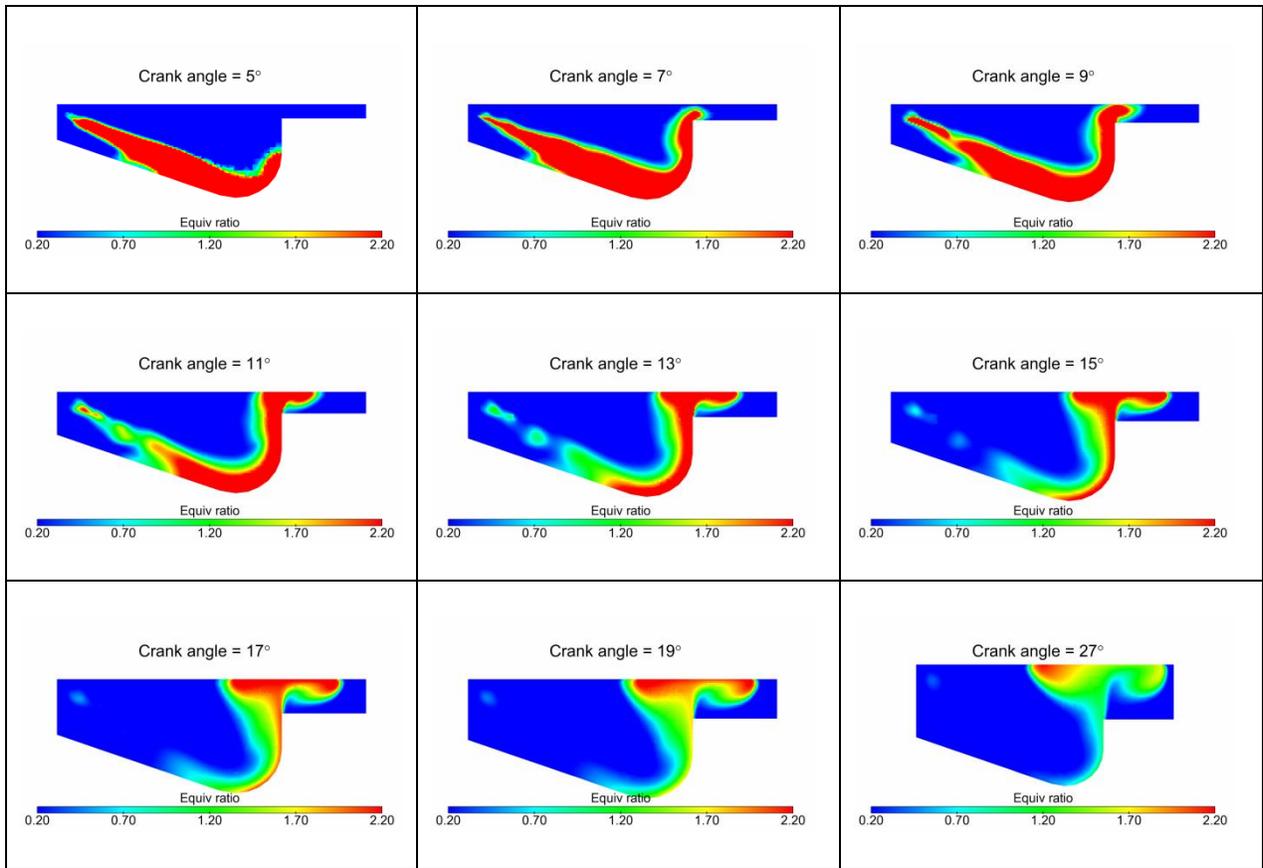
Figure C.2: ϕ distributions in diesel operation at 12% load at various crank angles
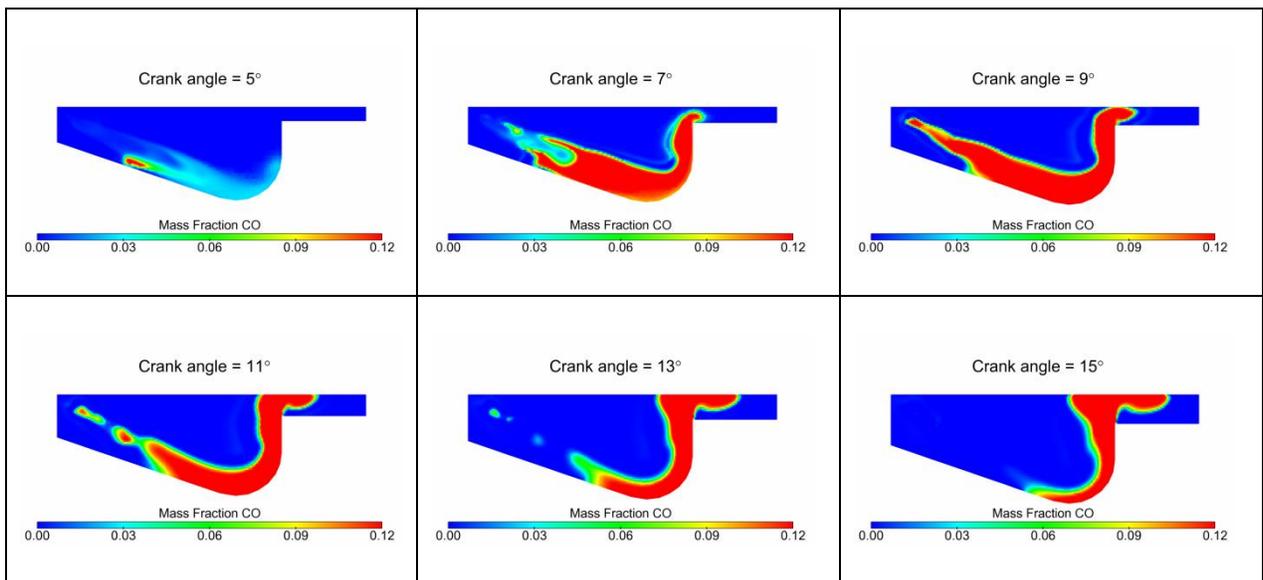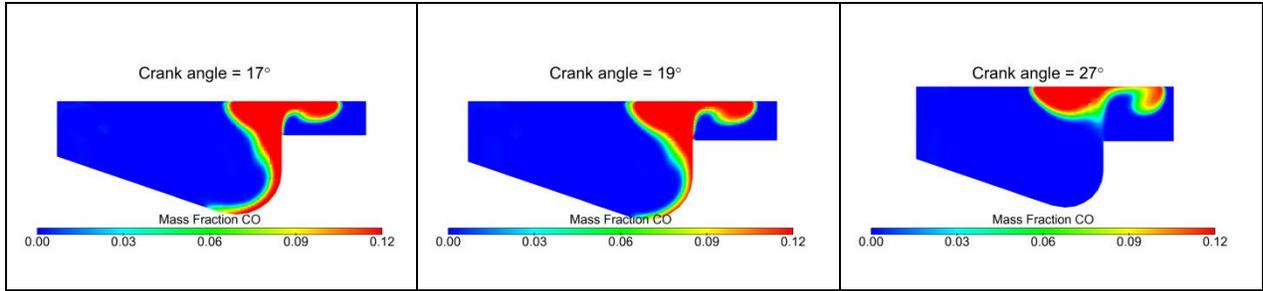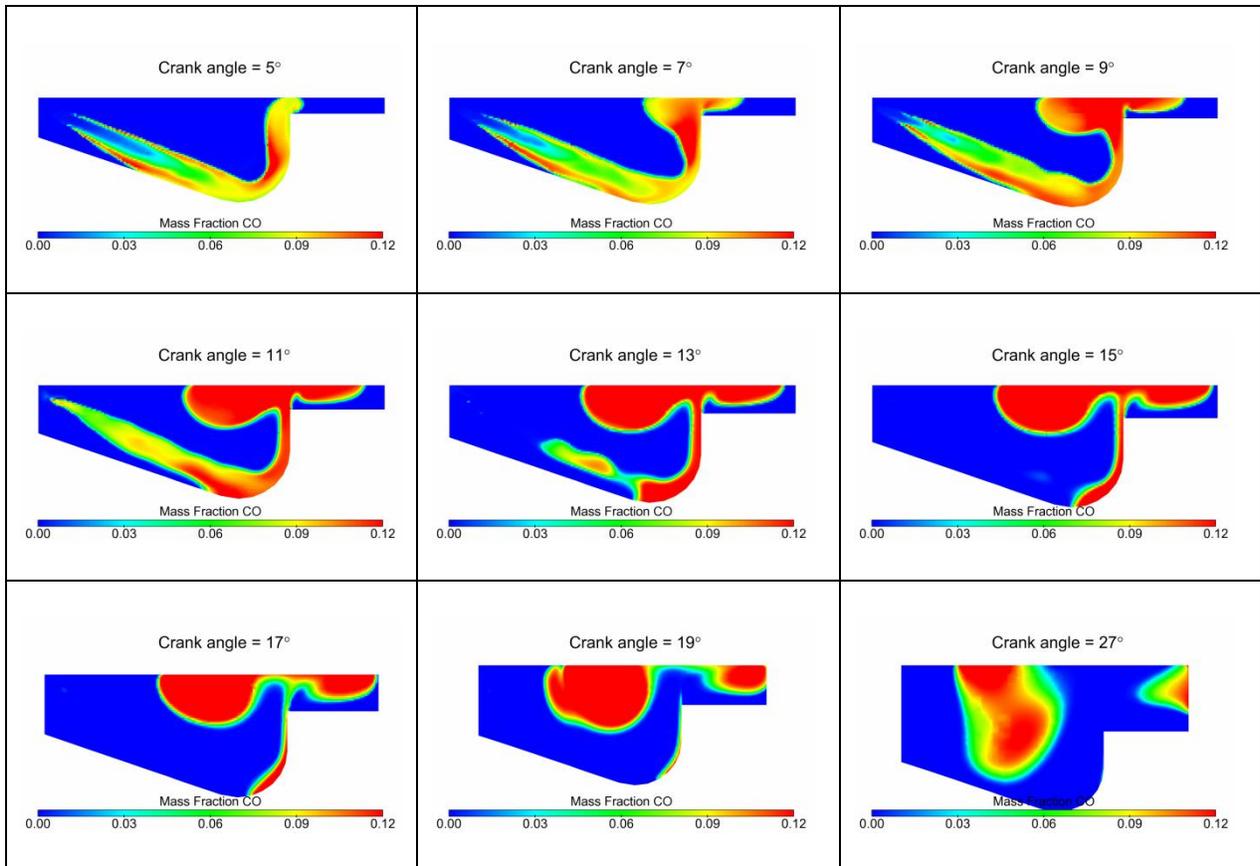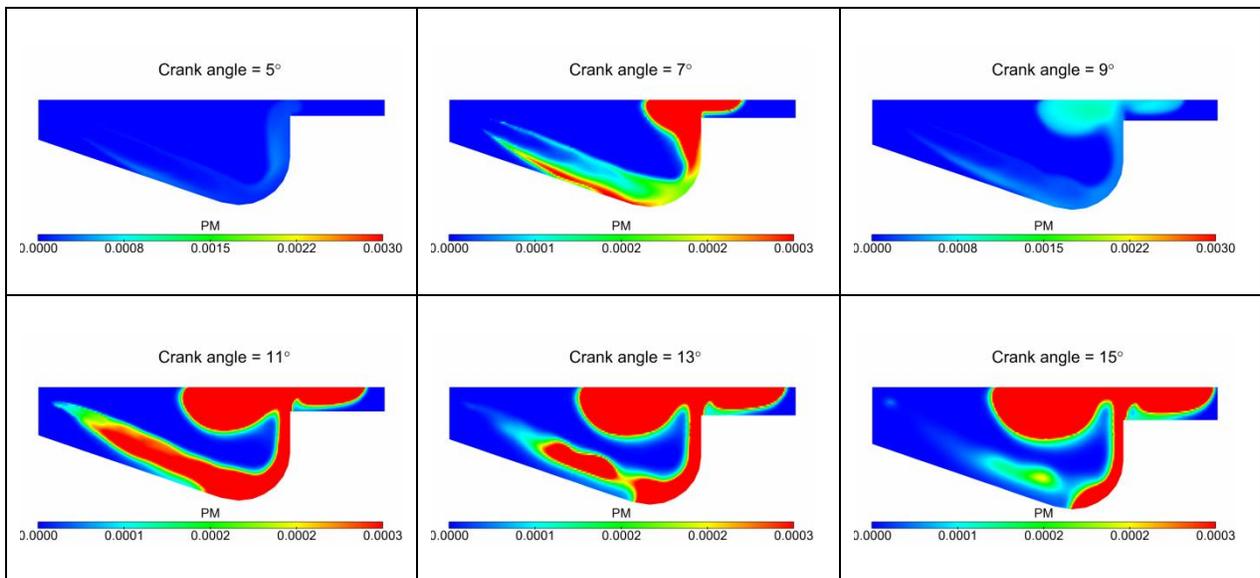
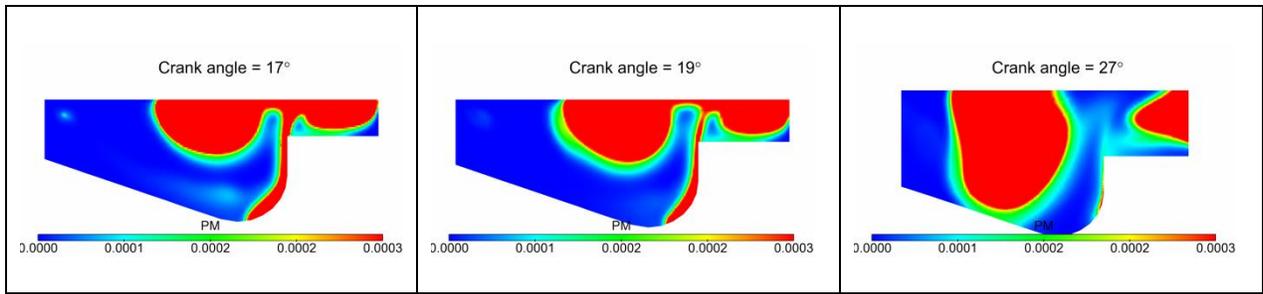Figure C.3: CO formations in diesel operation at 12% load at various crank angles
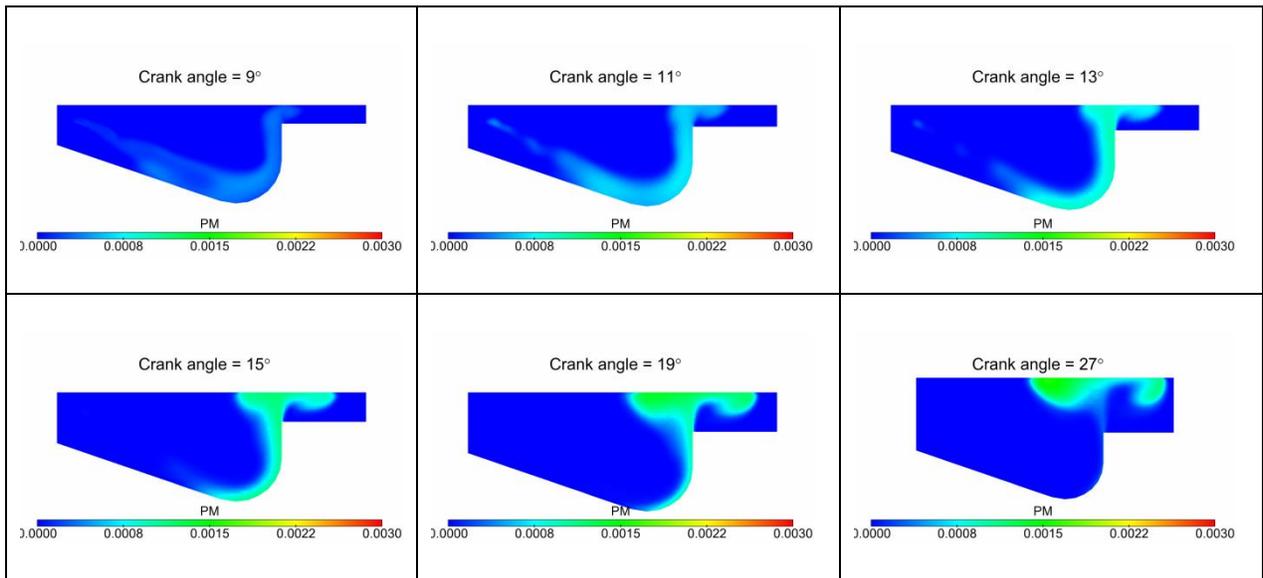
Figure C.4: PM formations in diesel operation at 12% load at various crank angles
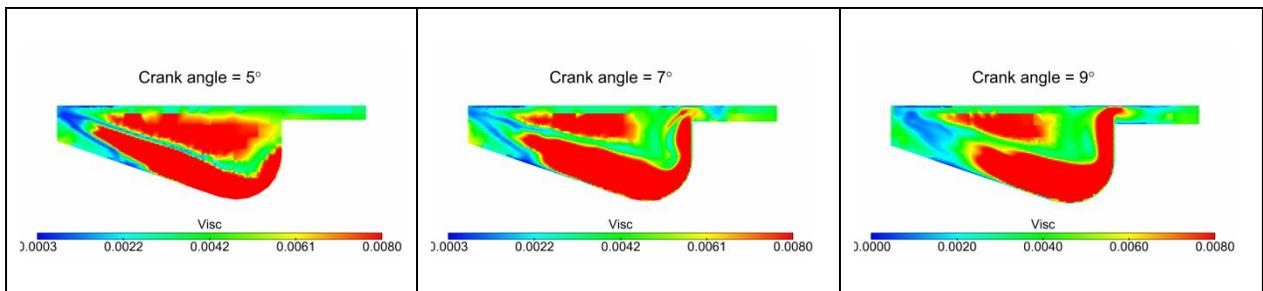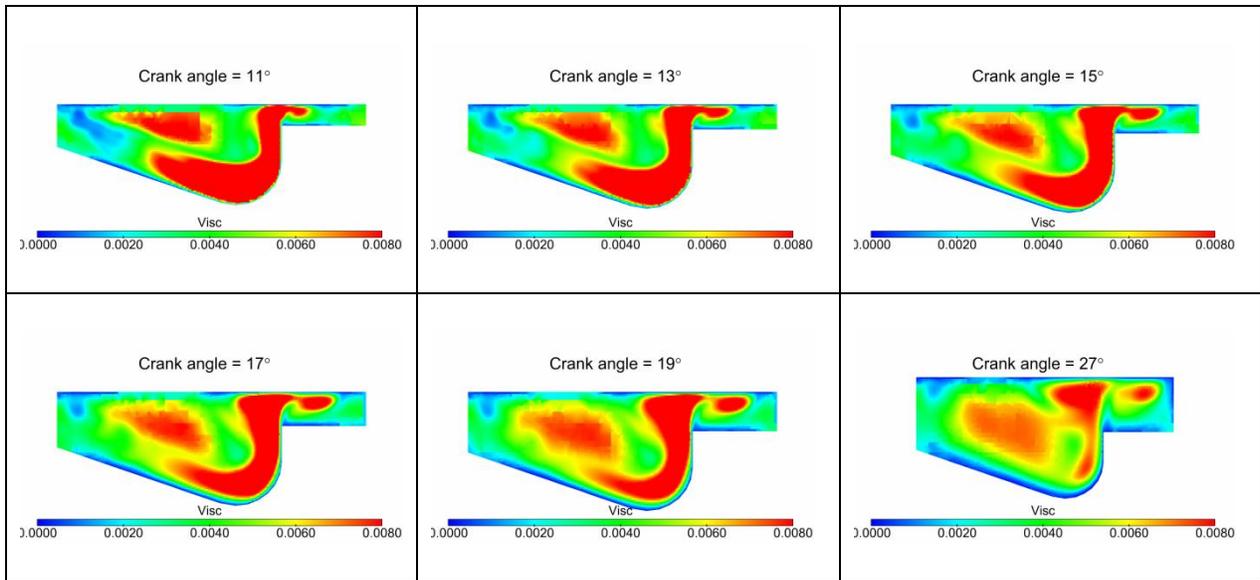
Figure C.5: Viscosity distributions in diesel engine at 12% load at various crank angles

Figure C.6 through Figure C.10 show temperature, ϕ, CO, PM and viscosity distributions in diesel operation at 12% load.
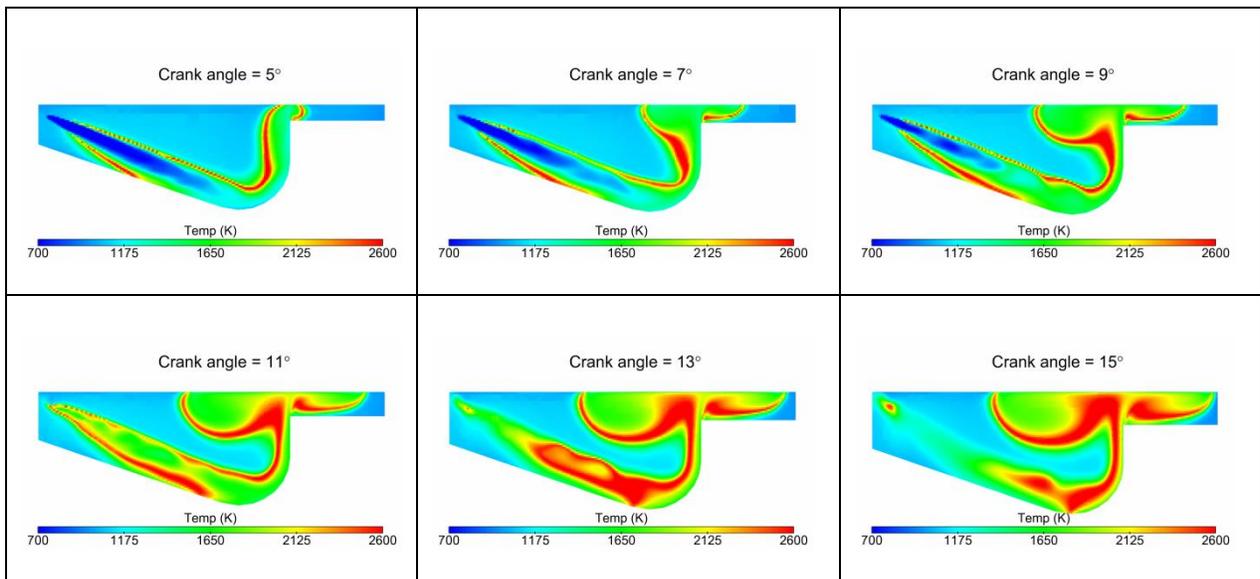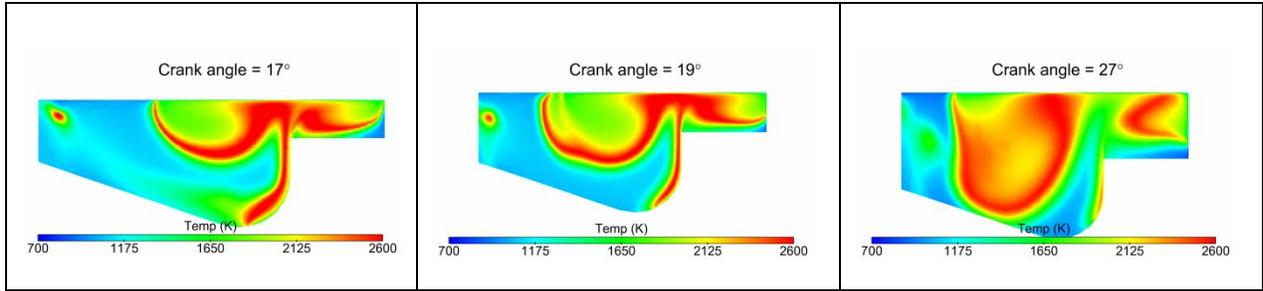
Figure C.6: Temperature distributions in diesel engine at 75% load at crank angles

Figure C.7: ϕ distributions in diesel operation at 75% load various at crank angles

Figure C.8: CO formations in diesel operation at 75% load at various crank angles

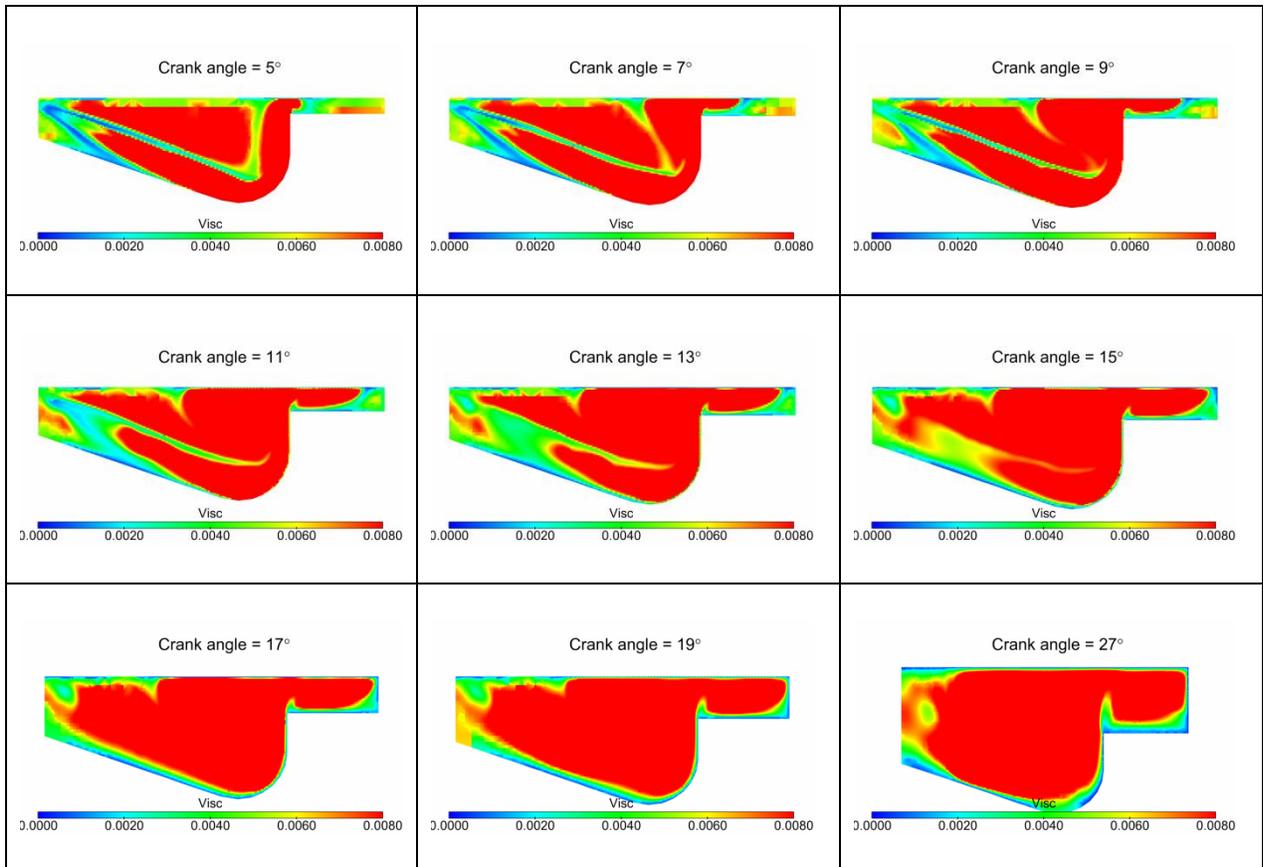Figure C.9: PM formations in diesel operation at 75% load at various crank angles

Figure C.10: Viscosity distributions in diesel engine at 75% load at various crank angles

APPENDIX D   DUAL FUEL ENGINE CFD RESULTS

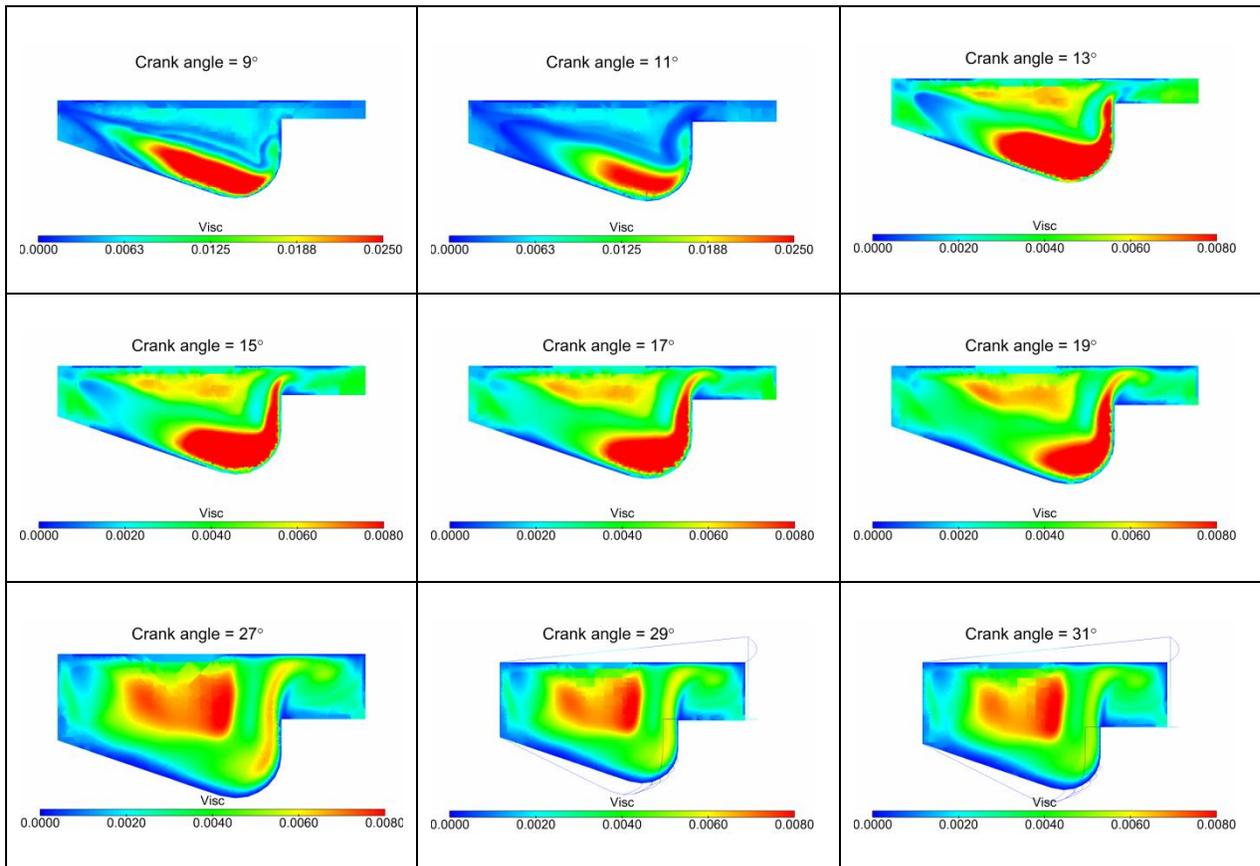Figure D.1 and Figure D.2 show viscosity distributions at 12% and 75% loads.

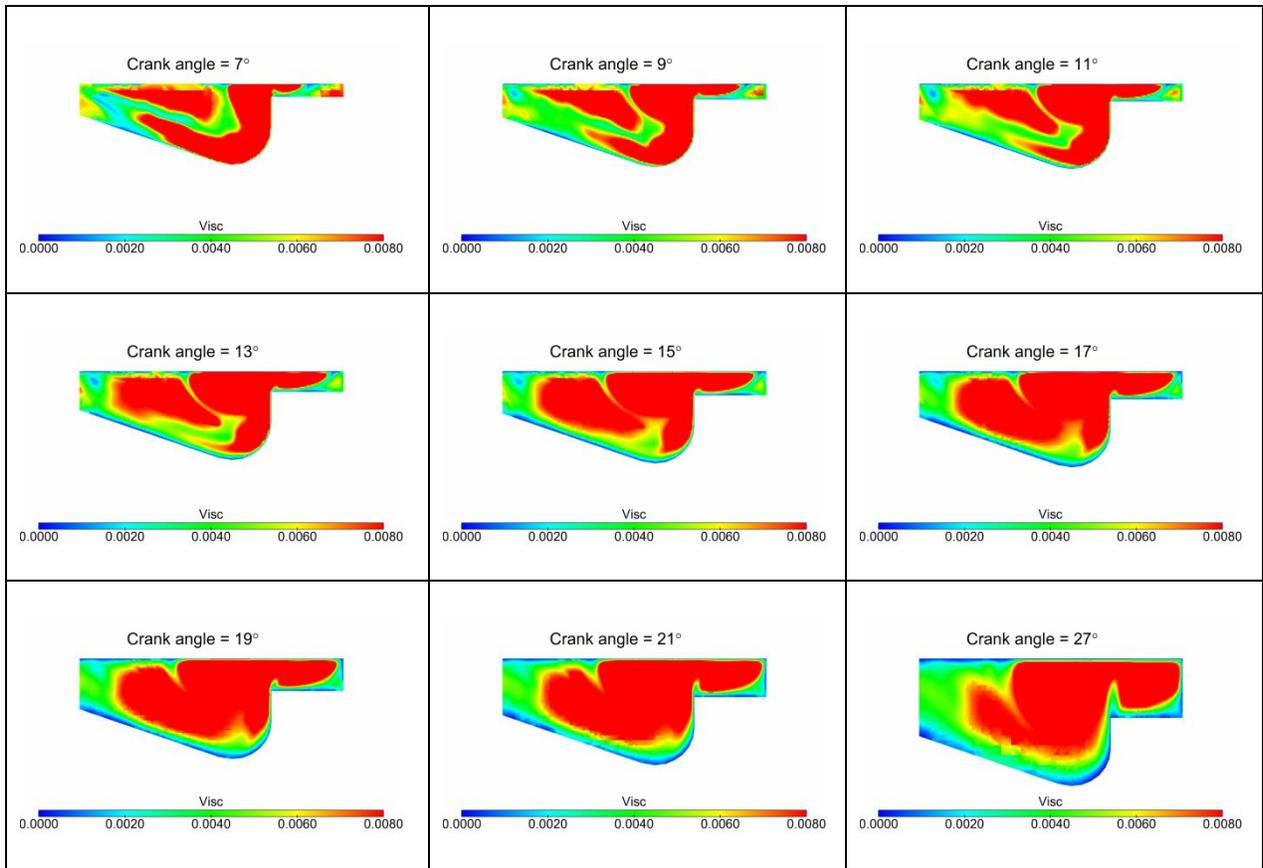Figure D.1: Viscosity distributions in dual fuel engine at 12% load at various crank angles

Figure D.2: Viscosity distributions in dual fuel engine at 75% load at various crank angles